UNIVERSITY OF CAMBRIDGE

MRC Laboratory of Molecular Biology

The role of EHD proteins in caveolae, and the role of caveolae in adipocytes

Ivana E-Ting Yeow

St. John's College

University of Cambridge

This dissertation is submitted for the degree of Doctor of Philosophy

November 2017

The role of EHD proteins in caveolae, and the role of caveolae in adipocytes

Ivana E-Ting Yeow

Abstract

Caveolae are 50-60 nm flask-shaped invaginations of the plasma membrane that protect the plasma membrane from damage under stretch forces. They are highly abundant in cells that experience high levels of stress forces such as adipocytes, endothelial cells and muscle cells. Caveolae are generated by the oligomerisation and association of caveolin and cavin proteins, which form the caveolar coat complex at the caveolar bulb and are progressively well characterised. However, less is known about the proteins that localise to the caveolar neck. Using the CRIPSR/Cas9 system to generate gene knock-in and knockout cell lines, the role of EHD proteins at caveolae was investigated. It was found that, in addition to EHD2 being at the neck, both EHD1 and EHD4 were also present. The recruitment of other EHD proteins was markedly increased in the absence of EHD2. This functional redundancy was confirmed by the generation of *EHD1*, *2* and *4* triple knockout cell lines, which displayed two striking sets of phenotypes. Firstly, the characteristic higher-order clusters of caveolae are lost in the absence of EHD proteins. And secondly, caveolae are destabilised and the plasma membrane is more likely to rupture when the *EHD1,2,4* knockout cells are subjected to cycles of stretch forces. The data identify the first molecular components that cluster caveolae into a membrane ultrastructure that potentially extends stretch buffering capacity. A second series of experiments tested different ideas about the function of caveolae in adipocytes. The insulin receptor and CD36 were found to at most partially colocalise with caveolae, and the role of caveolae in regulating signalling processes remains unclear. In contrast, the plasma membrane of adipocytes without caveolae is clearly more prone to rupture, confirming a mechanoprotective function.

The work described here was undertaken in the Cell Biology Division at the MRC Laboratory of Molecular Biology.

I hereby declare that this dissertation is the results of my own work and includes nothing which is the outcome of work done in collaboration except as declared in the Preface and specified in the text.

I further state that my dissertation has not been submitted, or, is being concurrently submitted for any degree or diploma or other qualification at the University of Cambridge or any other University or similar institution.

Finally, it does not exceed the prescribed word limit (60,000 words) for the Biology Degree Committee.

Preface

My dissertation on "The role of EHD proteins in caveolae, and the role of caveolae in adipocytes" is divided into five chapters. The first chapter introduces the reported functions of caveolae and the proteins involved in the formation of caveolae. It also details background information on chapters three and four. The materials and methods employed in chapters three and four are outlined in chapter two. Chapter three focuses on the role of EHD proteins in caveolae. EHD2 have been shown to localise to the neck of caveolae but other EHD proteins have not been conclusively shown to localise to caveolae. The goal of this study was to assess whether other EHD proteins are involved with caveolae, and if so, to elucidate their functions. Chapter four shifts the focus from proteins involved in the formation of caveolae to the function of caveolae in adipocytes. The insulin receptor and CD36 have been reported to associate with caveolae and are related to adipocyte function, however, contradictions to this are also available in the literature. The goal of this study was to attempt to shed some light onto the conflicting data, and to assess whether or not the mechanoprotective role of caveolae holds true in adipocytes.

Initially, I started my PhD work with the experiments described in chapter four, however from the experiments conducted, it became apparent that the insulin receptor and CD36 did not associate with caveolae to the extent that has been reported. However, caveolae did indeed have a mechanoprotective role in adipocytes both *in vitro* and *in vivo*. After obtaining ultimately inconclusive data on the localisation of the insulin receptor and CD36, I shifted my focus to the proteins involved in the formation of caveolae. The absence of EHD2 has been reported to have significant effects on the abundance and mobility of caveolae, however this could not be observed in our laboratory. This led me to investigate the role of other EHD proteins and they were indeed found to play a role in caveolar biology.

The majority of the work contained in chapter three is published in Yeow, I., et al., *EHD proteins cooperate to generate caveolar clusters and to maintain caveolae during repeated mechanical stress*. Curr. Biol., 2017., with elements from the publication adapted in the Materials and Methods, and figure legends.

It should be noted that Gillian Howard performed all the electron microscopy imaging presented in this thesis, the image presented in Figure 3.1.14 D was acquired by Ben Nichols, and live animal procedures were conducted by Jeroen Willems.

Acknowledgements

Firstly, I want to thank my supervisor Ben Nichols, I would not have been able to complete this PhD without his continuous guidance and support throughout the years. His knowledge and enthusiasm have been key to my progression in the PhD. I would also like to thank my second and University supervisors, Sean Munro and Antonio Vidal-Puig, for all their support. I would like to thank everyone in the lab, both present and past members who have made working in the lab a very enjoyable experience – Carolina, Kirsi, Jess, Tuula, Gill, Lena, Jade and Vasillis. In particular, I want to thank Lena, with whom I worked closely with, and Gill and Jess for doing all of the electron microscopy.

Secondly, I want to thank the facility teams at the LMB: Jon, Nick and Mathias in microscopy for training and helping me on the microscopes. Maria, Fan, Martyn and Nika in flow cytometry for sorting all my cell lines. Martin, Jeroen and Jo at ARES for taking care of the mice and doing the live animal procedures. The work completed in my PhD would not have been possible without funding from the Medical Research Council. I would also like to thank my college, St. John's, for the additional support.

Finally, my time in Cambridge would not have been so wonderful without my friends, especially Sarah and Lottie. I want to thank my sister Aoife for always being there when I needed someone to talk to, no matter what the issue. And last but not least, a huge thank you to my parents, Alison and Ricky, for all the support and understanding they have given me throughout my PhD and my life.

Table of Contents

Abbreviations

ANOVA: analysis of variance

ATP: adenosine triphosphate

BAR: bin-amphiphysin-Rvs167

bp: base pair

BSA: bovine serum albumin

BSS: buffered salt solution

CAV1: caveolin1

CBD: caveolin-binding domain

CD36: cluster of differentiation 36 (also known as fatty acid translocase)

cDNA: complementary DNA

CoA: coenzyme A

CRISPR: clustered regularly interspaced palindromic repeat

CSD: caveolin scaffolding domain

DAB: 3,3'-Diaminobenzidine

DMEM: Dulbecco's modified Eagle's medium

DNA: deoxyribonucleic acid

DRM: detergent resistant membrane

DSB: double-stranded break

DTT: dithiothreitol

ECL: enhanced chemiluminescence

EDTA: ethylenediaminetetraacetic acid

EE: early endosome

EGFR: epidermal growth factor receptor

EHD: Eps15 homology domain

eNOS: endothelial nitric oxide synthase

Eps15: epidermal growth factor receptor substrate 15

ERC: endocytic recycling compartments

F-BAR: FCH-BAR

FACS: fluorescence-activated cell sorting

FATP: fatty acid transport protein

FBS: foetal bovine serum

FCH: Fes-CIP4 homology

FITC: fluorescein isothiocyanate

FP: fluorescent protein

FRAP: fluorescence recovery after photobleach

GAPDH: glyceraldehyde 3-phosphate dehydrogenase

gDNA: genomic DNA

GFP: green fluorescent protein

GLUT4: glucose transporter type 4

GM1: monosialotetrahexosylganglioside

GPI: glycophosphatidylinositol

GTP: guanosine triphosphate

HDR: homology-directed repair

HRP: horseradish peroxidase

IR: insulin receptor

IRS1: insulin receptor substrate 1

kb: kilo base

kDa: kilo Dalton

KO: knockout

mCh: mCherry

MEF: mouse embryonic fibroblast

MESNA: sodium 2-mercaptoethanesulfonate

MHC: major histocompatibility complex

mRNA: messenger RNA

MURC: muscle-restricted coiled-coil protein (also known as cavin4)

NA: numerical aperture

NHEJ: non-homologous end joining

NPF: asparagine-proline-phenylalanine

OE: overexpressed

PACSIN: protein kinase C and casein kinase substrate in neurons

PAM: protospacer adjacent motif

PBS: phosphate-buffered saline

PCR: polymerase chain reaction

PFA: paraformaldehyde

PKC: protein kinase C

PP2A: protein phosphatase 2

PRD: Pro-rich domain

PRKCDBP: protein kinase C delta binding protein (also known as cavin3)

PTRF: polymerase transcript release factor (also known as cavin1)

PVDF: polyvinylidene difluoride

RNA: ribonucleic acid

ROCK: Rho/Rho-associated protein kinase

RT: room temperature

SDPR: serum deprivation protein response (also known as cavin2)

SDS-PAGE: sodium dodecyl sulfate polyacrylamide gel electrophoresis

SH3: Src homology 3

siRNA: small interfering RNA

SOCS3: Suppressor of cytokine signalling 3

STAT3: signal transducer and activator of transcription 3

STED: stimulated emission depletion

SV40: Simian virus 40

TALEN: transcription activator-like effector nuclease

TIR: total internal reflection

WT: wildtype

ZFN: zinc finger nuclease

Abstract

Caveolae are 50-60 nm flask-shaped invaginations of the plasma membrane that protect the plasma membrane from damage under stretch forces. They are highly abundant in cells that experience high levels of stress forces such as adipocytes, endothelial cells and muscle cells. Caveolae are generated by the oligomerisation and association of caveolin and cavin proteins, which form the caveolar coat complex at the caveolar bulb and are progressively well characterised. However, less is known about the proteins that localise to the caveolar neck. Using the CRIPSR/Cas9 system to generate gene knock-in and knockout cell lines, the role of EHD proteins at caveolae was investigated. It was found that, in addition to EHD2 being at the neck, both EHD1 and EHD4 were also present. The recruitment of other EHD proteins was markedly increased in the absence of EHD2. This functional redundancy was confirmed by the generation of *EHD1*, *2* and *4* triple knockout cell lines, which displayed two striking sets of phenotypes. Firstly, the characteristic higher-order clusters of caveolae are lost in the absence of EHD proteins. And secondly, caveolae are destabilised and the plasma membrane is more likely to rupture when the *EHD1,2,4* knockout cells are subjected to cycles of stretch forces. The data identify the first molecular components that cluster caveolae into a membrane ultrastructure that potentially extends stretch buffering capacity. A second series of experiments tested different ideas about the function of caveolae in adipocytes. The insulin receptor and CD36 were found to at most partially colocalise with caveolae, and the role of caveolae in regulating signalling processes remains unclear. In contrast, the plasma membrane of adipocytes without caveolae is clearly more prone to rupture, confirming a mechanoprotective function.

Chapter 1: Introduction

1.1 Specialised regions of the plasma membrane

All eukaryotic cells possess plasma membranes to protect and organise the cell by separating its inner contents from the outside. The lipid bilayer is the fundamental structure of plasma membranes, and is composed of phospholipids. Phospholipids contain a hydrophilic phosphate head group and hydrophobic fatty acid tail chains, and as such they are amphipathic. Due to their amphipathicity, phospholipids aggregate into bilayers with the hydrophobic tail chains aligning inwards and the hydrophilic head groups facing outwards. There are four major phospholipids – phosphatidylethanolamine and phosphatidylserine, which are primarily found on the inner leaflet of the lipid bilayer, and phosphatidylcholine and sphingomyelin, which are primarily found on the outer leaflet of the lipid bilayer. Membranes are semi-permeable barriers, as small molecules such as oxygen can diffuse rapidly across the membrane whereas larger molecules cannot and require membrane protein channels to facilitate crossing. In fact, membrane proteins account for approximately 50% of the cell membrane mass, most of which are transmembrane proteins [1]. In addition to phospholipids and proteins, the plasma membrane also contains cholesterol that helps regulate the fluidity of membranes and comprises of approximately 20% of the lipids in membranes [1].

Phospholipids interact via amphipathic properties, and like beads on a chain, if pulled laterally, membranes will break. The main function of the plasma membrane is to define cells by separating the inside from the outside. Therefore in order to resist pulling forces, the plasma membrane requires a mechanism to buffer for this, which could simply be by convolutions of the plasma membrane.

1.2 Introduction to caveolae

Caveolae are small 50-60 nm bulb-shaped invaginations of the plasma membrane and are particularly abundant in adipocytes, endothelial and muscle cells. The individual caveola can also form higher-order clustered arrays of two or more caveola bulbs.

These unique structures were first detected using electron microscopy in 1953 by Palade in blood capillaries, and in 1955 by Yamada in mouse gall bladder epithelium [2, 3]. However, despite their early observation, the molecular details of caveolae only started to become apparent in 1992 upon the discovery of caveolin1, an integral membrane protein that is a key component of caveolae [4]. Up until then, only the use of electron microscopy made it possible to examine these structures, but the discovery of caveolin1 allowed for the use of biochemical techniques to dissect the structure and roles of caveolae. Since then, two further homologues of caveolin have been discovered, caveolin2 and caveolin3 [5-7]. Caveolin1 is expressed in many cell types, other than in striated muscle, and is essential in the biogenesis of caveolae. Caveolin2 is generally expressed along with caveolin1 but it is not crucial in the formation of caveolae. Caveolin3 is specific to striated muscle and is key to the biogenesis of caveolae there. In addition to caveolins, a family of cytoplasmic proteins termed cavins, which have previously recognised functions, have been identified to cooperate with caveolins in the formation of caveolae [8-10]. Cavin1, also known as polymerase transcript release factor (PTRF), was initially described as a nuclear protein that induces the dissociation of paused ternary transcription complexes [11]. Without cavin1, caveolae do not form and caveolin protein expression is reduced despite normal caveolin mRNA expression [12]. Cavin2 and cavin3, also known as serum deprivation protein response (SDPR) and protein kinase C delta binding protein (PRKCDBP) respectively, were discovered as substrates for protein kinase C [13, 14]. Cavin4, also known as muscle-restricted coiled-coil protein (MURC), is specific to striated muscle and was suggested to modulate the Rho/Rho-associated protein kinase (ROCK) pathway in mouse cardiac muscle [15].

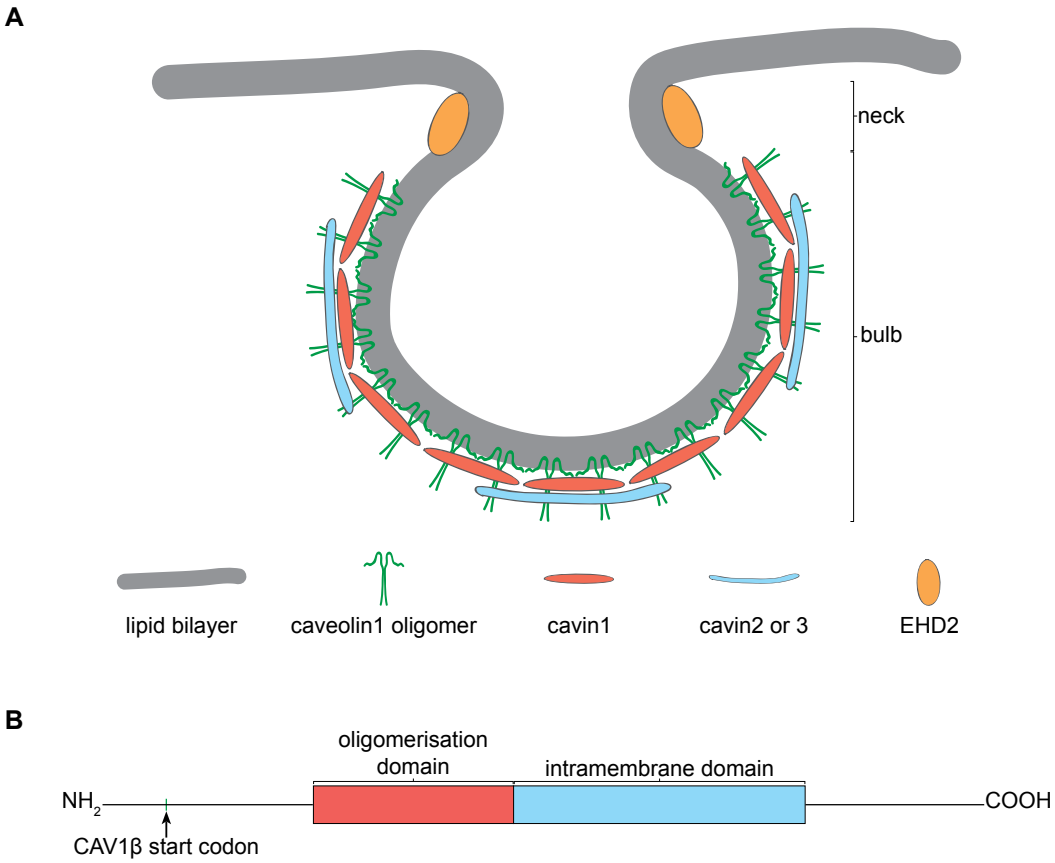

Figure 1.1 Structure and components of caveolae

A. Diagrammatic representation of a single caveola with the caveolar coat complex proteins (caveolin and cavin) represented in the bulb and EHD2 at the neck. Note: protein abundance not to scale. **B.** Schematic representation of caveolin1 domain organisation containing an oligomerisation domain and an intramembrane domain. The caveolin1 β isoform start codon is indicated with an arrow.

The discovery of the key components of caveolae and the identification of patients with mutations in these proteins have allowed for the study of the structure and function of caveolae, and the role of caveolae in disease. The apparent phenotypes in humans and mice lacking caveolae may reveal insights into the function of caveolae. Humans lacking functional cavin1 and therefore caveolae exhibit myopathy, cardiac arrhythmia, enlarged blood vessels, pulmonary hypertension and lipodystrophy [16-18]. Similar phenotypes are observed in mice that lack cavin1. They display pulmonary hypertension, lipodystrophy, are insulin resistant and have impaired glucose tolerance [12].

Caveolae have been implicated in a wide range of functions including endocytosis, lipid homeostasis, signal transduction, and mechanoprotection. However, the exact molecular mechanisms by which caveolae do so is still unclear and numerous proposed details remain controversial [19]. Many of these discrepancies have arisen from the use of overexpressed fluorescently tagged caveolin1 as a marker for caveolae. Overexpression of caveolin1-GFP has seen caveolins targeted to endosomes and lysosomes for degradation through non-caveolar pathways [20]. Consequently, colocalisation of proteins observed when using overexpressed caveolin1-GFP may in fact represent endosomal localisation of the protein, rather than colocalisation with caveolin1. Thus, the use of genome-edited caveolin1 and cavin1 to express fluorescent tags from the endogenous loci is key to dissecting caveolar biology [21].

1.3 Functions of caveolae

1.3.1 Endocytosis

The characteristic bulb-shape of caveolae has led to the idea of caveolae budding from the plasma membrane [2]. They have been proposed to act as transport vesicles, in particularly in endothelium where caveolae could transport albumin from one side to the other [22]. The abundance of caveolae may thus aid in the high flux of albumin across the endothelium. However, caveolae are highly stable structures at the plasma membrane and this has been seen by the relative immobility of caveolin1 in caveolae using fluorescence recovery after photobleaching (FRAP) [23, 24]. Further experiments of fused cells with different coloured caveolins confirm this, as there were no mixed coloured structures [25]. Indeed even during endocytosis, caveolae remain in a stable unit that fuses with endosomes and can recycle back to the plasma membrane as an intact structure [23]. Yet it is unclear as to whether caveolae only bud as single units, or if multiple caveolae connected by non-caveolar membrane can also detach from the membrane [26].

The fact that caveolae bud from the plasma membrane is long-standing, however, the exact molecular mechanisms and machinery responsible for this is just being elucidated [22, 27]. Cavin3, which is not essential for the formation of caveolae, has been shown to increase the surface dynamics of caveolae by interacting with cavin1

and caveolin1, perhaps destabilising caveolae for its release from the membrane [28, 29]. PACSIN2, dynamin2 and EHD2 have all been linked to caveolar mobility with PACSIN2 sensing and inducing membrane curvature, dynamin2 aiding in the scission of caveolae from the plasma membrane, and EHD2 confining caveolae at the membrane [30-34]. PACSIN2 phosphorylation at serine 313 by protein kinase C (PKC) decreases its membrane binding capacity resulting in caveolae destabilisation and the triggering of dynamin-mediated removal of caveolae [35].

Despite advances in elucidating caveolar endocytosis, the lack of specific markers and cargoes for this remains problematic. Several studies investigating the uptake of the simian virus 40 (SV40) indicated a direct role of caveolae budding in virus entry, leading to the possibility of SV40 virus as a specific cargo for caveolar endocytosis [36, 37]. However, later studies showed that overexpressed of caveolin1-GFP led to its degradation in late endosomes and subsequent examinations of SV40 revealed that it uses the classical endocytic pathway instead [20, 38, 39]. Another cargo that has been thought to be specific for caveolar endocytosis is cholera toxin B subunit [40, 41]. Both SV40 and cholera toxin B subunit binds to the ganglioside GM1 which is present in caveolae [42]. Again, later studies revealed that cholera toxin is also sorted into clathrin-coated pits and other endocytic structures, complicating previous data associating it with caveolae [40, 41]. It is not surprising that a specific marker of caveolar endocytosis has not been identified, since caveolae do not contribute greatly to overall endocytic trafficking [24, 26, 43]. A recent study supporting this used genome editing to endogenously tag caveolin1 and cavin1 with fluorescent proteins, and quantified the endocytic flux in these cells which revealed that only about 5% of the caveolae population undergo endocytosis within a 15 minute timeframe [21]. The low rate of caveolar endocytosis suggests that it is most likely not crucial for overall endocytosis in cells, but perhaps it may be important in trafficking and regulating certain proteins in the plasma membrane. Cargoes that have been connected to caveolae include the insulin receptor, some G-protein coupled receptors, sphingolipid analogs, vitamins D3, enterovirus and more [44-51]. Indeed it is also not entirely impossible that caveolar endocytosis observed is due to the regulation of caveolae abundance and distribution at the plasma membrane, rather than endocytosis of specific cargoes.

1.3.2 Lipid regulation

Caveolae are highly abundant in adipocytes, representing up to 50% of the plasma membrane surface in these cells [52]. Multiple lines of evidence have linked caveolae to lipid regulation in these cells. Caveolin1 binds cholesterol and fatty acids, and localises to lipid droplets under certain cellular conditions [53-57]. Lipid droplets serve as a reservoir for cholesterol and triglycerides, and release them during fasting. Thus a mechanism for trafficking and storing lipids is essential. Caveolin1 has been shown to increase the cellular levels of free cholesterol and facilitate fatty acid uptake into cells, even in the absence of the fatty acid transport protein CD36 [58-60]. Cholesterol is known to be required for caveolar stability and function [61, 62]. *Caveolin1* knockout mice have reduced fat mass, smaller adipocytes, are resistant to diet-induced obesity and are insulin resistant [63, 64]. Isolated lipid droplets from mice lacking caveolin1 display reduced levels of cholesterol, and in 3T3 L1 adipocytes the addition of cholesterol possibly stimulated the translocation of caveolin1 to lipid droplets [65]. Furthermore, these mice display decreased cholesterol synthesis [66]. In addition, a caveolin mutant that constitutively associates with lipid droplets led to an increase in neutral lipid storage in lipid droplets and a decrease in free cholesterol at the surface [56, 67]. Examination of enterocyte apical brush border membranes from *caveolin1* knockout mice showed a significant decrease in the uptake of fatty acids compared to wildtype [68]. *Cavin1* knockout mice display similar metabolic phenotypes as *caveolin1* knockout mice, and cavin1 may also play a role in lipid homeostasis [12, 69]. Taken together, the evidence here posits an important role for the presence of caveolae in lipid homeostasis, but the exact mechanisms by which caveolae do so is yet to be identified [70].

1.3.3 Signalling

Caveolae have been linked to a range of signalling pathways and are suggested to regulate them by retaining signalling proteins in an inactive state until a release cue is received [71, 72]. If that is the case, then an important question of how cells that inherently lack caveolae signal normally remains unanswered. Mild phenotypes observed in mice and humans lacking caveolae suggest that signalling processes are not severely perturbed by the absence of caveolae. A plethora of signalling molecules such as endothelial nitric oxide synthase (eNOS), insulin receptor, mitogen-activated protein, and epidermal growth factor receptor (EGFR), have been associated with

caveolae [45, 73-82]. These signalling proteins have been suggested to bind through its caveolin-binding domain (CBD) to the conserved alpha-helical caveolin scaffolding domain (CSD) at residues 82-101 of caveolin1 [77, 83, 84]. However, more recent studies have undermined the CBD/CSD interaction [85, 86]. Structural analysis of the CBD, which is suggested to exist in many proteins, revealed that the CBD is not exposed at the surface of many signalling proteins, and is therefore unlikely to interact with caveolin. In fact, analysis of the CBD of 40 potential interaction partners of caveolin1 did not reveal any concurrent structural motifs [85, 86]. Furthermore, the CSD is located at the N-terminal of caveolin1 and is thought to have membrane-binding capacities and may even insert into the caveolar membrane [87-89]. It has been proposed that caveolin1 is inserted into the plasma membrane in such a way that the CSD is concealed by its close proximity to the phospholipid bilayer, thereby unable to interact with cytoplasmic proteins [85, 90].

Although it seems that caveolin1 does not have a direct effect in signalling via CBD/CSD interactions, caveolae may still contribute to signalling indirectly through other proteins associated with caveolae such as caveolin2 and cavin3, or by more complex mechanisms [72]. Fatty acylation and phosphorylation of caveolin2 prevents suppressor of cytokine signalling 3 (SOCS3) interacting with the insulin receptor, thereby allowing the activation of insulin receptor substrate 1 (IRS1) and the nuclear translocation of activated STAT3 [91-93]. Caveolae can also change the activity of signalling proteins by altering their subcellular location [94, 95]. Loss of caveolin1 accelerates the endocytosis of the insulin receptor, which normally resides at the surface of the plasma membrane [94].

An alternative mechanism for caveolae signalling could involve compartmentalisation and caveolae-mediated membrane organisation into domains. Caveolae may provide a segregated platform in insulin signalling. Ceramide-mediated inhibition of insulin occurs through PKC in cells abundant with caveolae, whereas it acts via the phosphatase PP2A in cells lacking caveolae [96]. As mentioned, caveolae have the ability to regulate plasma membrane lipid composition. In cells lacking caveolin1, the ganglioside GM1 and the glycosylphosphatidylinositol (GPI)-anchored proteins, which are components of membrane nanoclusters, are significantly decreased [97]. Hence, altered lipid composition by caveolae causes perturbation of membrane

nanoclusters implying that caveolae may affect signalling indirectly through regulating membrane lipid composition.

1.3.4 Mechanoprotection

Cells subjected to mechanical stress have evolved mechanisms to protect the cells from such stress, and this has been referred to as mechanoprotection. Caveolae have been proposed to be involved in mechanoprotection as far back as 1975, when Dulhunty and Franzini-Armstrong stretched frog skeletal muscle fibres and found that caveolae opened up to increase the effective cell surface area [98]. They suggested that caveolae could acts as "safety valves" that open up and flatten out to prevent plasma membrane rupture (Figure 1.2 A). Recent studies have confirmed that caveolae flatten out in an ATP- and actin-independent manner in response to plasma membrane stretching, with cavins dissociating from the plasma membrane (Figure 1.2 B) [99, 100]. In addition to *in vitro* experiments showing a loss of caveolae upon stress, *in vivo* studies with more physiological conditions have confirmed this apparent function of caveolae [101, 102]. Lo *et al*. observed that in isolated intact mouse muscle fibres caveolae were primarily assembled into multi-lobed rosettes, and that they flattened upon increased membrane tension, highlighting the importance of caveolar clusters. They also found that vigorous muscle activity in live zebrafish embryos that lack caveolae led to cell damage [101]. In a study conducted by Cheng *et al*., mechanical stress was induced pharmacologically. Dobutamine was injected into mice which stimulated cardiac output, increased blood flow and thus induced mechanical stress on endothelial cells of the heart, causing the disassembly of endothelial caveolae [102]. Moreover, endothelial cells lacking caveolae were more susceptible to plasma membrane damage. Mice and humans lacking caveolae display cardiomyopathy and cardiac arrhythmias [103-107]. Re-expression of caveolin1 in mice deficient of it rescued its cardiovascular phenotypes implying that endothelial cell damage may underlie these phenotypes [108]. The concept of caveolae playing a role in membrane repair upon damage is consistent with the muscular dystrophy phenotypes caused by caveolae deficiency [104, 109-113].

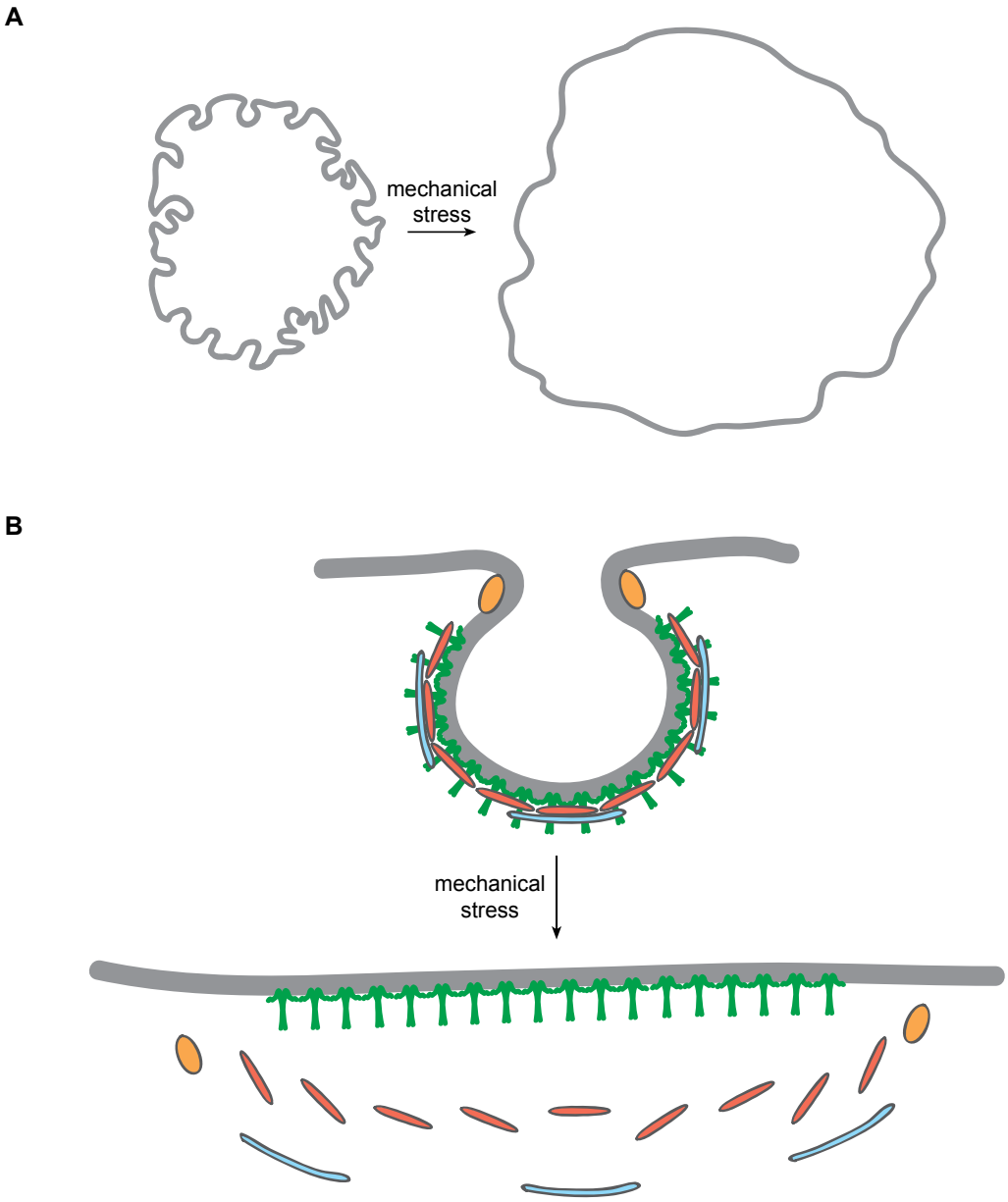

Figure 1.2 Mechanoprotective role of caveolae
A. Expansion of a single cell (left of arrow) with caveolae to provide more surface area upon mechanical stress (cell right of arrow). **B.** Disassembly of caveolae upon mechanical stress, with cavin proteins released into the cytosol. (See Figure 1.1 for the components of caveolae.)

Membrane tension is typically induced by mechanical stretch or hypo-osmotic shock and the disassembly of caveolae after stress is commonly measured via loss of morphologically defined caveolar structures detected by electron microscopy. Thus, the loss of caveolae may also be due to internalisation of caveolar structures rather than flattening of caveolae. Corrotte *et al*. showed that regions of membrane that were

damaged by the pore-forming toxin streptolysin O triggered the formation and clustering of caveolae, and the subsequent removal of the lesion by endocytic caveolar vesicles and lysosomal degradation [114]. Electron microscopy displayed a considerable accumulation of caveolae-like vesicles proximal to the regions of damaged membrane, suggesting that the pores generated by streptolysin O were removed from the plasma membrane via internalisation in caveolae. The two mechanisms presented here, flattening versus internalisation, may pose a potential paradox, however they are not mutually exclusive. Caveolae flatten out in response to membrane tension to protect cells from membrane damage, and caveolae endocytosis aids in the repair of membrane lesions. This highlights the complexity of caveolar biology and the requirement of further experiments to unravel this. The presence of caveolar clusters add to the complexity as they may allow for greater expansion in the plasma membrane upon stress forces, but have also been observed in the repair of membrane lesions. Additionally, how caveolae "know" when to disassemble is still uncertain. It may be solely due to mechanical forces, as caveolae can flatten out independently of ATP, but increasing evidence suggests a mechanosensing role of caveolae as well.

The endothelial cell surface is sensitive to changes in hydrostatic pressure and shear stress. Persistent exposure to shear stress of cultured endothelial cells caused an increase in surface localisation of caveolae due to caveolin1 redistribution from the Golgi [115, 116]. Furthermore, caveolin1 phosphorylation was observed and specific signalling pathways, including ones involving ERK and Akt, were activated [117]. *In vivo*, mice lacking caveolin1 showed defects in blood vessel remodelling and dilation that depended on blood flow, but this was rescued by re-expression of caveolin1 in the endothelium indicating a role for caveolin1 in sensing flow [118]. More evidence for caveolae as mechanosensors comes from studies in smooth muscle cells. Caveolin1 is rapidly redistributed to focal contacts in smooth muscle cells when they are under cycles of stretch and in cells lacking caveolin1, cell cycle progression was inhibited [119]. Mechanisms allowing caveolae to transduce mechanical signals remain unclear.

1.4 Structure and components of caveolae

1.4.1 Structure of caveolae

The characteristic shape of caveolae is in some ways similar to that of clathrin-coated pits. Indeed, caveolae do form hollow cavities but unlike clathrin-coated pits, they are not transient. Caveolae also do not have a hallmark electron-dense coat that clathrin-coated pits display when observed under electron microscopy [120]. However, they do exhibit striations around the caveolar bulb, resembling something of a protein coat [121]. More recent experiments have revealed that this protein coat is composed of caveolins and cavins which assemble into an 80S complex termed the caveolar coat complex, which forms around the caveolar bulb [122]. They demonstrated that other proteins associated with caveolae, such as EHD2, are not a part of the complex around the bulb, and that EHD2 remained in a different domain of caveolae. What is not fully understood though is whether pre-formed caveolae arrive at the plasma membrane and fuse with it creating a caveolar bulb protruding from the inner leaflet of the membrane, or if caveolae assemble as flat structures in the plasma membrane that then bud inward and produce the characteristic bulb shape. A study conducted by Hayer et al. suggests the latter, as they observed that cavin1 only associates with caveolin1 when at the plasma membrane [62]. Deep etch electron micrographs of caveolae display varying degrees of invagination, from flat caveolae to fully budded caveolae [123]. Not only are caveolae observed in different degrees of invagination, they are also observed in clusters. Caveolae have the ability to associate together to form higher-order clusters. These clusters have been observed in cultured cells and *in vivo* in tissues such as white adipose tissue and endothelium [22, 124-126]. However, the molecular mechanisms of how these complex multi-lobed structures are formed or the proteins responsible for linking them are not known. As caveolae have been observed to have two distinct regions, the bulb and the neck, it is likely that proteins at the neck of caveolae play an important role in aiding the generation of these higher-order clusters [122].

1.4.2 Caveolins and cavins

Caveolae have two distinct regions, the bulb which is shaped by the caveolar coat complex composed of caveolins and cavins, and the neck in which membrane-

deforming proteins such as EHD2, PACSIN2 and dynamin2 have been associated with (Figure 1.1 A) [30-32, 122, 127]. The stoichiometry of the caveolar coat complex is likely to be 12 caveolin:3 cavin1:1 cavin2 or cavin3 molecules, with each caveola estimated to have 140-150 caveolin1 molecules [128]. The main mammalian caveolin in non-muscle cells is caveolin1, which is an essential component of caveolae and lack of it results in the absence of caveolae in non-muscle tissues [63, 129]. It is a 21 kDa integral membrane protein with a hairpin domain that inserts into the inner leaflet of the plasma membrane, and is held in place by multiple acylation (Figure 1.1 B) [130, 131]. Both the N-terminus and C-terminus of caveolin1 is located in the cytoplasm of the cell. Genes encoding caveolins are conserved across metazoans, although it is unclear when caveolins acquired the ability to form caveolae, as caveolin in *Caenorhabditis elegans* (*C.* elegans) is apparently unable to form caveolae, thus caveolin must have acquired the ability during evolution [90].

There are two isoforms of caveolin1 in mammals, alpha and beta, with caveolin1β lacking part of the N-terminus where a tyrosine phosphorylation site resides [132]. Caveolin1 are synthesised at the rough endoplasmic reticulum as integral membrane proteins where they homo-oligomerise via amino acids 61-101 and are transported to the Golgi where they assemble into larger complexes [133-136]. The caveolin1 assemblies are delivered to the plasma membrane where hetero-oligomeric cavin complexes associate with them [25, 62]. Cavin complexes appear to initially assemble in the cytosol, and continue to do so after binding to caveolin1 [62]. Once assembly has occurred, the caveolar coat is stable and does not undergo cycles of disassembly and assembly, unlike clathrin coated pits [25].

Although the cavin family of proteins were discovered independently, they share common structural motifs such as phosphatidylserine binding sites and leucine zippers, and form a defined family of homologous proteins. Cavin proteins have a coiled-coil (helical region 1) domain at the N-terminus and a membrane association (helical region 2) domain towards the C-terminus [137]. The coiled-coil domains of cavins have been shown to promote homo- and heteromeric cavin-cavin interactions [138]. Cytosolic cavin proteins form heterotrimers via the coiled-coil domain, consisting of three cavin1 or two cavin1 with one cavin2 or cavin3, and upon doing so

form the membrane association domain [138]. These two domains together are important for cavin complexes to associate with the plasma membrane. They stabilise the caveolin oligomers, and without cavins, caveolae do not form due to the degradation of caveolin1 [12, 139]. This suggests that caveolin1 is only stable in the plasma membrane when inside the caveolar coat, despite its ability to generate membrane vesicles, in the absence of cavins, when expressed in bacteria [140].

Recent studies have implied that the striations observed around the bulb of caveolae are due to the cavin complexes [141, 142]. In a study by Stoeber *et al.*, purified cavin1 complexes and purified caveolin oligomers were analysed, and it was found that cavin1 assumed a net-like mesh structure which formed polyhedral lattices, and caveolin oligomers formed disc-shaped arrangements [141]. Analysis, by Ludwig *et al.*, of the caveolar coat complex that shapes the bulb of caveolae revealed two layers, an inner coat comprised of caveolin units in a polyhedral cage and an outer filamentous coat formed from cavins [142]. The studies suggest a dodecahedron structure with caveolin units occupying the pentagonal face and cavin oligomers aligning the vertices [141, 142]. In addition to caveolin and cavin proteins, there have been several non-essential proteins associated with caveolae.

1.4.3 Proteins associated with caveolae

With caveolae displaying highly curved membrane surfaces, it is not surprising that membrane-deforming proteins such as PACSIN2, dynamin2 and EHD2 have been associated with caveolae. The bin-amphiphysin-Rvs167 (BAR) domain-containing superfamily of proteins contain a highly conserved protein dimerisation domain and are capable of shaping membranes by sensing membrane curvature [143]. The negatively charged inner surface of the plasma membrane allows for the binding of these positively charged domains, which bend the plasma membrane according to its protein structure. Members include the Fes-CIP4 homology (FCH)-BAR (F-BAR) domain-containing proteins such as CIP4, FBP17, Toca-1 and Protein kinase C and casein kinase substrate in neurons (PACSIN) [143, 144]. The PACSIN family of proteins are also known as syndapins and there are three mammalian PACSIN proteins. These are PACSIN1 which is neuron specific and implicated in synaptic vesicle recycling in the brain, PACSIN2 which is almost ubiquitously expressed, and PACSIN3 which is primarily expressed in lung and muscle tissues [145-148].

PACSINs are peripheral membrane proteins and consist of an N-terminal F-BAR domain with a Src homology 3 (SH3) domain at the C-terminus (Figure 1.3 A). Proteins containing F-BAR domains are involved in organising the membrane during clathrin-mediated endocytosis, while the SH3 domain has been shown to bind to dynamin [146, 149-152]. PACSINs have been implicated in dynamin-mediated endocytosis [147]. The F-BAR domain of PACSIN2 has an alpha-helical coiled-coil region that possesses a concave surface enriched in positively charged residues, allowing it to bind and shape membranes [153, 154]. The membrane bending activity of the F-BAR domain in PACSIN2 is regulated by autoinhibition by the SH3 domain [153, 154]. The SH3 domain acts as a molecular clamp and is only released when it binds to dynamin [155, 156]. PACSIN2 has been reported to associate with caveolae [30, 127]. Senju *et al.* show that the F-BAR domain of PACSIN2 directly interacts with caveolin1, although colocalisation was limited, and that it helps shape caveola plasma membrane [30]. In addition, Hansen *et al.* demonstrate that loss of PACSIN2 results in an accumulation of caveolin1 in the plasma membrane and a loss of morphologically defined caveolae, despite only partially colocalising with caveolin1 [127]. It seems that PACSIN2 plays an important role in helping to shape caveolae, however the exact step in which it is involved has yet to be determined.

With PACSIN2 being associated with dynamin, it is not surprising that dynamin2 is found to regulate caveolae endocytosis [31, 32]. Dynamin is a cytosolic GTPase and the founding member of the family of GTPases, dynamin-like proteins (DLPs), which have diverse roles in membrane remodelling, especially in the scission of endocytic membranes [157]. It has a G-domain at the N-terminus, followed by a stalk region, a pleckstrin homology (PH) domain, a GTPase effector domain (GED) and a Pro-rich domain (PRD) at the C-terminus (Figure 1.3 B) [158, 159]. Dynamin's GTPase activity is located in its G domain, and is key for clathrin-mediated endocytosis [160-163]. During endocytosis, dynamin assembles into a helical polymer at the neck of budding vesicles. Upon GTP hydrolysis, the G domains of the dynamin helix dimerise and conformational changes occur resulting in the scission of budding vesicles, thus producing a free endocytic vesicle [164-167]. In mammals, there are three dynamin genes encoding for three proteins, *dynamin1*, *dynamin2* and *dynamin3* [159]. They share the same domain organisation and 80% homology, however, they have very

different expression patterns. Dynamin1 is neuronal specific, dynamin2 is ubiquitously expressed and dynamin3 is found mostly in the brain and testis [159, 168-171]. Dynamin2 has been localised to the neck of caveolae, binding to caveolin1 through its PRD and it has been indicated to function at caveolae when it binds to the SH3 domain of PACSIN2 [155, 156, 172]. It appears that PACSIN2 aids in the formation of caveolar bulbs, while dynamin2 aids in the scission of caveolar vesicles, and that perhaps these two proteins work in conjunction with each other [30-32, 127]. Having said that, both proteins have been shown to bind to caveolin1 directly, and both proteins only show partial colocalisation with caveolin1 [30-32, 172]. It is quite possible that caveolin1 recruits these proteins only when they are required, and that PACSIN2 and dynamin2 only work in concert when either is already present at caveolae.

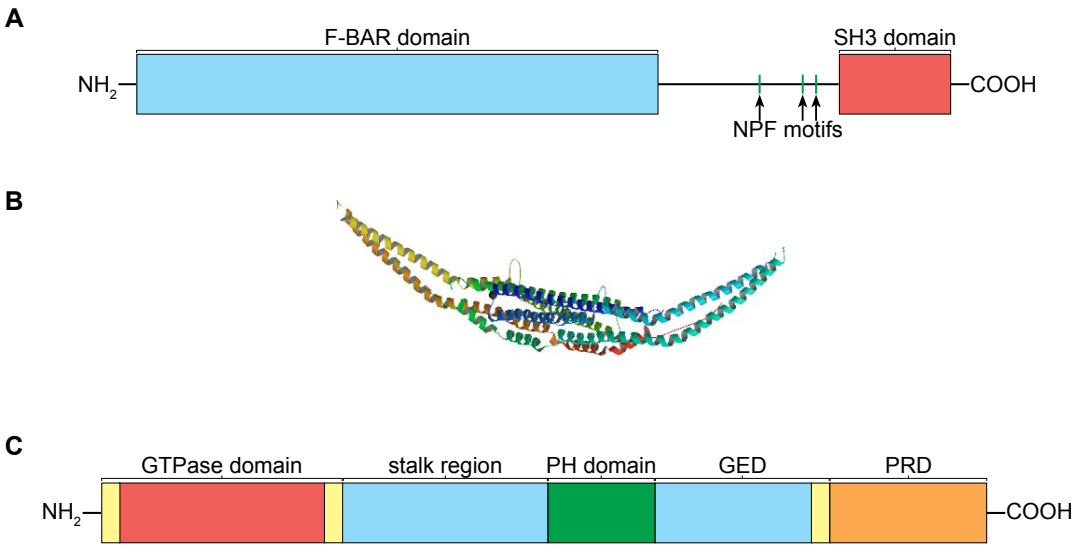

Figure 1.3 Schematic representations of PACSIN2 and dynamin2
A. Schematic representation of PACSIN2 domain organisation containing an F-BAR domain, three NPF motifs, followed by an SH3 domain. **B.** Crystal structure of human PACSIN2 F-BAR domain [173]. **C.** Schematic representation of dynamin2 domain organisation, with the G domain contained within the GTPase domain.

Another protein that has been associated with caveolae is the dynamin-like ATPase EHD2, which has also been localised to the necks of caveolae but in the case of

EHD2, almost perfect colocalisation is observed [33, 127]. EHD proteins and the role they have in caveolar biology are discussed below.

1.5 Role of EHD proteins in caveolae

1.5.1 EHD proteins structure and function

Eps15 homology domain (EHD) proteins are dynamin-related ATPases that associate with membranes and are involved in regulating various steps during intracellular membrane trafficking [174]. There are four mammalian EHD proteins, EHD1-4, and they share 70%-86% amino acid sequence homology (Figure 1.4 A and B). Despite their high level of sequence identity, EHD proteins have been found to have different localisations and functions. They are expressed in most tissues with EHD1, 2 and 4 highly expressed in lung, heart and spleen and EHD3 highly expressed in kidney and brain [175]. All EHD proteins are seen to be located in vesicular structures and only endogenous EHD1 and EHD4 have been observed to localise to tubular structures as well [176, 177]. These structures are likely to be endocytic compartments associated with the recycling functions of EHD proteins. However, whether EHD1 and EHD4 tubulate membranes or bind to pre-existing tubular membranes is unclear. Although the crystal structure has only been solved for EHD2, the high sequence homology between the EHD proteins suggest that all four EHD proteins are composed of an N-terminal ATP-binding dynamin-like G-domain, a central helical domain followed by a linker region, and a C-terminal Eps15 homology (EH) domain (Figure 1.4 C) [178]. The EH domain is a specialised protein-interaction module that binds tightly to the tripeptide asparagine-proline-phenylalanine (NPF) found in proteins involved in endocytosis [179, 180]. While EH domains are normally found at the N-terminal and generally have a negatively charged surface area, the EH domain of EHD proteins are at the C-terminal and has a positively charged surface [181]. EHD interaction partners, such as PACSIN2, contain NPF residues followed by at least two acidic residues, indicating that they selectively bind to certain NPF-containing proteins [182-184]. Dimerisation of EHD proteins occurs via a highly conserved and hydrophobic interface of the G-domain [178].

A

		sequence identity
EHD1	EHD2	71%
EHD1	EHD3	86%
EHD1	EHD4	75%
EHD2	EHD3	71%
EHD2	EHD4	68%
EHD3	EHD4	75%

B

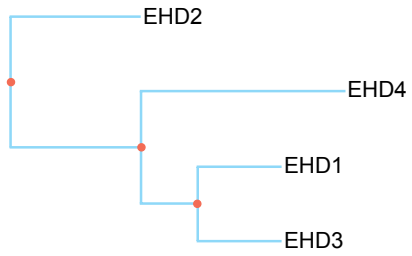

C

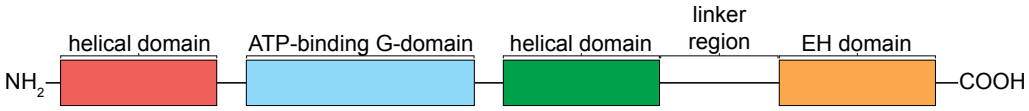

D

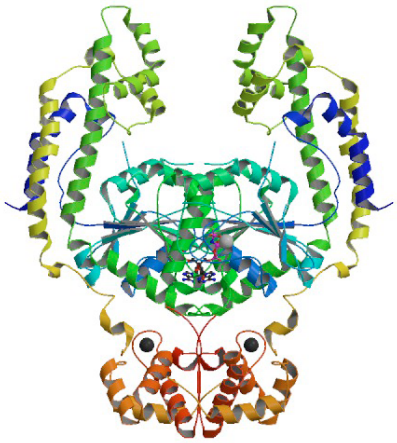

Figure 1.4 EHD proteins structure and homology

A. Sequence identity between each EHD protein ranging from 68% to 75%. **B.** Sequence homology between EHD proteins. **C.** Schematic representation of EHD proteins domain organisation with a helical domain at the N-terminus, followed by an ATP-binding G-domain, another helical domain, then a linker region and finally an EH domain at the C-terminus. **D.** Crystal structure of mouse EHD2 [178].

The EHD1 amino acid sequence is most similar to that of EHD3 and has the highest level of sequence homology to the single EHD ortholog expressed in invertebrate organisms. The *C. elegans* ortholog of EHD1 (Rme-1) was shown to control the recycling of internalised receptors from endocytic recycling compartments (ERCs) to the plasma membrane [185]. Mice lacking EHD1 are still viable and display relatively minor phenotypes, however, there is a delay in transferrin recycling to the plasma membrane in isolated embryonic fibroblasts and EHD1 appears to be essential for

spermatogenesis in mice [186, 187]. EHD1 has been demonstrated to regulate the recycling of a broad range of receptors, including the transferrin receptor, the GLUT4 glucose transporter, major histocompatibility complex (MHC) class I proteins and MHC class II molecules [176, 188-190]. It does so by promoting ERC to plasma membrane recycling, as seen by studies investigating transferrin receptor recycling [175, 188, 191].

EHD2 is the most distant in sequence homology to the other EHD proteins and as well as being implicated in ERC to plasma membrane recycling, EHD2 is the only EHD protein that has been conclusively localised to caveolae [33, 34, 127, 175]. Structural insights into EHD2 showed that EHD2 oligomers *in vitro* adopted ring structures with varying diameters that matched the distinct size of caveolae [178]. Knockdown of *EHD2* with small interfering RNA (siRNA) resulted in accumulation of transferrin in the perinuclear region, indicating a role of EHD2 in ERC to plasma membrane recycling [175]. EHD2 is unique amongst the EHD proteins in that it also has a nuclear localisation signal and potentially regulates transcription within the nucleus [192]. In addition, EHD2 appears to form primarily homo-oligomers whereas the other EHD proteins have been shown to hetero-oligomerise [177, 193, 194]. An examination by Hoernke *et al*. extended further studies of EHD2 structure, and showed that when ATP binds to the EHD2 dimer, it is released from an autoinhibited state to an open-conformation allowing EHD2 membrane insertion and oligomerisation [178, 195]. After ATP hydrolysis, EHD2 oligomers are disassembled and released, destabilising the membrane [178, 195].

Although EHD3 shares the highest level of sequence identity with EHD1, its expression is more variable [175]. Though unlike EHD1, EHD3 appears to regulate transport from early endosome (EEs) to ERCs as evident by studies using knockdown of EHD3 [175, 196]. It has also been implicated in EE to Golgi retrograde transport [197]. Additionally, EHD3 depletion has been shown to affect the expression and function of the sodium/calcium exchanger through its interaction with ankyrin-B [198]. EHD1 and EHD3 have been shown to cooperate with each other, for example in vesicle trafficking steps critical for early events in the establishment of primary cilium [199-201]. The lack of severe effects in *Ehd1* knockout mice may indicate functional redundancy of EHD1 with EHD3.

EHD4 has been suggested to regulate receptor transport from EEs to ERCs and from EEs to the lysosomal degradation pathway [175, 177]. It has been shown to hetero-oligomerise with EHD1, though it is localised to a subset of EEs and implicated to function upstream of EHD1 [175, 177]. Oligomerisation of EHD4 with EHD1 allows its cooperation in controlling NgCAM endocytosis [202]. Studies have shown a role for EHD4 in neuronal cells however no profound neurological phenotypes have been reported in *Ehd4* knockout mice [203-205]. *Ehd4* knockout mice display similar phenotypes to *Ehd1* knockout mice, in that mice lacking EHD4 display defects in pre-pubertal testis size and mice lacking EHD1 exhibit defects in spermatogenesis and male fertility [187, 206]. The mild phenotypes in conjunction with lack of neurological ones, again suggest a possible functional overlap between the EHD proteins.

1.5.2 EHD proteins and caveolae

EHD2 was first associated with caveolae in a study conducted by Aboulaich *et al*., where they conducted proteomic analysis on biochemically-isolated caveolae from purified human adipocyte plasma membrane [207]. Subsequently, Hansen *et al*. confirmed the recruitment of EHD2 to caveolae, and also showed that EHD2 is found in caveolae by electron microscopy [127]. However, EHD2 siRNA experiments did not reveal any coherent phenotypes, which may have been due to residual EHD2 expression [127]. EHD2 has been shown to be an ATPase involved in membrane remodelling, and this is indeed the role of EHD2 with regards to caveolae [33, 34, 178]. A study conducted by Morén *et al*. demonstrated that EHD2, but not other EHD proteins, specifically and stably associates with caveolae in an ATP-dependent manner [34]. They showed that EHD2 interacts with cavin1 and PACSIN2, and that binding of one EHD2 dimer to one molecule of PACSIN2 is mediated by the EH domain of EHD2 and NPF motifs in PACSIN2 [34]. Limited PACSIN2 colocalisation with caveolin1 and EHD2 was observed, as previously demonstrated [34, 127]. EHD2 has also been reported to bind actin but the relevance of this remains unclear [33]. Depletion of *EHD2* with siRNA showed that caveolae could form independently of EHD2, and that the oligomeric state of caveolae and caveolin1 were not disrupted, indicating that EHD2 is not essential for the formation of caveolae [33, 34]. Later studies show that EHD2 is in the neck region of caveolae distinct from the bulb [122, 142]. Knockdown of *EHD2* also resulted in increased dynamics of plasma membrane

caveolin1, and expression of a dominant-negative mutant of dynamin2 decreased the movement of caveolae [33, 34]. This led to the interpretation that EHD2 acts to stabilise caveolae at the plasma membrane, positing the role of EHD2 as the opposite of dynamin2.

Taken together, the current model of EHD2 function at caveolae presents itself thus far as: ATP binding to EHD2 dimers allow for its membrane binding and oligomerisation. EHD2 oligomers associate with static plasma membrane caveolae to control membrane curvature and stabilise caveolae in an ATPase activity-dependent manner. EHD2 undergoes continuous cycles of association and dissociation, and with the slow hydrolysis rate of EHD2, as compared to dynamin, it may allow for the slow and tightly controlled dynamics of caveolae [33, 34, 178]. However, the exact mechanism in which EHD2 is recruited to caveolae or the way in which EHD2 activity is involved in caveolae budding is unknown. EHD2 was diffusely distributed in the cytosol and plasma membrane of mouse embryonic fibroblasts (MEFs) lacking caveolin1. Expression of *caveolin1* in these cells was sufficient to restore the punctate distribution of EHD2 indicating that caveolin1 or caveolae somehow recruit EHD2 [33]. It may be triggered by membrane curvature of caveolae or influenced by lipid composition of the caveolar membrane.

The only evidence of other EHD proteins being associated with caveolae is from a study by Stoeber *et al*. where they observed partial colocalisation of EHD4 with caveolin1 [33]. It should be noted that overexpressed fluorescently tagged EHD1, EHD3 and EHD4 were used, and analogous with the atypical effects noted in caveolin1 overexpression, the observations made about overexpressed EHD colocalisation to caveolin1 may not reflect the endogenous situation.

1.5.3 Reason for study

The goal of this study was to elucidate the functions of EHD proteins in relation to caveolae. Firstly, do other EHD proteins associate with caveolae, other than EHD2? Secondly, what is the role of EHD proteins in the generation of caveolae? And finally, is the mechanoprotective role of caveolae compromised when cells lack EHD proteins? The laboratory has employed genome-editing techniques to produce NIH 3T3 cell lines expressing GFP-tagged caveolin1 and mCherry-tagged cavin1 from the

endogenous loci [21]. More recently the laboratory used CRISPR/Cas9 to generate NIH 3T3 cells where mutations in *EHD2* led to the loss of EHD2 protein expression [208]. There was no loss of morphologically defined caveolae in these cells compared to wildtype NIH 3T3 cells, consistent with previous studies using siRNA to deplete EHD2 (Figure 1.5 A) [33, 34]. However, unlike prior studies, FRAP analysis to assess the dynamics of caveolae in endogenously tagged caveolin1-GFP *EHD2* knockout cells did not reveal any altered mobility of caveolae (Figure 1.5 B) [208]. In these earlier studies, fluorescently tagged caveolin1 was either overexpressed or stably expressed and EHD2 depletion was induced by siRNA [33, 34]. The discrepancy seen in caveolar dynamics in the absence of EHD2 may be attributed to artefacts generated by the overexpression of caveolin1 [20]. The difference may also be due to the acute effects of siRNA knockdown compared to genome-edited cells. The short period in which siRNA induces EHD2 depletion may not allow enough time for the cell to respond, especially seeing the slow turnover of caveolae [25], whereas in genome-editing, cells have time to recover and compensate. Further to the lack of effects in caveolar dynamics, the subcellular localisation of caveolin1 did not change in *EHD2* knockout cells (Figure 1.5 C) [208]. Endocytic compartments were specifically labelled and the proportion of endogenously GFP-tagged caveolin1 colocalising to them was the same in both wildtype and *EHD2* knockout NIH 3T3 cells. The lack of clear effects on caveolar abundance, dynamics and sub-cellular distribution in *EHD2* knockout cells contrasts with the increased dynamics and internalisation observed in cells depleted of EHD2 using siRNA [33, 34]. Some variable and limited colocalisation has been observed between overexpressed and tagged EHD1, EHD3, or EHD4 and caveolar markers [33]. Owing to the fact that EHD proteins can associate with each other and perform similar functions, this study set out to elucidate the roles of other EHD proteins in caveolar biology [175, 187, 199-201, 206].

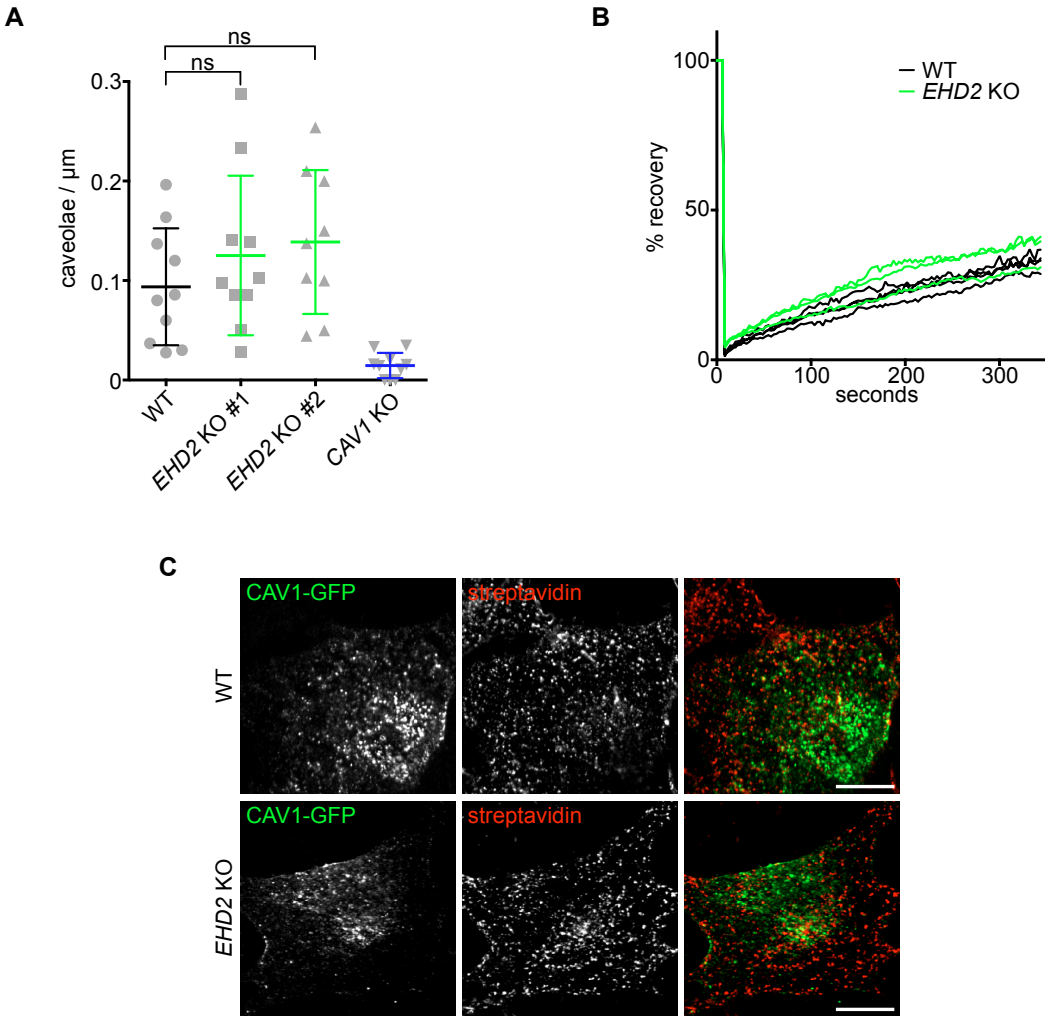

Figure 1.5 Reason for study

A. Quantification of morphologically-defined caveolae in knockout cells. For each genotype / clone complete reconstructions of the perimeter of 10 cells were generated from 15-70 high resolution micrographs per cell. Two different clones of *EHD2* knockout cells were analysed. One-way ANOVA with Dunnett's multiple comparison test, not significant. **B.** Fluorescence recovery after photobleaching of caveolin1-GFP in wildtype NIH 3T3 cells and three different *EHD2* knockout clones. Each line is a mean from >7 individual photobleached regions. **C.** Internalisation assay to reveal intracellular caveolin1-GFP. Biotinylation of all surface proteins with sulfo-NHS-SS-biotin was followed by MESNA treatment to remove non-internalised biotin moieties and streptavidin-labelling to reveal endocytic compartments. Internalisation was for 15 minutes.

Note: all figures are adapted from [208].

1.6 Caveolae in adipocytes

1.6.1 Role of caveolae in adipocytes

With caveolae covering approximately 50% of the plasma membrane surface area in adipocytes, and striking adipocyte-related phenotypes observed in mice lacking caveolae, it is no surprise that caveolae have been linked to a range of functions with regards to the adipocyte [12, 52, 63, 64, 69]. Mice and humans lacking caveolae are insulin resistant, and display marked lipodystrophy and hypertriglyceridaemia, most likely due to deregulations of adipose tissue [63, 209-211]. Adipose depots from *cavin1* knockout mice are reduced compared to wildtype mice [69]. In addition, adipocytes are smaller in size, adipose tissue is fibrotic and infiltrated with macrophages, indicating that the tissue has been damaged [69]. However, it is not clear whether reduced adipose depots are due to the smaller adipocyte size or whether it is due to decreased absolute numbers of adipocytes in adipose tissue. It is also unclear if the phenotypes observed are due to caveolae components themselves, as slight differences are seen between *cavin1* and *caveolin1* knockouts, or if they are due to the caveolar bulb as a whole. Evidence has linked caveolae to various adipocyte-associated roles including insulin signalling and fatty acid transport, though there is also data challenging these claims [45, 59, 60, 76, 77, 212, 213].

1.6.2 Insulin receptor and CD36 association to adipocyte caveolae

The insulin receptor has been suggested as a potential cargo for caveolar endocytosis, and caveolae suggested to act as a platform for insulin receptor signalling [44-46]. The insulin receptor has also been shown to colocalise with caveolae, however conflicting data contradicts this and undermines the link between caveolae and insulin signalling [45, 213-215]. An initial study by Mastick *et al*. postulated that insulin stimulates the tyrosine phosphorylation of caveolin, although they did not provide sufficient evidence of the insulin receptor localising to caveolae [216]. Then in 1999, Gustavsson *et al*. were the first to show the insulin receptor localising to caveolae of adipocytes [45]. Immunogold electron and immunofluorescence microscopy were employed to visualise insulin receptor localising to caveolae and colocalisation of insulin receptor with caveolin1 respectively. A following study proposed that the insulin receptor actually catalyses the tyrosine phosphorylation of caveolin1 [217].

However, subsequent studies question the link between the insulin receptor and signalling from caveolae [213, 215]. Using immunogold electron microscopy, Souto *et al*. did not find the insulin receptor localising to caveolae [213]. Moreover, the insulin receptor was not present in immunopurified adipocyte caveolae [213]. A subsequent study expressed varying amounts of caveolin1 in a cell line where endogenous caveolin1 expression is very low [215]. They found that the levels of insulin receptor present in the cells expressing varying amounts of caveolin1 were comparable to the levels in the parental line. Likewise, to assess insulin signalling, insulin-dependent receptor autophosphorylation and IRS1 were measured, and again the levels in the caveolin1-expressing cell lines were comparable to that of the parental line [215]. To add to the discord, in a different study, the insulin receptor was shown to associate with the neck of caveolae in electron micrographs [214]. The phenotypes observed when caveolae are absent supports an association of caveolae with the insulin receptor, however, a lack of consensus still exists, and the idea of caveolae being important for insulin signalling has possibly lead to undue bias in the literature [44, 45, 77, 86, 213-219].

Insulin resistance and impaired insulin signalling have been shown to be induced by fatty acids [220, 221]. Mice lacking caveolae have smaller adipocytes, with an elevation in free fatty acid and triglyceride levels, which can act as mild detergents and be toxic to cells [60, 63, 222]. It may be that elevated fatty acid and triglyceride levels due to impaired transport are influencing the insulin resistant phenotype observed in animals lacking caveolae, rather than the association of insulin receptor with caveolae. Triglycerides derived from dietary intake are lipolysed and fatty acids taken up by adipocytes, the main energy storage site in the body, and are stored as triglycerides until the body requires energy and is released as fatty acids. However, the exact mechanism by which fatty acids cross the plasma membrane is still in debate. A number of membrane proteins have been described to be involved in fatty acid transport, these include fatty acid transport proteins (FATPs), CD36 and caveolin1 [54, 59, 223-226]. Additionally, transmembrane fatty acid movement has been shown to occur without the participation of proteins by simple passive diffusion, although there is evidence disputing this [227-230]. FATPs are acyl CoA ligases that convert fatty acids to fatty acyl CoA derivatives and their activity may drive transmembrane movement by creating an inward gradient for fatty acid diffusion

[231-233]. CD36, also known as fatty acid translocase, is an integral membrane protein that belongs to the class B scavenger receptor family of cell surface proteins and is expressed in tissues including adipose tissue. Mice lacking CD36 have a significant decrease in fatty acid uptake in adipose tissue, a similar phenotype to that of humans lacking CD36, indicating the importance of CD36 in fatty acid movement [226, 234, 235]. Plasma membrane CD36 is preferentially localised to detergent resistant membranes (DRMs) and its positioning there is crucial to its function [58, 236]. Disruption of the DRM structure by cholesterol depletion results in a decrease in fatty acid uptake, although this does not indicate whether is it directly caused by CD36 or by the general disruption of membranes [58, 236]. A study by Ring *et al*. suggested that caveolin1 is required for CD36 localisation and function at the plasma membrane [237]. Caveolin1 is a key component of DRMs and has been shown to be a fatty acid binding protein [54]. In addition, it was demonstrated to play a role in transmembrane fatty acid movement, even in the absence of CD36 and other fatty acid transport proteins [59]. It should be noted that caveolar bulbs were not observed in that study, thus effects of caveolin1 may have been solely due to its ability to form DRMs rather than its involvement in caveolar bulbs [59]. Taken together the data implies that the presence and integrity of DRMs is essential for fatty acid transport across the membrane. As suggested, caveolin1 may influence fatty acid uptake by regulating surface availability of CD36 [59, 237]. The exacts mechanism by which fatty acid transport occurs is still open to question, however multiple lines of evidence show that caveolin1, DRMs and CD36 play a pivotal role in this.

1.6.3 Reason for study

The goal of this study was to shed light onto the role of caveolae in adipocytes. More specifically, do proteins such as the insulin receptor and CD36 directly colocalise with caveolae, and if so, what are their roles in relation to caveolae? Furthermore, do caveolae have a mechanoprotective role in adipocytes, as reported in other cell types? It is evident that caveolae play a role in adipocytes from the striking phenotypes observed in mice and humans lacking caveolae [63, 209-211]. It would seem that the insulin receptor is involved as studies have linked it to caveolae and insulin resistance is a phenotype detected [45, 214, 217]. However, there is also evidence in the literature that contradicts this, dissociating caveolae from the insulin receptor and signalling [213, 215]. As the understanding of caveolar biology progresses and the

development of new techniques become available, it is apparent that the opposing results may have arisen from artefacts of the dated methods employed to exam caveolae. To add to the uncertainty, fatty acids have been shown to induce insulin resistance and impaired insulin signalling, implying that perhaps the insulin resistant phenotype observed is merely due to increased free fatty acid levels as it is another phenotype noted [220, 221]. A range of studies have linked fatty acid uptake to caveolae, though the exact mechanisms by which caveolae aid in the uptake of fatty acids in unclear [54, 59, 225, 226, 237]. It could be that it acts as a scaffold for proteins such as the fatty acid translocase CD36, although caveolin1 itself has been shown to participate in fatty acid movement in the absence of CD36 [59, 237]. In addition, there is evidence that transmembrane fatty acid movement can occur by passive diffusion without, and with, the participation of other proteins [227-230, 238].

It is clear that there does not seem to be an agreed consensus on the contributions of adipocyte caveolae to the phenotypes. Therefore, it would be key to employ new techniques such as super-resolution microscopy to understand the relationships between caveolae and the insulin receptor and CD36. Not only that, but it should not be discounted that a role of caveolae in adipocytes may be to act as a membrane buffer to mechanical forces as it has been seen to do so in other cell types [98, 101, 102]. It is plausible that in order for adipocytes to accommodate the levels of fatty acid it uptakes, caveolae are required to provide more membrane surface area for when the cell needs to expand due to the uptake. It suggests that without caveolae, the cells cannot expand and are hence small, and will most likely rupture releasing its fatty acid content. This correlates well with the small adipocyte size and macrophage-infiltrated and fibrotic environment of adipose tissue devoid of caveolae as in addition to the damaged cells, fatty acids can act as detergents, damaging the cells further [239, 240]. An inability to store lipids lead to hyperlipidaemia, and an imbalance in lipid uptake and lipolysis contributes to a lipodystrophic and insulin-resistant phenotype [69]. Adipocytes contain large fat reservoirs and are inherently fragile due their thin layer of cytoplasm and small network of cytoskeletal proteins. Thus, adipocytes are more prone to cell damage, which leads to the release of free fatty acids, triggering macrophage infiltration in response to the damage inflicted [60, 222, 241]. It would therefore be of great value to assess the mechanoprotective roles of

caveolae in adipocytes, in addition to reassessing the relationship between the insulin receptor and CD36 with respect to adipocyte caveolae.

1.7 Genome editing

Genome editing employs the use of programmable sequence-specific endonucleases to enable the precise editing of endogenous genomic loci. It allows for DNA to be inserted, deleted or replaced, therefore enabling the tagging of specific genes with fluorescent protein tags, or the deletion of them. Systems used to apply genome editing include zinc-finger nucleases (ZFNs), transcription activator-like effector nucleases (TALENs) and the clustered regularly interspaced palindromic repeat (CRISPR)-Cas9 nuclease system [242-245]. These methods work by inducing double-stranded breaks (DSBs) at targeted genomic locations. Upon cleavage the targeted breaks undergo DNA damage repair via the high-fidelity homology-directed repair (HDR) or the error-prone non-homologous end joining (NHEJ). In HDR, a homology sequence is used as a template to repair the DSB. Although it occurs at a lower and more variable rate than NHEJ, this can be exploited to produce exact modifications to the target locus. The exogenously-introduced repair template contains homology arms that flank an insertion sequence, such as a fluorescent protein sequence, so that when the DSB is repaired by HDR, the desired sequence is inserted into the genome. In this way, genes of interest can be endogenously-tagged with fluorescent proteins, or other markers. However, in the absence of a repair template, DSBs are repaired via the NHEJ pathway. It uses a variety of enzymes to directly ligate the DSB which leads to the formation of insertion or deletion mutations. This can be utilised to mediate gene knockouts as errors in the coding exon can lead to frameshift mutations and premature stop codons. A combination of multiple DNA targets can be used to remove different sections of DNA, creating multiple gene knockouts.

ZFN and TALEN nuclease activity cuts DNA non-specifically and require the tethering of endonuclease catalytic domains to modular DNA-binding proteins in order to induce targeted DSBs. They are linked to peptides which recognise specific DNA sequences such as zinc fingers for ZFNs and transcription activator-like effectors for TALENs. ZFNs contain a zinc finger DNA-binding domain, which can

be designed to target specific DNA sequences, and a DNA-cleavage domain which executes the DSBs [246]. The DNA-binding domain of ZFNs usually contain three to six individual zinc finger repeats recognising between 9 and 18 base pairs, however it depends on the surroundings of the zinc finger and the repeats can overlap [246]. TALENs are similar to ZFNs in that they also contain a binding domain, the transcription activator-like effector DNA-binding domain, that can also be modified to target precise sequences of DNA, and a DNA-cleavage domain [247]. The DNA-binding domain of TALENs contain a repeat of highly conserved amino acids, with two highly variable residues that aid in specific nucleotide recognition. By selecting a combination of repeat segments containing the appropriate two residues, TALENs can be used to specifically target the genome [247].

Unlike ZFNs and TALENs, CRISPR-Cas9 cuts DNA specifically through base pairing with the target DNA [248-250]. It originated from the microbial adaptive immune system CRISPR-Cas. CRISPR is a family of viral DNA sequence fragments found in bacteria. They are sequences from viruses that have attacked the bacterium and the bacterium utilises this to protect itself by recognising and destroying its target. RNA containing the guide target sequence recognises the DNA target and guides the Cas nuclease to cut the exogenous DNA. The target DNA is immediately preceded by a protospacer adjacent motif (PAM) which varies between different CRISPR systems. For example, in *Streptococcus pyogenes* Type II CRISPR system a 5'-NGG PAM sequence must immediately follow the target DNA sequence. The Type II CRISPR system consists of the Cas9 endonuclease, the CRISPR RNA (crRNA) array that encodes the guide RNAs and the trans-activating CRISPR RNA (tracrRNA) that aids in the processing of the crRNA array [249, 250]. The targeting of Cas9 with a 20-nucleotide guide RNA is the basis on which the CRISPR-Cas9 technology has developed. The *S. pyogenes* CRISPR-Cas9 has been modified into a more practical system by fusing the crRNA and tracrRNA together to create a chimeric single-guide RNA. The Cas9 nuclease exerts its DNA cleaving activity through its conserved RuvC and HNH nuclease domains. Mutating the RuvC catalytic domain at an exact position (D10A) allows the Cas9 to nick the DNA creating a single-stranded break rather than a DSB.

As displayed by the artefactual effects of caveolin1 overexpression, it is key to examine caveolar biology with endogenous levels of the proteins involved. *S. pyogenes* CRISPR-Cas9 is used in this study to generate cell lines that encode endogenously fluorescent-tagged proteins, and gene knockout cell lines as it has several advantages over ZFNs and TALENs. Firstly, Cas9 is easier to customise than ZFNs or TALENs as it only involves generating short RNA sequences to convey specificity rather than creating custom proteins for each targeted DNA sequence. Secondly, Cas9 cuts specifically 3 base pairs upstream from the PAM meaning that the exact site of DSB is known when designing. ZFNs and TALENs cleave DNA non-specifically with the FokI restriction endonuclease. And finally, Cas9 can be used to target several genomic loci simultaneously by the use of multiple guide RNAs. A description of the generation of the cell lines used is detailed below in Materials and Methods.

Chapter 2: Materials and Methods

2.1 Antibodies and reagents

The following antibodies were used: rabbit anti-cavin1 (Abcam ab48824), rabbit anti-caveolin1 (BD Biosciences 610060), mouse anti-GFP (Roche 11814460001), rabbit anti-RFP (to detect for mCherry, MBL PM005), mouse anti-tubulin (Sigma T9026), goat anti-EHD2 (Abcam ab23935), rabbit anti-EHD1 (Abcam ab109311), rabbit anti-EHD4 (Proteintech 11382-2-AP), mouse anti-CD36 (Abcam ab23680), mouse anti-insulin receptor (kind gift from K. Siddle, MRL) and rabbit anti-FABP4 (Abcam ab66682). HRP-conjugated secondary antibodies were from DAKO and fluorophore-conjugated antibodies and streptavidin were from Molecular Probes (Invitrogen).

2.2 Cell culture

NIH 3T3 cells (kind gift from McMahon lab, MRC-LMB) were grown in DMEM (Gibco) supplemented with penicillin and streptomycin and 10% calf serum (Gibco).

Primary pre-adipocytes were isolated from gonadal adipose tissue from 6-8 week old mice and grown in DMEM supplemented with penicillin and streptomycin, 10% neonatal calf serum (Gibco), 1% L-Glutamine (Gibco), 2.4 nM insulin (Sigma) and 150 μM sodium ascorbate (Sigma). Tissues were minced finely, digested with collagenase type 2 (Sigma) in Hanks BSS (Gibco) and 7.5% w/v BSA (Sigma) at 37°C for 40 minutes, filtered through a 100 μm mesh and incubated on ice for 20 minutes. The upper white fat layer was removed and equal volumes of growth media was added to the cells. Cells were centrifuged at 700 *g* for 10 minutes, washed in media, and plated into appropriate vessels. The medium was changed every day for the first three days, then every two days after that and experiments performed nine days after initial culture.

2.3 Animals and *in vivo* experiments

All experiments using mice were conducted under the appropriate UK Home Office license, and were approved by the Ethical Review Committee of the Medical Research Council, Laboratory of Molecular Biology. *Caveolin1* knockout mice have the first two exons of the *caveolin1* gene deleted [251].

For the *in vivo* stretching of mice, mice aged approximately 20 weeks old were intravenously injected with propidium iodide and FITC-albumin to visualise broken cells and blood vessels respectively. The mice were then anaesthetised, abdominal hairs removed and the mouse placed on a mechanical agitator heated to 37°C (Figure 2.1). Mice were agitated across the abdomen for 20 minutes before dislocation of the neck and exsanguination. Subcutaneous fat was removed, submerged in PBS and imaged using a 20x W Plan-Apochromat 1.2 NA water immersion objective on a Zeiss 710 NLO upright microscope.

For the high fat diet mice, weaned mice at approximately 3 weeks old were placed on a high fat diet (60% kcal in fat, Research Diets D12492-1.5Vi) until 20 weeks of age.

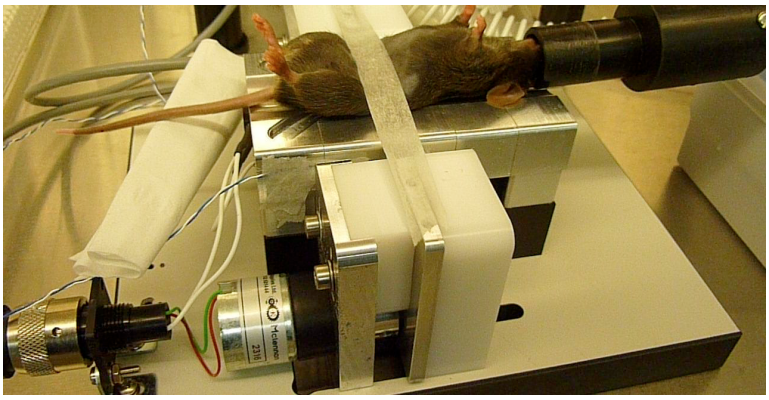

Figure 2.1 Set up for *in vivo* mice subcutaneous fat agitation
Mouse was placed on the agitator with the abdomen exposed and nose inserted into a nose cone for anaesthesia. Tape was stuck tightly across the abdomen for agitation.

2.4 DNA constructs and transient transfections

Different combinations of mCherry-EHD1, mCherry-EHD2, mCherry-EHD3, mCherry-EHD4, GFP-EHD2 (kind gift from the McMahon lab, MRC-LMB), GFP empty, and Mito-V5-APEX (kind gift from the Munro lab, MRC-LMB (Addgene plasmid #42607)) plasmids were singly or co- transiently transfected into the appropriate cells using the Neon transfection system (Invitrogen) or Fugene reagent

according to manufacturers instructions (Promega). Cells were cultured for 20-24 hours and experiments conducted after.

2.5 Genome editing

NIH 3T3 cell lines expressing caveolin1-GFP or cavin1-mCherry tagged from endogenous loci were generated previously [21]. GFP-tagged EHD2 and *EHD2* knockout cell lines were previously made in the laboratory [208]. For the tagging or deletion of endogenous EHD1, EHD3 and EHD4 proteins, Cas9 was used as described in [242]. For each cleavage site, two potential guide RNA sequence were designed using the Feng Zhang lab software at http://crispr.mit.edu/ and the chosen nucleotide sequences were used for insertion into pSpCas9(BB)-2A-GFP (PX458) or pSpCas9(BB)-2A-Puro (PX459), gifts from Feng Zhang (Addgene plasmid #48138 and #48139).

Donor DNA constructs containing flanking regions for gap repair by homologous recombination and the appropriate fluorescent protein DNA were produced as follows. Approximately 1 kb of genomic DNA sequence on either side of the *EHD1*, *EHD3* and *EHD4* stop codons were amplified from genomic DNA using primers listed in Table 1. DNAs coding for GFP or mCherry originated from pEGFP-N1 or pCherry-N1 (Clontech) respectively, were amplified using the primers listed in Table 1. In donor constructs, the stop codons of *EHD1*, *EHD3* or *EHD4* genes were deleted and the cDNA of fluorescent protein was fused with a linker as described in [252] and inserted into pBlueScript SK (-)- using Gibson Master kit assembly (New England BioLabs) according to manufacturer's instructions.

Primer name	Sequence	Gene	Goal
EHD1 cleavage C-term pair	CACCGAAGTCACTCGTGCCTCCGTT AAACAACGGAGGCACGAGTGACTTC	EHD1	Knock-in
EHD4 cleavage C-term pair	CACCGTGGGCCCTCAGTCAGCCTT AAACAAGGCTGACTGAGGGCCCAC	EHD4	Knock-in
EHD3 cleavage C-term pair	CACCGACCTCCTCCCTCCATCTAAG AAACTTAGATGGAGGGAGGAGGTC	EHD3	Knock-in
Left arm for	AGGGGTTCCGCGCACATTTCCCCTCGAGTGGTGAACA ACCTGGGAGAG	EHD1	Knock-in
Left arm rev	CGGGCCCGCGGTACCGTCGACTGCAGAATTCTCGTGC CTCCGTTTGGAG	EHD1	Knock-in
Right arm for	TCTCGGCATGGACGAGCTGTACAAGTAACTTCCATGC CTGAGATACCC	EHD1	Knock-in
Right arm rev	GATAACCGTATTACCGCCATGGCGGCCGCCAGGTCAC AGGGCCTACTG	EHD1	Knock-in
Left arm for	ATAGGGGTTCCGCGCACATTTCCCCTCGAGAGCAGAT GTGGCCCCTCG	EHD4	Knock-in
Left arm rev	CGGGCCCGCGGTACCGTCGACTGCAGAATTGTCAGCC TTTGGCAGGGAC	EHD4	Knock-in
Right arm for	TCACTCTCGGCATGGACGAGCTGTACAAGTAAGGGCC CACAGCTGGGG	EHD4	Knock-in
Right arm rev	GATAACCGTATTACCGCCATGGCGGCCGCGCCCAGAT AGGCACTCCTG	EHD4	Knock-in
Left arm for	AGGGGTTCCGCGCACATTTCCCCTCGAGGTTGCCTTG GTTTCCCACCC	EHD3	Knock-in
Left arm rev	CGGGCCCGCGGTACCGTCGACTGCAGAATTTTCTGAT ACTTTCCTCTTAGATGG	EHD3	Knock-in
Right arm for	GGCGGCATGGACGAGCTGTACAAGTAGGAGAGCCAG GTAACCTCAGAC	EHD3	Knock-in
Right arm rev	ATAACCGTATTACCGCCATGGCGGCCGCTCACAGAAC TGGGACAGAGG	EHD3	Knock-in
GFP for	AATTCTGCAGTCGACGGTACCGCGGGCCCGATGGTGA GCAAGGGCGAGG	GFP (for EHD1 and 4)	Knock-in
GFP rev	TTACTTGTACAGCTCGTCCATG	GFP (for EHD1 and 4)	Knock-in
mCherry for	AATTCTGCAGTCGACGGTACCGCGGGCCCGATGGTGA GCAAGGGCGAGG	mCh (for EHD3)	Knock-in
mCherry rev	CTACTTGTACAGCTCGTCCATG	mCh (for EHD3)	Knock-in
EHD1 cleavage N-term pair1	CACCGCAAGGATGCCCGCCGCAAGA AAACTCTTGCGGCGGGCATCCTTGC	EHD1	Knockout
EHD1 cleavage N-term pair2	CACCGCATCCGCCACCTGATCGAGC AAACGCTCGATCAGGTGGCGGATGC	EHD1	Knockout
EHD4 cleavage N-term pair1	CACCGCTGGCGGGCGCGAGCGCTC AAACGAGCGCTCGCGCCCGCCAGC	EHD4	Knockout
EHD4 cleavage N-term pair2	CACCGCTGGTGGGCCAGTACAGCA AAACTGCTGTACTGGCCCACCAGC	EHD4	Knockout
EHD3 cleavage N-term pair1	CACCGTAACGATGATCGCCGCAAGA AAACTCTTGCGGCGATCATCGTTAC	EHD3	Knockout
EHD3 cleavage N-term pair2	CACCGTGGTCTTGCCGGTAGAGTAC AAACGTACTCTACCGGCAAGACCAC	EHD3	Knockout

Table 1. Primers used for genome editing

For generation of genome-edited NIH 3T3 cell lines with tagged proteins, PX459 plasmids with appropriate guiding RNA sequences and donor plasmids were co-transfected into cells using the Neon transfection system. After transfection, cells were cultured for 5 days to recover and express protein of interest, and sorted for relevant fluorescent signals using a Sony iCyt Synergy Dual Channel High Speed Cell Sorter or Beckman Coulter MoFlo High Speed Cell Sorter to obtain populations of positive cells.

For generation of genome-edited NIH 3T3 cell lines deleted of the protein of interest, PX458 plasmids with appropriate guiding RNA sequences were transfected into cells using the Neon transfection system and sorted for GFP-positive signal. For generation of cells deleted of two or three genes, cell were co-transfected with several PX458 plasmids simultaneously. Cell lines with gene knockouts were cloned and screened as individual clones. Correct gene targeting was determined by PCR and Western blotting.

2.6 Western blot

Samples were lysed in sample buffer (Novex) with 100 mM DTT, boiled for 10 minutes at 95°C and run on pre-cast 4-20% Tris-Glycine gels (Invitrogen). The gels were blotted using wet transfer (Bio-Rad) onto PVDF membranes (Millipore). The membranes were blocked in PBS containing 5% dried skimmed milk powder, incubated with the appropriate primary antibodies overnight at 4°C, washed in 0.1% PBS Tween 20 (National Diagnostics) and incubated with HRP-conjugated secondary antibodies. The blots were developed using Immobilon Western Chemiluminescent HRP Substrate (Millipore) or ECL Western Blot Detection Reagent Kit (GE Healthcare) onto Fuji Super RX X-ray films.

2.7 Immunoprecipitations

Cells were washed with ice-cold PBS and lysed with IP lysis buffer (50 mM Tris-HCl pH 7.4, 300 mM NaCl, 5 mM EDTA and 0.5 % (v/v) Triton X-100, supplemented with ‘cOmplete’ protease inhibitors (Roche)). The lysates were centrifuged at 50,000 rpm for 30 minutes at 4°C. The supernatants were pre-cleared for 1 hour at 4°C with agarose beads (Chromotek), then incubated with GFP-Trap agarose beads

(Chromotek) for 1 hour at 4°C. Proteins were eluted from the beads with sample buffer containing 100 mM DTT for 10 minutes at 95°C. Samples were subjected to Western blotting.

For pulse-chase samples, cells were washed with ice-cold PBS and lysed with IP lysis buffer (20 mM Tris-Hcl pH7.4, 100 mM NaCl, 5 mM EDTA, 1% Triton X-100 and 1% (w/v) octyl-glucoside, supplemented with protease inhibitors). The lysates were centrifuged at 20,000 *g* for 20 minutes at 4°C. The supernatants were pre-cleared for 1 hour at 4°C with Protein A Sepharose beads (GE Healthcare), then incubated with Protein A Sepharose beads and rabbit anti-caveolin1 antibody overnight at 4°C. Proteins were eluted from the beads with sample buffer plus 100 mM DTT for 10 minutes at 95°C.

2.8 Polymerase chain reaction (PCR)

Genomic DNA (gDNA) was extracted from cells using cell lysis and protein precipitation solution (Qiagen). The gDNA was PCR amplified using KOD Hot Start DNA Polymerase (Novagen) as per manufacturers instructions. Primers used for amplification are listed in Table 2. Amplified PCR products were ran on 1%-3% agarose gels.

Primer name	Sequence	Gene	Goal
EHD1 expression forward	CCAAGCTGCTGGATACAGTG	EHD1	EHD1 expression
EHD1 expression reverse	GAACACGGCTAGCAGGAAAC	EHD1	EHD1 expression
EHD3 expression forward	CACTGAAGAGCAAGCTGCTG	EHD3	EHD3 expression
EHD3 expression reverse	GTGCCCTATGGAGGTTTCTC	EHD3	EHD3 expression
EHD4 expression forward	CACTGAAGCCCAAGCTGATC	EHD4	EHD4 expression
EHD4 expression reverse	GGCAGAAACTCTCTGTTCTG	EHD4	EHD4 expression
EHD1 C-terminal forward	GTAGTTGGCAAGGACAAGCC	EHD1	Knock-in genotyping
EHD1 C-terminal reverse	ATCCAAGCATCACCCATGCC	EHD1	Knock-in genotyping
EHD3 C-terminal forward	GCGGGACAAGCCTATGTATG	EHD3	Knock-in genotyping
EHD3 C-terminal reverse	GGTGGGCCATCTGTGTTAAC	EHD3	Knock-in genotyping
EHD4 C-terminal forward	GTCGTGGCTAAAGACAAGCC	EHD4	Knock-in genotyping
EHD4 C-terminal reverse	TTCGACAGCCTGTGTCACAC	EHD4	Knock-in genotyping
EHD1 N-terminal forward	CCGTCCTGTAGCAGCCAG	EHD1	Knockout genotyping
EHD1 N-terminal reverse	CCGTGCATGACCGCGATG	EHD1	Knockout genotyping
EHD2 N-terminal forward	CTCTCCACCTTGTAGTCTCC	EHD2	Knockout genotyping
EHD2 N-terminal reverse	CAGGGGAAGAAGTTTCGTGC	EHD2	Knockout genotyping
EHD3 N-terminal forward	GGAGCTCGAGCATCCTTTAG	EHD3	Knockout genotyping
EHD3 N-terminal reverse	GGAAGACTTTCCACGTCACC	EHD3	Knockout genotyping
EHD4 N-terminal forward	GGTTCTTACTGAAGTGCGGC	EHD4	Knockout genotyping
EHD4 N-terminal reverse	CCTTGGCAACAGCAAGGAAG	EHD4	Knockout genotyping

Table 2. Primers used for knock-in and knockout PCR genotyping

2.9 Transferrin uptake assay

Cells were grown on glass chamber slides (Ibidi), incubated with 5 μg/ml transferrin conjugated to Alexa Fluor 647 (Invitrogen) in serum-free medium for 30 minutes at 37°C. Cells were subsequently fixed with 4% PFA and stained with the appropriate antibodies.

2.10 Fluorescence recovery after photobleach (FRAP)

FRAP studies were conducted on live NIH 3T3 cells expressing endogenous caveolin1-GFP. Cells were seeded in glass chambers (Ibidi) for 48 hours prior to experiment. Measurements were taken in growth media supplemented with 10 mM HEPES (Sigma), and the temperature maintained at 37°C with a heated stage incubator insert. Experiments were performed using a 63x 1.4 NA objective on an inverted Zeiss LSM510 confocal microscope. Three frames were taken before photobleaching to determine the average pre-bleach fluorescence at the starting point. Three defined regions of interest (ROI; 8 μm diameter) were photo bleached at full laser power. Recovery of fluorescence was monitored by scanning the ROI at low laser power in movies taken at a rate of one frame per 3 seconds (120 frames per movie). The mean fluorescence intensity in the ROIs and the mean non-cellular background were determined from the images using LSM510 software. After subtracting the background, the ROI fluorescence values were normalised to an unbleached region to correct for the loss in fluorescence caused by imaging. To be able to compare FRAP curves from different cells, the average fluorescence from 3 frames taken before photobleaching was set to 100% and the relative recovery in each cell was normalised to its initial level. 6-9 cells were imaged in each independent experiment.

2.11 Quantitative PCR

Total RNA was isolated from cells using the RNeasy Mini Kit (Qiagen) and reverse transcribed using the High-Capacity RNA-to-cDNA Kit (Applied Biosystems). Quantitative PCR analysis of *CAV1* and *PTRF* was performed using the CAV1 TaqMan probe (Mm01129316_m1) and PTRF TaqMan probe (Mm00477266_m1) respectively, and TaqMan Universal Master Mix II, with UNG (Applied Biosystems)

on a ViiA7 Real-Time PCR System (Applied Biosystems). This was normalised against GAPDH (Mm99999915_g1).

2.12 Pulse-chase

Cells were depleted of methionine and cystine by incubating with DMEM without methionine or cysteine (Gibco) supplemented with dialysed FBS for 1 hour at 37°C. Cells were pulsed with 50 μCi/ml EasyTag EXPRESS ^{35}S Protein Labelling Mix (PerkinElmer) for 2 hours at 37°C, and washed in normal growth media before chasing in normal growth media for 24, 48, and 72 hours. Cells were lysed in 1% Triton X-100 plus 1% octyl-glucoside, lysates were subjected to immunoprecipitation and samples were run on pre-cast 4-20% Tris Glycine gels. Gels were fixed in 10% acetic acid, incubated with Amplify Fluorographic Reagent (GE Healthcare) and subsequently dried onto Whatman paper. Samples were exposed at -80°C on Fuji Super RX X-ray films and developed.

2.13 Cell surface biotinylation and internalisation assay

For the internalisation assay, cells seeded on fibronectin-coated glass chambers were washed twice with PBS pH 7.9 and cell surface molecules were biotinylated with 0.2 mg/ml sulfo-NHS-SS-biotin in the same buffer at 37°C. The reaction was quenched 15 minutes later with 50 mM Tris and then surface exposed biotin was removed by incubating the cells for 3 x 7 minutes in 100 mM sodium 2-mercaptoethanesulfonate (MESNA) in MESNA buffer (50 mM Tris, 100 mM NaCl, 1 mM EDTA, 0.2% (w/v) BSA, pH 8.6 at 25°C). Quantification of the proportion of caveolin1-GFP in endosomes, using a pixel mask generated from signal from fluorescent streptavidin, was conducted as in [43]. In brief, a binary mask was produced from one channel of a two-colour image. This was used to isolate pixels from the second channel that are positive in the mask. It was also used to isolate pixels from an offset of the second channel to determine the amount of overlap by chance. Mean fluorescence intensity was quantified by drawing cell outlines as regions of interests in FIJI.

2.14 Cell stretching

Cells were grown on fibronectin-coated deformable chambers to fit a ShellPa cell stretching device (Menicon Life Science). Cells were stretched for 1 hour by 20%

extensions with cycles at 1.5 Hz. For membrane rupture assays, the cell culture medium was supplemented with FITC-DEAE dextran 150 kDa (Sigma) at 100 mg/ml, and NucRed Live 647 nuclear stain (Invitrogen) added before imaging. For electron microscopy, cells were fixed whilst still undergoing stretch for 5 minutes, before removal of the chambers and further fixation.

2.15 Cytotoxicity assay

Cells grown on fibronectin-coated deformable silicon chambers were incubated with MultiTox-Fluor Multiplex Cytotoxicity Assay reagents (Promega) for 1 hour whilst stretching by 20% extension at 1.5 Hz cycles. Fluorescent intensity of the reagent was measured according to manufacturer's instructions and dead:live cells ratios obtained.

2.16 Fatty acid uptake assay

Primary pre-adipocytes were cultured and differentiated as describe. Once confluent, cells were serum-starved with serum-free DMEM for 1 hour. The appropriate ^{3}H-labelled fatty acid (0.5 μM; Perkin Elmer) in 0.1% fatty acid-free BSA (Sigma) in PBS was added to the cells at times 0, 10, 20, 30, 45 and 60 minutes. After fatty acid loading, cells were washed with ice-cold fatty acid-free BSA and lysed on ice with ice-cold RIPA buffer (50 mM Tris-HCl pH7.4, 1% NP-40, 0.5% Na-deoxycholate, 0.1% SDS, 150 mM NaCl and 2 mM EDTA, supplemented with protease inhibitors). This was incubated for 5 minutes before centrifuging at 16,000 *g* for 10 minutes. Cell lysates were added to scintillation fluid in scintillation tubes and counted using the PerkinElmer Tri-Carb 2910 TR Liquid Scintillation Counter.

2.17 Adipocyte membrane rupture assay

Primary cells were cultured as described above in fibronectin-coated deformable silicon chambers. Cells were stained with Nile red (Sigma), stretched for 10 minutes by 20% extensions with cycles at 1 Hz, in media containing SYTOX Green (Invitrogen). Samples were imaged immediately with a 20x 0.50 NA objective on an inverted Zeiss LSM510 confocal microscope. Control cells were not subjected to stretching. Images were quantified using FIJI and statistical analysis performed using GraphPad Prism.

2.18 Light microscopy

For indirect immunofluorescence, cells grown in Ibidi glass chambers were washed in PBS, fixed in 4% PFA for 10 minutes, blocked in 5% FBS supplemented with 0.1% Triton X-100 (Sigma) for 30 minutes to permeabilise, and incubated with the appropriate antibodies.

All confocal imaging was carried out using a Zeiss LSM510 inverted confocal microscope with a 63x 1.4 NA objective or 20x 0.50 NA objective, driven by Zen software. TIR images were acquired using an Olympus TIR microscope equipped with 488, 546 and 647 nm lasers and fitted with a 100x 1.45 NA objective.

Super-resolution images were acquired on a Leica TCS SP8 X gate STED inverted confocal microscope using a HCX PL APO 100x 1.4 NA objective.

2.19 Electron microscopy

Note: this procedure was carried out by Gillian Howard

For counting of morphological caveolae, cells grown on MatTek glass bottomed Petri dishes were fixed in 2.5% glutaraldehyde, 2% paraformaldehyde in 0.1 M cacodylate buffer. Cells grown on fibronectin-coated silicon chambers for stretching were fixed whilst stretching by adding double strength fixative to an equal volume of culture medium for 5 minutes, before removal of the chambers and exchanging to fresh normal strength fixative. Cells were then processed on their growing substrate for electron microscopy: post fixed in 1% osmium tetroxide, dehydrated in an ascending ethanol series and embedded in CY212 resin. Cells were cut perpendicular to their growing substrate and ultrathin sections of cells were stained with 4% aqueous uranyl acetate and Reynolds lead citrate and viewed on a FEI Tecnai Spirit operated at 80kV. Quantification of caveolae were carried out by acquiring images to trace the outline of cells at 6500x magnification, assembling these images into complete profile of the cell using Adobe Photoshop, and then scoring morphological caveolae blind to the identity of the sample.

For immunolabelling, cells were grown on glass bottom Petri dishes (MatTek) or on fibronectin-coated silicon chambers, and fixed in 4% PFA in 0.1 M phosphate buffer

pH 7.4 overnight at 4°C. For fixation while stretching, normal strength fixative was added to the cells whilst undergoing stretching and replaced with fresh fixative. After washing, cells were treated with either 0.1% sodium borohydride or 50 mM glycine in phosphate buffer for 15 minutes to block reactive aldehydes, and then permeabilized using 0.03% saponin in 20 mM phosphate buffer, 150 mM sodium chloride. Cells were incubated in normal goat serum (Aurion 905.002) for 40 minutes before incubation in either rabbit anti-caveolin1 antibody used at 1:200 or rabbit anti-GFP (Abcam ab6556) used at 1:100 for 4.5 hours at RT. After washing, cells were incubated in a 1:200 dilution of F(ab')2 goat anti-rabbit ultrasmall gold (Aurion 100.166) overnight at 4°C. Cells were fixed with 2% glutaraldehyde in 0.1 M phosphate buffer for 30 minutes, washed with distilled water followed by silver enhancement of gold using R-Gent SE-EM (Aurion 500.033) reagent. Cells were then post fixed with 0.5% osmium tetroxide in water for 15 minutes on ice and processed for electron microscopy as above. Quantification was carried out by acquisition of 50 images at 6500x magnification, all selected to contain gold staining, and then assignation of gold-positive membranes to the different classes shown. All image analysis was blind to the identity of the samples.

For 3'3'-diaminobenzidine (DAB) staining of EHD1,2,4/mitochondrial APEX transfected cells, transiently transfected and non transfected cells grown on MatTek dishes were fixed in pre-chilled 2% glutaraldehyde in 0.1M cacodylate buffer plus 2 mM calcium chloride for 1 hour on ice. All subsequent steps were carried out on ice until resin infiltration. After 5 washes in buffer, cells were treated for 5 minutes in buffer containing 20 mM glycine to quench unreacted fixative, followed by several washes. Freshly prepared DAB (working concentration 0.5 mg/ml), prepared using free base DAB dissolved in 0.1 M HCl plus hydrogen peroxide (0.03%) were mixed and filtered (0.2 mm) directly onto cells for 10 minutes. The reaction was stopped by washing in buffer. Cells were post fixed in 1% osmium tetroxide for 1 hour followed by processing for electron microscopy as above. Cells containing DAB stained mitochondria identified by transmitted light were cut out from the discs of resin and mounted on dummy resin blocks with superglue. Ultrathin sections were cut parallel to the growing surface.

2.20 Quantifications and statistics

Quantification of colocalisation was performed by measuring pixel overlap based on [43]. In brief, a binary mask was produced from one channel of a two-colour image. This was used to isolate pixels from the second channel that are positive in the mask. It was also used to isolate pixels from an offset of the second channel to determine the amount of overlap by chance. Mean fluorescence intensity was quantified by drawing cell outlines as regions of interests in FIJI. Statistical significance was determined using GraphPad Prism.

Chapter 3: Role of EHD proteins in caveolae

As results regarding the role of EHD2 in caveolar biology obtained in the laboratory did not show any significant effects, the aim of this study was to determine the effects of other EHD proteins on caveolae as some variable and limited colocalisation has been observed between other EHD proteins and caveolar markers [33]. Variations in the results from our laboratory and the literature are likely to have arisen from the different approaches used to detect for caveolae markers and EHD2. In previous studies, fluorescently tagged caveolin1 was either overexpressed or stably expressed and the depletion of EHD2 was induced acutely by siRNA [33, 34]. Experiments from our laboratory employed a more physiological approach by endogenously tagging caveolae markers and EHD2 with fluorescent proteins [208]. There is evidence in the literature that overexpression of caveolin1 causes its mislocalisation [20]. Thus, to avoid potential artefacts and misleading results, this study employs a genome editing approach to assess the function of EHD proteins in caveolae. It should be noted that cell lines annotated with "cavin1-mCh" or "CAV1-GFP" have cavin1 or caveolin1 endogenously tagged with mCherry or GFP respectively, as described in [21].

3.1 Results

3.1.1 Recruitment of EHD1 to cavin1 is significantly increased in EHD2 knockout cells

The presence of EHD1 and EHD4 in caveolae and the lack of clear effects of *EHD2* knockout cells on caveolar biology, as detailed in the Introduction Part 1.5.3, convey the impression that the EHD proteins may work in conjunction with each other. Wildtype and *EHD2* knockout cells were stained with anti-EHD1 antibody, with cavin1-mCherry expressed endogenously. A striking increase in colocalisation of EHD1 and cavin1 is observed in confocal images (Figure 3.1.1 A) and this is confirmed by the quantification of confocal images acquired. Images were analysed with the two fluorescent channels offset by approximately 1.5 μm to give an indication of the values expected due to chance overlap. Significant differences between original and offset images indicate true colocalisation. Colocalisation between EHD1 and cavin1 was observed in both wildtype and *EHD2* knockout cells,

with a significant increase in the *EHD2* knockout cells (Figure 3.1.1 B). This increase in colocalisation was not correlated with an increase in the abundance of EHD1 or EHD4 protein as seen in the Western blots of wildtype and EHD2 knockout lysates (Figure 3.1.1 C), indicating that lack of EHD2 causes the relocation of EHD1 to caveolae.

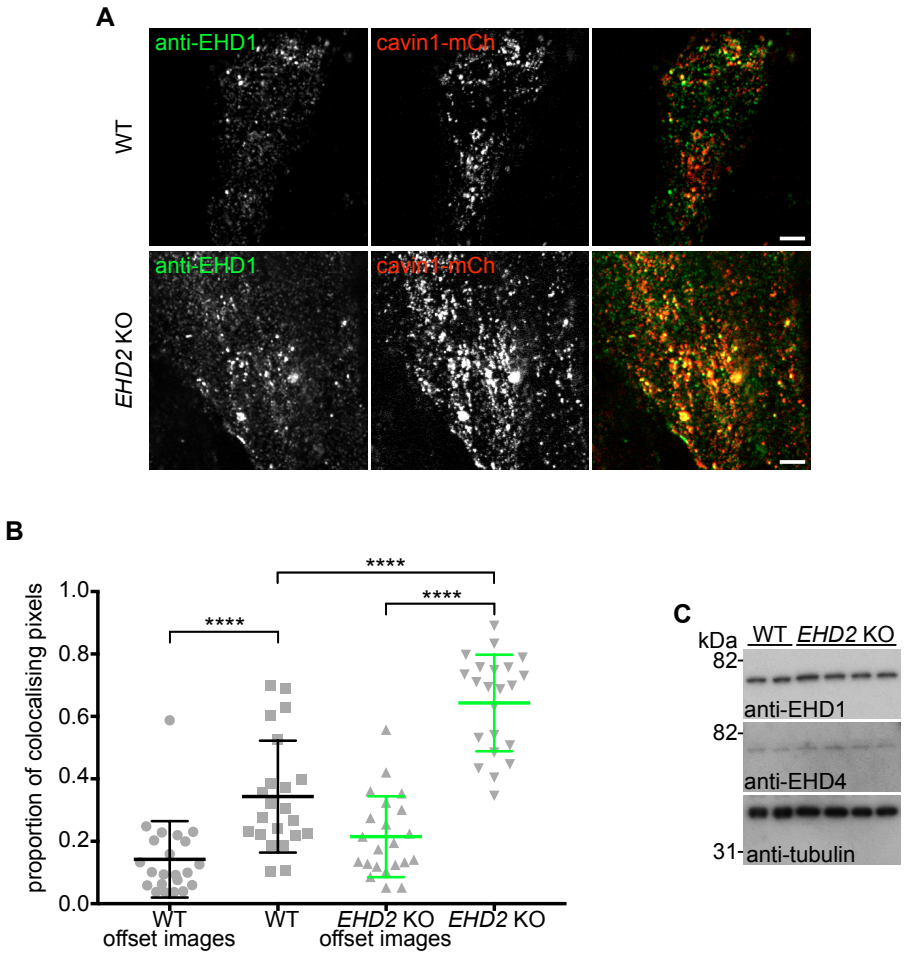

Figure 3.1.1 Recruitment of EHD1 to cavin1 is significantly increased in *EHD2* knockout cells

A. Confocal images of wildtype and *EHD2* knockout NIH 3T3 cells stained by indirect immunofluorescence with antibodies shown. Both express cavin1-mCherry from the endogenous locus. Bar 5 µm. **B.** Quantification of the colocalisation between EHD1 and cavin1-mCherry as in A. Images were analysed with the two fluorescence channels offset by approx. 1.5 µm to give an indication of the values expected due to chance overlap. Student's t-test, ****P≤0.0001. **C.** Western blots to show abundance of EHD1 and EHD4 proteins in two cultures of wildtype NIH 3T3 and four clones of *EHD2* knockout cells.
Experiments were conducted three times.

3.1.2 Overexpressed EHD1 and EHD4 colocalise with caveolin1 in NIH 3T3 cells

To confirm that EHD1, and to assess whether EHD3 and EHD4 are also associated with caveolae, NIH 3T3 cells with caveolin1-GFP expressed from the endogenous locus were transiently transfected to express mCherry-EHD1, mCherry-EHD3, or mCherry-EHD4. A small degree of colocalisation was observed between mCherry-EHD1 and caveolin1-GFP (Figure 3.1.2 A) and also mCherry-EHD4 and caveolin1-GFP (Figure 3.1.2 B). However, mCherry-EHD3 did not yield the same amount of colocalisation (Figure 3.1.2 C).

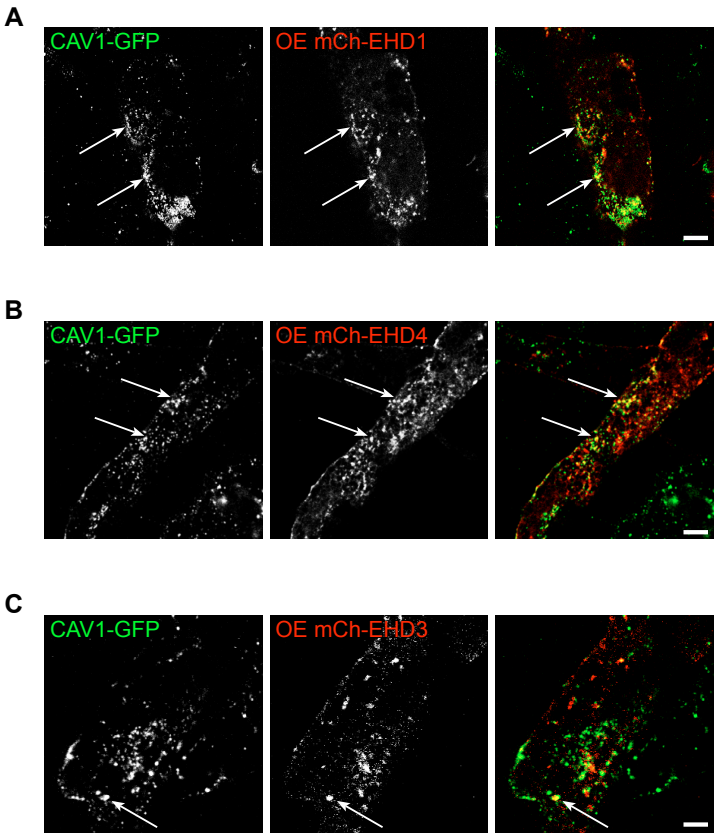

Figure 3.1.2 Overexpressed EHD1 and EHD4 co-localise with caveolin1 in NIH 3T3 cells

A. Confocal images showing co-localisation between mCherry-EHD1 expressed by transient transfection and caveolin1-GFP expressed from the endogenous locus in NIH 3T3 cells. Bar 5 µm. **B.** Confocal images showing co-localisation between mCh-EHD4 expressed by transient transfection and caveolin1-GFP expressed from the endogenous locus in NIH 3T3 cells. Bar 5 µm. **C.** Confocal images showing co-localisation between mCherry-EHD3 expressed by transient transfection and caveolin1-GFP expressed from the endogenous locus in NIH 3T3 cells. Bar 5 µm. Experiments were conducted two times.

3.1.3 EHD1 and EHD4, but not EHD3, are expressed in NIH 3T3 cells

Western blots of lysates from wildtype NIH 3T3 cells and NIH 3T3 cells transiently transfected with mCherry-tagged EHD1, EHD3 and EHD4 showed that EHD1 and EHD4 are both endogenously expressed in this cell line and commercially available antibodies readily detect the proteins (Figure 3.1.3 A). However, it is to be noted that the EHD4 antibody appears to detect EHD1 as well since a band is detected in the lane containing overexpressed mCherry-EHD1. EHD3 on the other hand does not seem to be expressed endogenously in this cell line as the antibody only detected the overexpressed tagged protein (Figure 3.1.3 A). This observation is confirmed by agarose gel electrophoresis of PCR products from NIH 3T3 genomic DNA and cDNA. Primers were designed for each of the EHD proteins to amplify the region of DNA that would be translated for the protein. Both *EHD1* and *EHD4* are present in the cDNA of NIH 3T3 cells indicating that mRNA for these proteins is produced (Figure 3.1.3 B). However, no product is present in the cDNA for *EHD3*, suggesting that no mRNA thus protein is produced for EHD3 (Figure 3.1.3 B). As a control, the same primer pairs were used against genomic DNA to indicate that the primers do indeed detect the regions of interest.

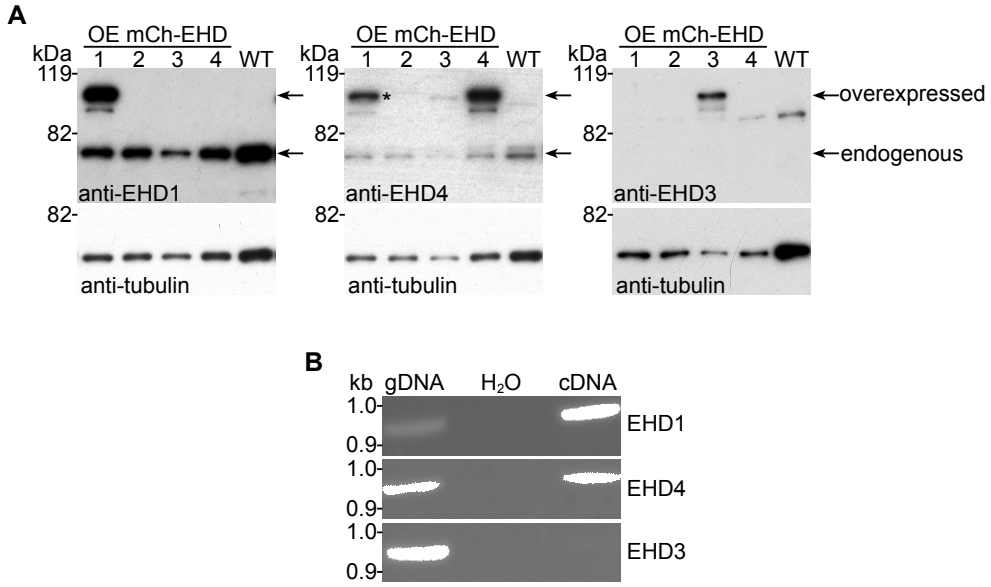

Figure 3.1.3 EHD1 and EHD4, but not EHD3, are expressed in NIH 3T3 cells
A. Western blots with antibodies shown of lysates from NIH 3T3 cells transiently transfected with mCherry-tagged EHD proteins to show EHD1, EHD4, and EHD3 protein expression and antibody specificity. Asterisked band most likely due to cross-reactivity of antibody. **B.** Agarose gel electrophoresis showing PCR products from NIH 3T3 genomic DNA and cDNA.
Experiments were conducted two times.

3.1.4 Generation of NIH 3T3 knock-in cell lines

NIH 3T3 cells expressing GFP fused to the C-terminus of endogenous EHD1 and EHD4 were produced using CRISPR/Cas9. Guiding RNAs were designed to target Cas9 to the C-terminal stop codon of *EHD1* or *EHD4*. Respective donor DNA plasmids with the GFP sequence between flanking homology arms for *EHD1* and *EHD4* were produced. The guide RNA and associated donor DNA were transfected into NIH 3T3 cells and populations of GFP-tagged EHD1 or EHD4 were obtained by FACS. Endogenously tagged EHD1 and EHD4 can be detected by their respective antibodies, although a band at the endogenous size of the protein is still readily detected indicating that not all of the alleles were tagged with GFP (Figure 3.1.4 A). The same technique did not produce detectable expression of EHD3 tagged with GFP or mCherry (Figure 3.1.4 B). Western blots with anti-EHD3 antibody did not detect endogenous or tagged EHD3 but did detect only the overexpressed mCherry-EHD3. The asterisk indicates a non-specific band. To confirm the lack EHD3 protein, tagged EHD1 cells were used as a control for GFP and mCherry protein expression. Western blots with anti-GFP and anti-mCherry antibodies did not detect any tagged EHD3 (Figure 3.1.4 B). Insertion of fluorescent protein coding DNA into *EHD1*, *EHD4* and *EHD3* loci were confirmed via PCR products of the C-terminus of the genes, as shown by agarose gel electrophoresis (Figure 3.1.4 C). Untagged EHD is detected at approximately 500 bp with the tagged versions detected at approximately 1,200 bp, the size of the product plus GFP or mCherry. It is presumed here that EHD3 is not expressed in the cells used, and all further experiments in this study use EHD proteins and caveolar markers (caveolin1 and cavin1) fused to fluorescent proteins expressed from their endogenous genomic loci in NIH 3T3 cells, and will be referred to as the expressed fusion protein (i.e. EHD1-GFP etc.). EHD1-GFP and EHD4-GFP cells were stained via indirect immunofluorescence with anti-GFP antibody to boost signals from endogenously tagged protein and the respective EHD antibody to show correct tagging of the protein (Figure 3.1.4 D and E).

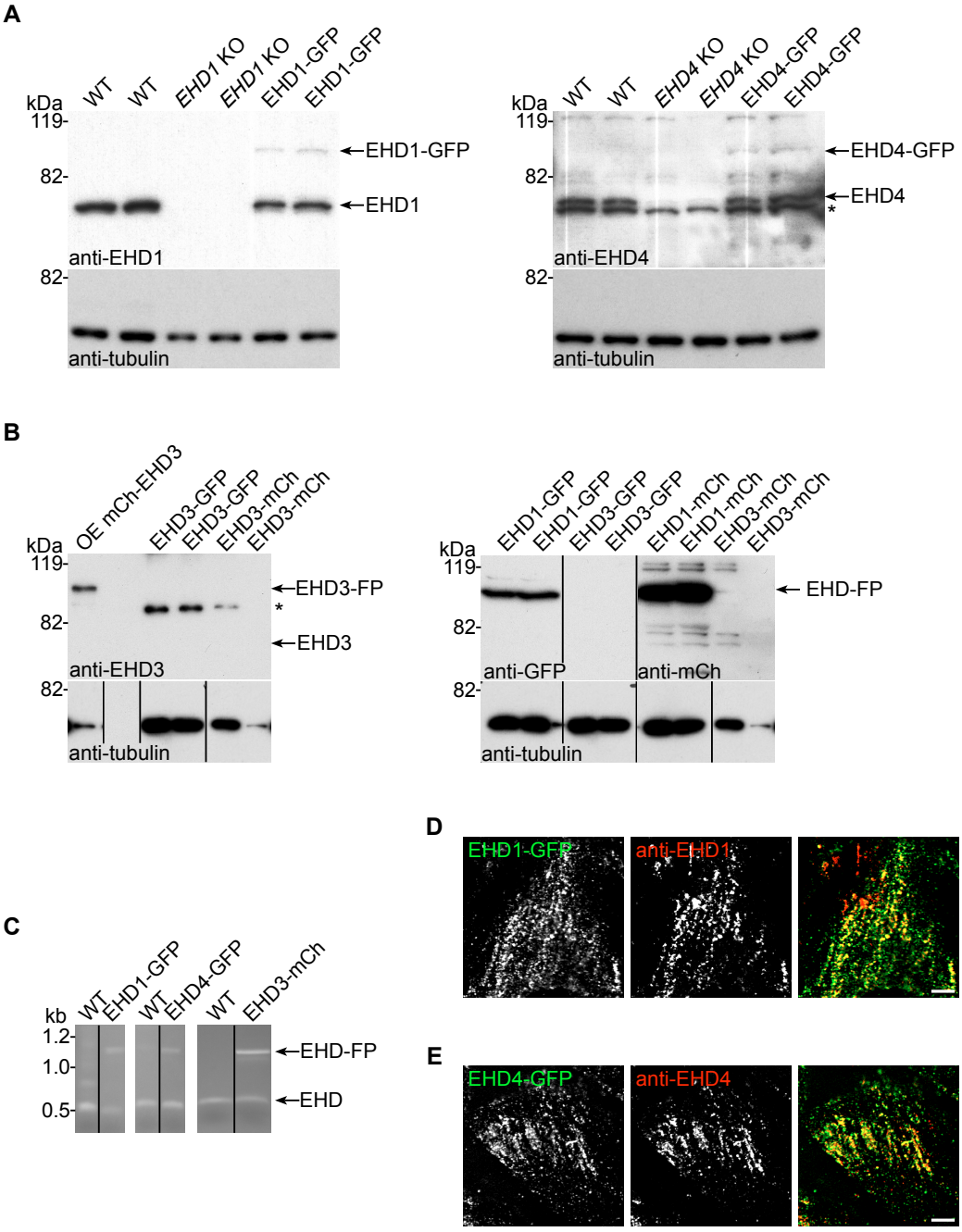

Figure 3.1.4 Generation of NIH 3T3 knock-in cell lines

A. Western blots with antibodies shown of EHD1-GFP and EHD4-GFP knock-in cell lines **B.** Western blots with antibodies shown of EHD3-GFP and mCherry knock-in cell lines. **C.** Agarose gel electrophoresis showing PCR products from genotyping of EHD knock-in cell lines. **D.** Confocal images of EHD1-GFP stained by indirect immunofluorescence with anti-EHD1 antibody, and anti-GFP antibody to boost signals from endogenously tagged protein. Bar 5μm. **E.** Confocal images of EHD4-GFP stained by indirect immunofluorescence with anti-EHD4 antibody, and anti-GFP antibody to boost signals from endogenously tagged protein. Bar 5 μm.
Experiments were conducted two times.

3.1.5 Generation of NIH 3T3 knockout cell lines

To aid in the study of the involvement of EHD proteins in caveolar biology, EHD protein knockout NIH 3T3 cell lines were generated. Single *EHD1*, *EHD2* (already made in the laboratory) and *EHD4* knockout, as well as *EHD1* and *EHD4* double knockout, and *EHD1*, *EHD2* and *EHD4* triple knockout NIH 3T3 cells were produced using CRISPR/Cas9. The strategy employed involved using two guide RNAs targeting either side of the start codon (Figure 3.1.5 B). Successful targeting resulted in the removal of the start codon and consequently the absence of EHD protein production. Western blots with EHD antibodies and tubulin as a loading control showed the successful knockout of the proteins (Figure 3.1.5 A). Asterisks indicate cross-reactivity of the antibodies, most likely due to other EHD proteins as the band disappears in the EHD1,2,4 triple knockout cell lines. Agarose gel electrophoresis of PCR products from genomic DNA as in Figure 3.1.5 B shows the larger full wildtype product (indicated with "x") above the smaller knockout cleaved product (indicated with "y") (Figure 3.1.5 C). Asterisks shows band close to the size of band x which may have resulted from a small insertion as the cell attempted to repair the cleavage. In any case, no protein was detected by Western blot. With these tools created, experiments were conducted to elucidate the role of EHD proteins in caveolar biology.

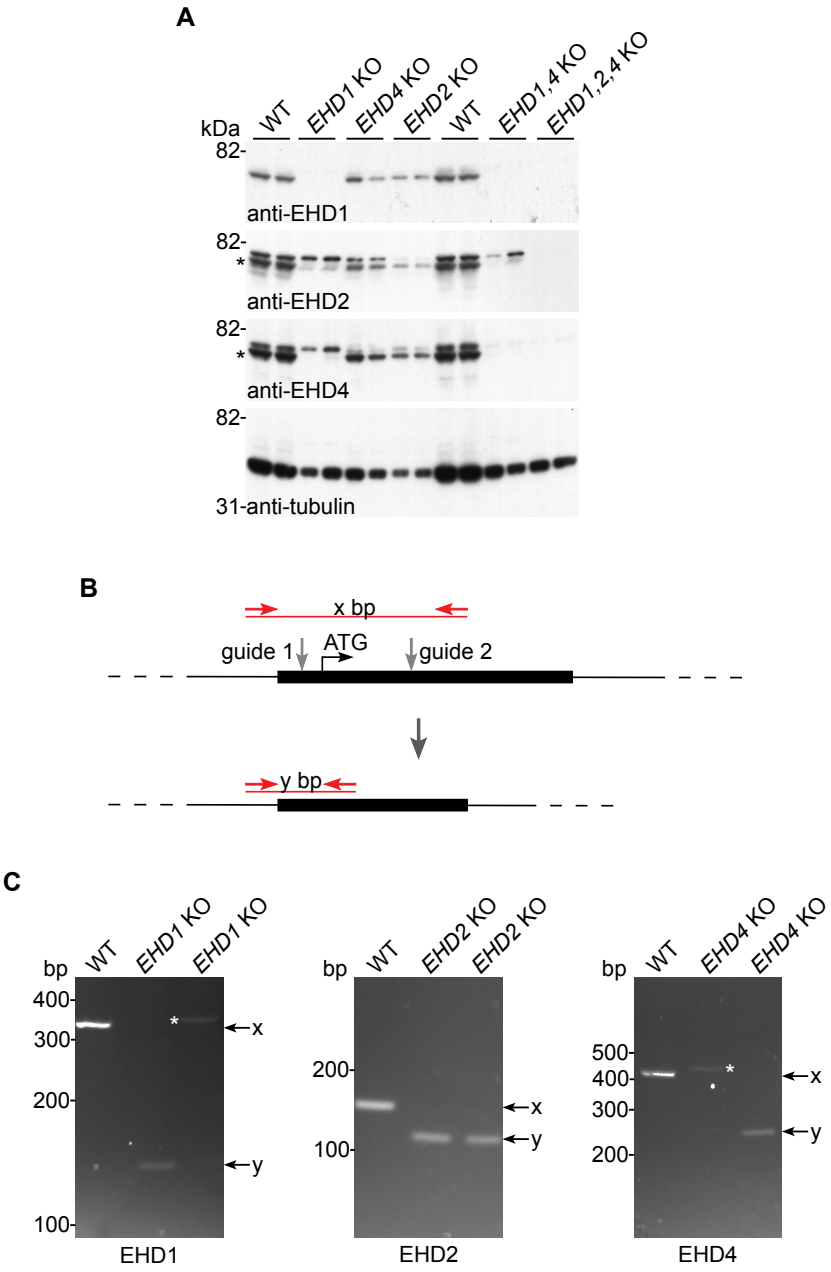

Figure 3.1.5 Generation of NIH 3T3 knockout cell lines

A. Cartoon showing strategy employed using CRISPR to generate knockout cell lines. Red lines indicate position of primers used in PCR genotyping. **B.** Western blots with antibodies shown. Two different clones of each EHD knockout cell line and two cultures of the parental wildtype NIH 3T3 is shown. Asterisks indicate cross-reactivity of the antibody, most likely to other EHDs as the band disappears in the triple knockout. **C.** Agarose gel electrophoresis of PCR products as in B. Asterisks shows bands close to the size of band x which may have resulted from incorrect attempt to repair the cleavage. No protein was detected by Western blot in all cases. Experiments were conducted three times.

3.1.6 EHD1-GFP and EHD4-GFP are present in caveolae when expressed at endogenous levels

Firstly experiments were carried out to confirm the presence of endogenous EHD1 and EHD4 in caveolae, as suggested by the overexpression of these proteins. Transferrin-647 was added to EHD1-GFP and EHD4-GFP cells to identify endosomes and the cells were subsequently fixed and stained for indirect immunofluorescence with anti-GFP antibody to boost GFP signal. EHD1-GFP and EHD4-GFP displayed punctate structures that partially colocalised with endocytosed transferrin and cavin1-mCherry (Figure 3.1.6 A). TIR microscopy of the EHD1-GFP and EHD4-GFP cell lines generated revealed both proteins to reside closely to the plasma membrane, and they also colocalised with cavin1-mCherry frequently (Figure 3.1.6 B and C). However, not all of the EHD1 or EHD4 expressed colocalised with cavin, and vice-versa, hence only a fraction of the total amount of EHD1 or EHD4 expressed is recruited to some caveolae. In experiments conducted by Gillian Howard, EHD1-GFP and EHD4-GFP were subjected to immunoelectron microscopy using affinity-purified anti-GFP antibody to confirm its localisation to caveolae. Indeed, both proteins can be detected in caveolae and gold particles were often detected at the neck of caveolae, which is in agreement with the reported distribution of EHD2 at the caveolar neck (Figure 3.1.6 D and E) [122]. Cells lacking GFP did not show specific labelling.

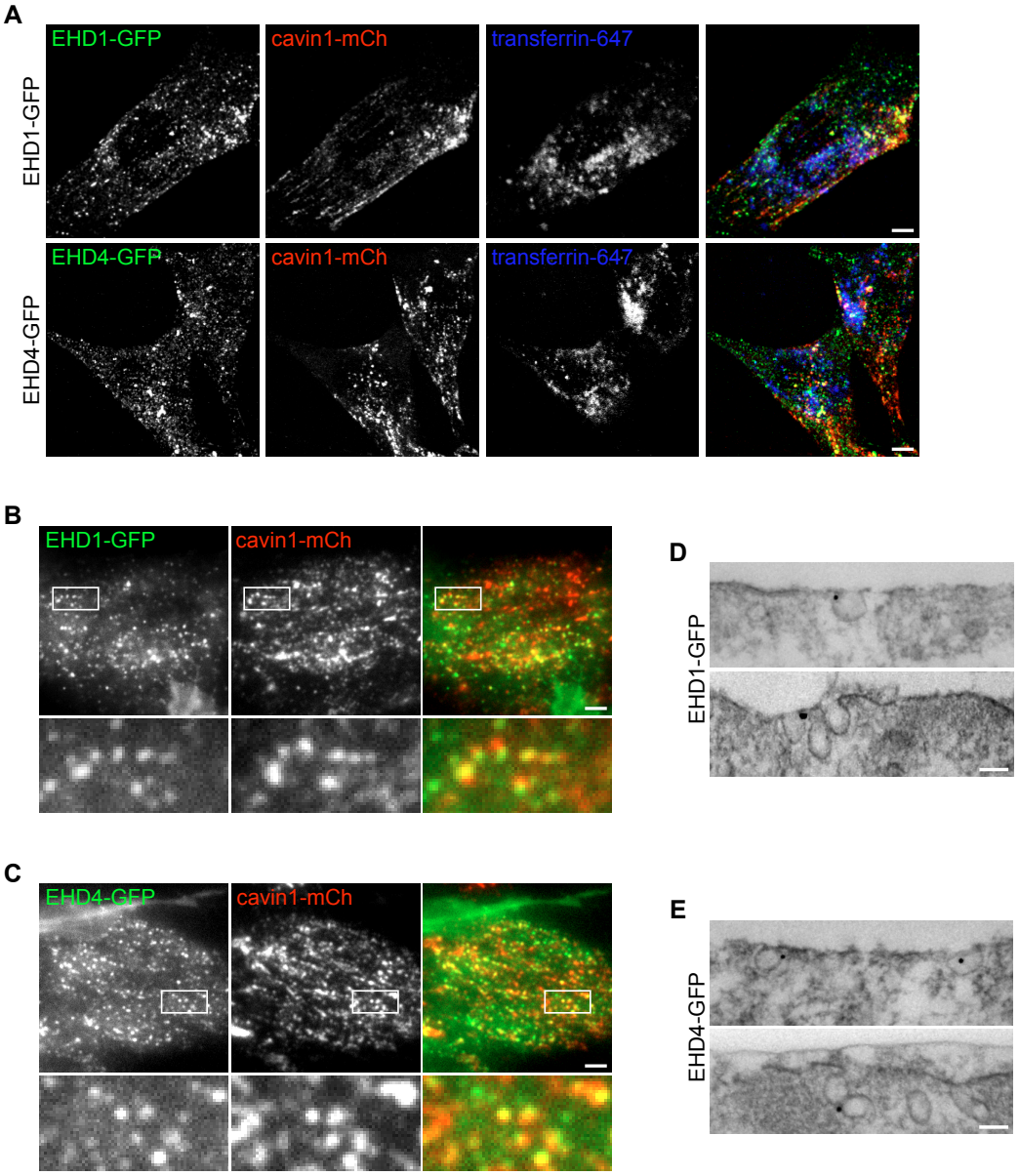

Figure 3.1.6 EHD1-GFP and EHD4-GFP are present in caveolae when expressed at endogenous levels

A. Cells expressing either EHD1-GFP or EHD4-GFP, and cavin1-mCherry from the endogenous loci were loaded with transferrin-647 for 30 minutes then fixed. Indirect immunofluorescent labelling with anti-GFP antibody was used to boost endogenously-tagged protein signals. Bar 5 µm. **B.** TIR imaging of EHD1-GFP and cavin1-mCherry expressed endogenously in live NIH 3T3 cells. Bar 5 µm. **C.** TIR imaging of EHD4-GFP and cavin1-mCherry expressed endogenously in live NIH 3T3 cells. Bar 5 µm. **D.** Immunoelectron microscopy with anti-GFP antibody in cells expressing EHD1-GFP. Bar 100 nm. **E.** Immunoelectron microscopy with anti-GFP antibody in cells expressing EHD4-GFP. Bar 100 nm.
Experiments were conducted three times.

3.1.7 EHD1 and EHD4 single knockout cells, and EHD1 and EHD4 double knockout cells do not affect caveolin1 and cavin1 colocalisation

Previous work from the laboratory has shown that lack of EHD2 does not affect caveolin1 and cavin1 colocalisation. Since EHD1 and EHD4 colocalise with caveolae to some extent, perhaps they have an effect on the colocalisation of caveolin1 and cavin1. Wildtype, *EHD1* knockout, *EHD4* knockout, and *EHD1* and *EHD4* double knockout NIH 3T3 cells were stained via indirect immunofluorescence with anti-caveolin1 antibody. Cavin1-mCherry was expressed from the endogenous loci. Here is it seen that cells lacking EHD1 or EHD4 or both EHD1 and EHD4 also display unperturbed levels of colocalisation between caveolin1 and cavin1, as with *EHD2* knockout cells (Figure 3.1.7). This suggests that the assembly of the 80S caveolar coat complex is not dependent on EHD protein expression.

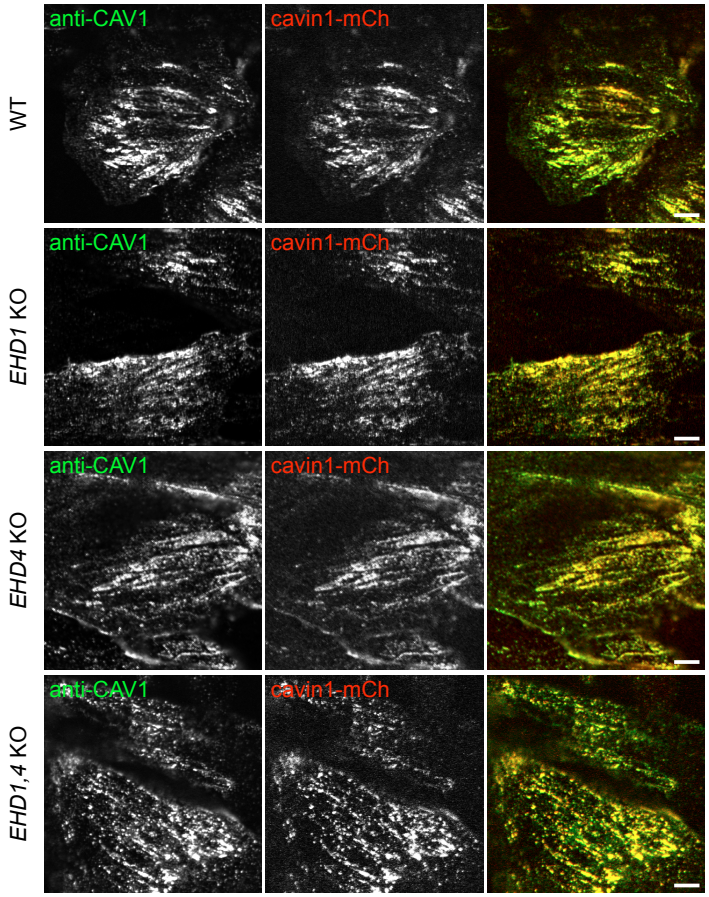

Figure 3.1.7 *EHD1* and *EHD4* single knockout cells, and *EHD1* and *EHD4* double knockout cells do not affect caveolin1 and cavin1 co-localisation
Confocal images of wildtype NIH 3T3 cells and cells that do not express EHD1, EHD4 or EHD1 and EHD4 stained by indirect immunofluorescence with anti-caveolin1 antibody. All cells express cavin1-mCherry from the endogenous locus. Bar 5 µm.
Experiments were conducted three times.

3.1.8 EHD2 colocalises with cavin1 in EHD1,4 knockout cells to the same extent as in wildtype NIH 3T3 cells

Wildtype and *EHD1,4* knockout cells, both with cavin1-mCherry expressed from the endogenous locus, were transiently transfected with GFP-EHD2. Confocal images acquired did not display a difference in EHD2 colocalisation with cavin1 (Figure 3.1.8 A) and this was confirmed by quantification (Figure 3.1.8 B). Although some degree of colocalisation is noted in both wildtype and *EHD1,4* knockout cells, there is no significant difference between the two. Thus, it is unlikely the EHD1, EHD2 and EHD4 co-depend on each other for the recruitment to caveolae, as without EHD1 and EHD4, EHD2 is still recruited to caveolae. Therefore, EHD1 and EHD4 could compensate when EHD2 is absent, and vice versa.

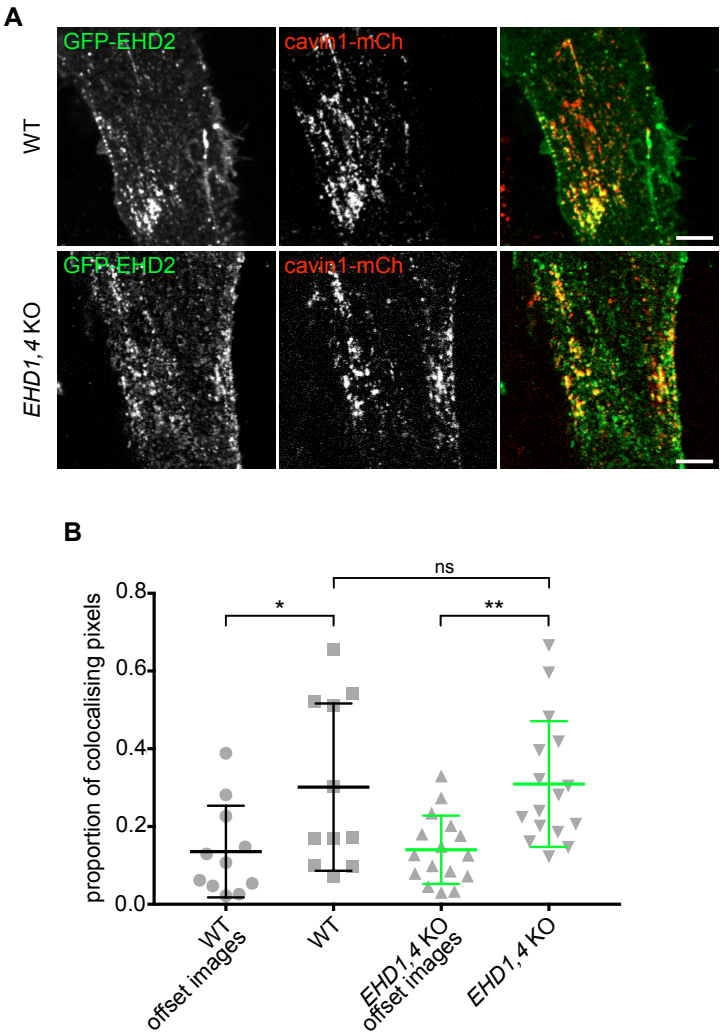

Figure 3.1.8 EHD2 colocalises with cavin1 in *EHD1,4* knockout cells to the same extent as in wildtype NIH 3T3 cells

A. Confocal images showing colocalisation between GFP-EHD2 expressed by transient transfection and cavin1-mCherry expressed from the endogenous locus, in wildtype and *EHD1,4* knockout NIH 3T3 cells that do not express EHD1 or EHD4. Bar 5 µm. **B.** Quantification of colocalisation between EHD1 and cavin1-mCherry. Images were analysed with the two fluorescence channels offset by approximately 1.5µm to give an indication of the values expected due to chance overlap. Student's t-test, *P≤0.05, **P≤0.01 and not significant.

Experiments were conducted three times.

3.1.9 EHD1 and EHD4 associate with EHD2, and EHD proteins assemble into hetero-complexes without the requirement for all three proteins

With both EHD1 and EHD4 being found in caveolae, as well as EHD2, it is possible that they may form heteromeric complexes. EHD2-GFP was effectively immunoprecipitated with anti-GFP antibodies and resulted in the specific co-precipitation of both EHD1 and EHD4 (Figure 3.1.9 A). The same immunoprecipitation in GFP control cells did not yield any co-precipitation of EHD1 and EHD4. The reverse immunoprecipitation of EHD1-GFP and EHD4-GFP, and then blotting for endogenous EHD2 also showed an association between EHD1 or EHD4 and EHD2 (Figure 3.1.9 B). The data imply that EHD2 can form complexes with both EHD1 and EHD4. To confirm these complexes and to ask whether both EHD1 and EHD4 are required for the interactions, cells lacking EHD1, EHD2 and EHD4 (*EHD1,2,4* knockout cells as described in Figure 3.1.5) were transiently transfected to express GFP-EHD2 and either mCherry-EHD1 or mCherry-EHD4. Again, anti-GFP antibody beads were used for immunoprecipitation. Both EHD1 and EHD4 displayed a specific association to EHD2, and on that account, the formation of EHD2-EHD1 and EHD4-EHD2 complexes were not dependent on the presence of all three EHD proteins (Figure 3.1.9 C). The same *EHD1,2,4* triple knockout cells transiently transfected to express only GFP and either mCherry-EHD1 or mCherry-EHD4 did not co-precipitate either EHD1 or EHD4, confirming that the interactions observed is explicit to EHD2. The data here support the idea that the EHD proteins can act independently of each other, as in Figure 3.1.8.

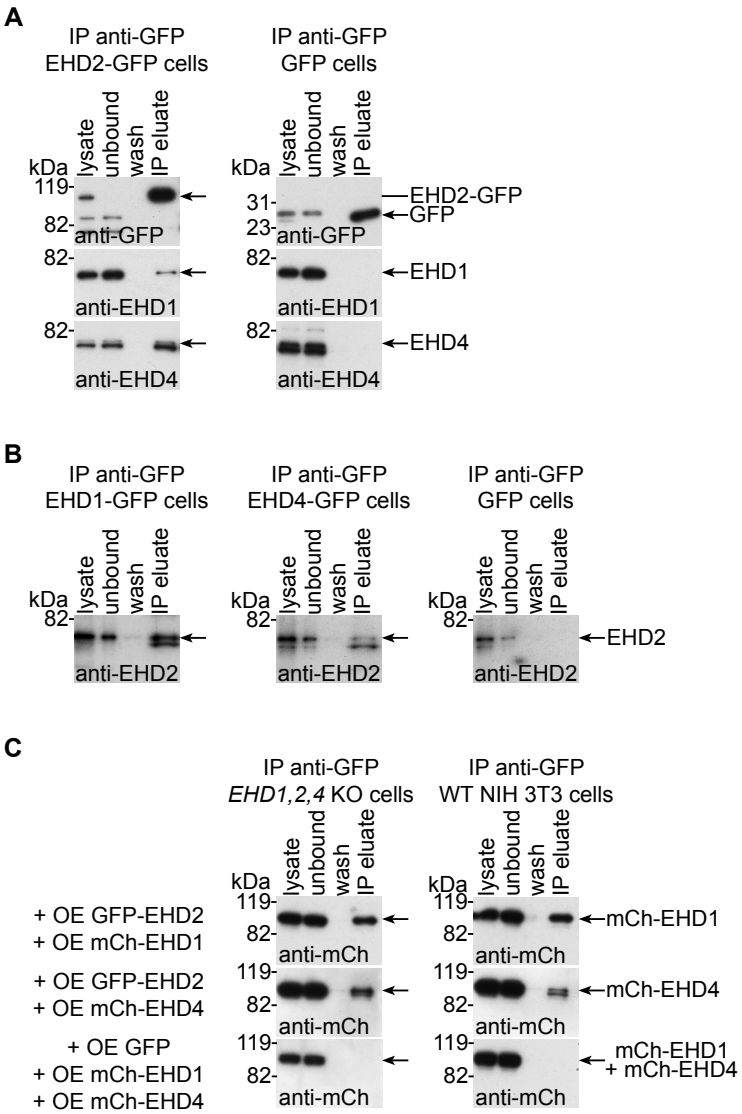

Figure 3.1.9 EHD1 and EHD4 associate with EHD2 and EHD proteins assemble into hetero-complexes without the requirement for all three proteins

A. Lysates from cells expressing EHD2-GFP from the endogenous locus, or negative controls expressing GFP alone, were incubated with anti-GFP-antibody beads. Lysates after this incubation are shown as 'unbound', and washes from the isolated beads as 'wash'. 'IP eluate' refers to the sample eluted from the beads with sample buffer, and is concentrated 10x relative to the lysate. **B.** Lysates from cells expressing EHD1-GFP or EHD4-GFP from the endogenous locus, or negative control cells stably transfected with plasmid to express GFP alone, were incubated with anti-GFP-antibody beads as in A. The eluate was concentrated 50x relative to the lysate. Anti-EHD2 antibodies cross-react with EHD1 and EHD4, asterisks indicates the cross-reacting bands, the EHD2 band is arrowed. **C.** Lysates from *EHD1,2,4* triple knockout NIH 3T3 cells transiently transfected with EHD-expressing or GFP-expressing plasmids as shown were incubated with anti-GFP-antibody beads. The eluate was concentrated 10x relative to the lysate.

Experiments were conducted two times.

3.1.10 Caveolae distribution and the ultrastructure of the caveolar neck are EHD protein dependent

As single knockouts of each of the EHD proteins and double knockout of EHD1 and EHD4 did not yield any detectable effects in the colocalisation of caveolin1 and cavin1, *EHD1,2,4* triple knockout cell lines were produced, as described in Figure 3.1.5, to test the hypothesis of EHD protein functional redundancy. The number of morphologically-defined caveolae by electron microscopy was not significantly different between wildtype and *EHD1,2,4* knockout cells (Figure 3.1.10 A). Confocal analysis of wildtype and *EHD1,2,4* knockout cells stained via indirect immunofluorescence with anti-caveolin1 and anti-mCherry antibodies showed indistinguishable levels of colocalisation between caveolin1 and cavin1 in both cell lines (Figure 3.1.10 B). Together, the observation that the numbers of caveolae are not different between wildtype and *EHD1,2,4* knockout cells, and the confocal analysis of colocalisation, illustrates that caveolar bulb formation is not dependent on EHD proteins. However, a more dispersed caveolae staining, with smaller puncta, was seen in the triple knockout cells (Figure 3.1.10 B).

With EHD proteins likely to localise to the neck of caveolae (Figure 3.1.6 D and E) and to not be an essential part of the machinery required to generate caveolar bulbs, it is plausible that they have a role at the neck of caveolae [122]. An examination of the neck of individual caveolae in wildtype and *EHD1,2,4* knockout cells showed that the neck of caveolae was more constricted in cells lacking EHD proteins (Figure 3.1.10 C). It was also apparent in the superimposition of multiple membrane profiles of individual caveolae (Figure 3.1.10 C). The diameters of caveolar necks were measured and confirmed the constricted neck phenotype, which is not seen in the cells lacking only EHD2 (Figure 3.1.10 D).

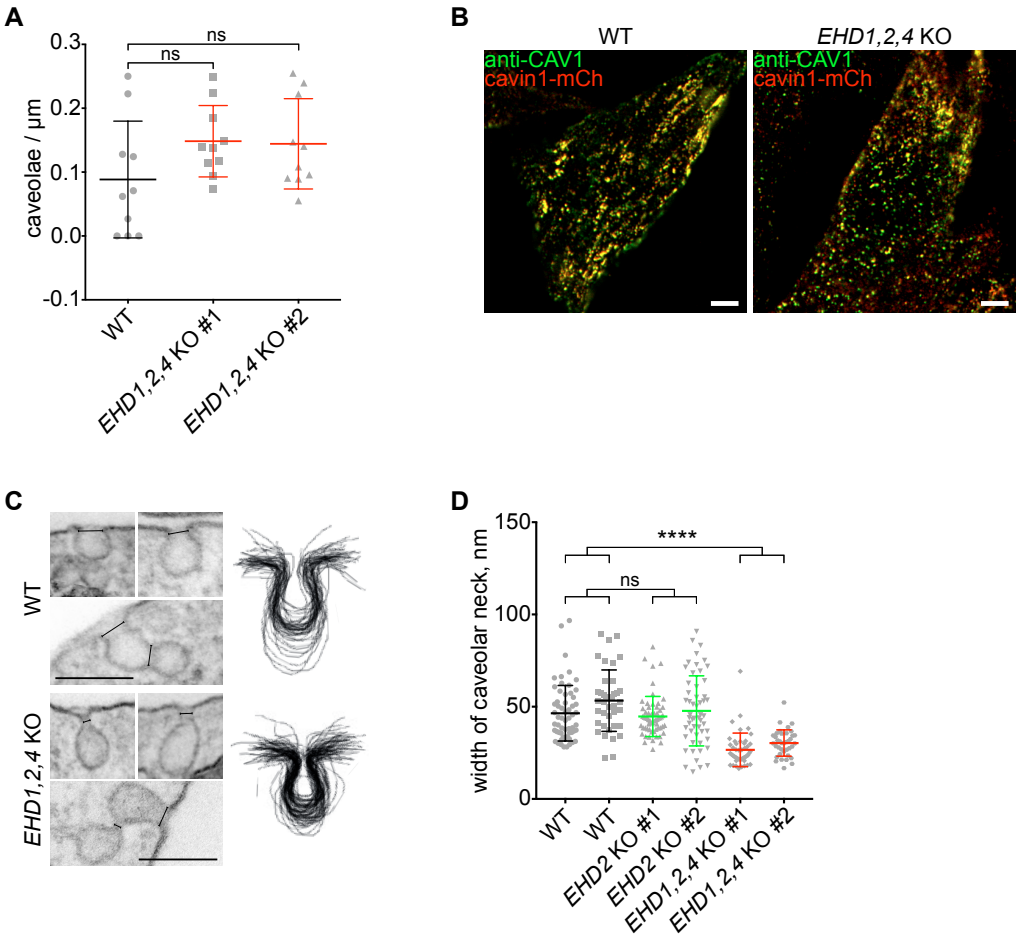

Figure 3.1.10 Caveolae distribution and the ultrastructure of the caveolar neck are EHD protein dependent

A. Quantification of morphologically-defined caveolae in *EHD1,2,4* knockout NIH 3T3 cells. One-way ANOVA with Dunnett's multiple comparison test, not significant. **B.** Confocal images to show distribution of caveolin1 in wildtype and *EHD1,2,4* knockout NIH 3T3 cells stained by indirect immunofluorescence with anti-caveolin1 antibodies. Both express cavin-mCherry from the endogenous loci. Bar 5 µm. **C.** Electron micrographs showing ultrastructure of the caveolar neck in wildtype and *EHD1,2,4* triple knockout NIH 3T3 cells. The right hand images present aggregated membrane profiles from 40 individual caveolae of each genotype. Bar 100 nm. **D.** Measurement of the width of caveolar neck, as shown in C, for multiple caveolae from two cultures of wildtype, two clones of *EHD2* knockout, and two clones of *EHD1,2,4* knockout NIH 3T3 cells. One-way ANOVA with Dunnett's multiple comparison test, ****P≤0.0001 and not significant.

Experiments A, C and D were conducted once in duplicates, and experiment B was conducted three times.

3.1.11 The formation of clustered arrays of caveolae is dependent on EHD proteins

Using immunoelectron microscopy, the morphology of caveolin1-positive structures in two cultures of wildtype, two clones of *EHD2* knockout and *EHD1,2,4* knockout cells were analysed. Caveolin1-positive structures were classified as either flat membrane, single caveolae or clustered caveolae (Figure 3.1.11 A). There was a slight increase in the amount of caveolin1 found in flat membrane patches in *EHD2* knockout and *EHD1,2,4* knockout cells compared to wildtype control cells (Figure 3.1.11 B). Quantifying the caveolin1-positive morphologically defined caveolae (single caveolae or clusters of two or more caveolae) in the same samples, it was apparent that there was marked decrease in the number of clusters of caveolae in the *EHD1,2,4* triple knockout cells, as compared to the wildtype or *EHD2* knockout cells (Figure 3.1.11 C). Furthermore, analysis of the cluster sizes in the samples show that clusters of more than three caveolae are abolished in cells lacking EHD1, 2 and 4 (Figure 3.1.11 D). To confirm this observation, cells lacking EHD proteins were transiently transfected with mCherry-EHD1, mCherry-EHD2 and mCherry-EHD4 as well as mitochondria-targeting APEX to allow for the unambiguous visualisation of transfected cells under electron microscopy through electron-dense polymerised diaminobenzidine staining within the mitochondrial matrix. Clusters of multiple caveolae were easily detected in transfected cells while this was not the case for untransfected cells (Figure 3.1.11 E). The electron microscopy was done by Gillian Howard.

Experiments A-D, shown in Figure 3.1.11, were conducted once in duplicates, and experiment E conducted two times.

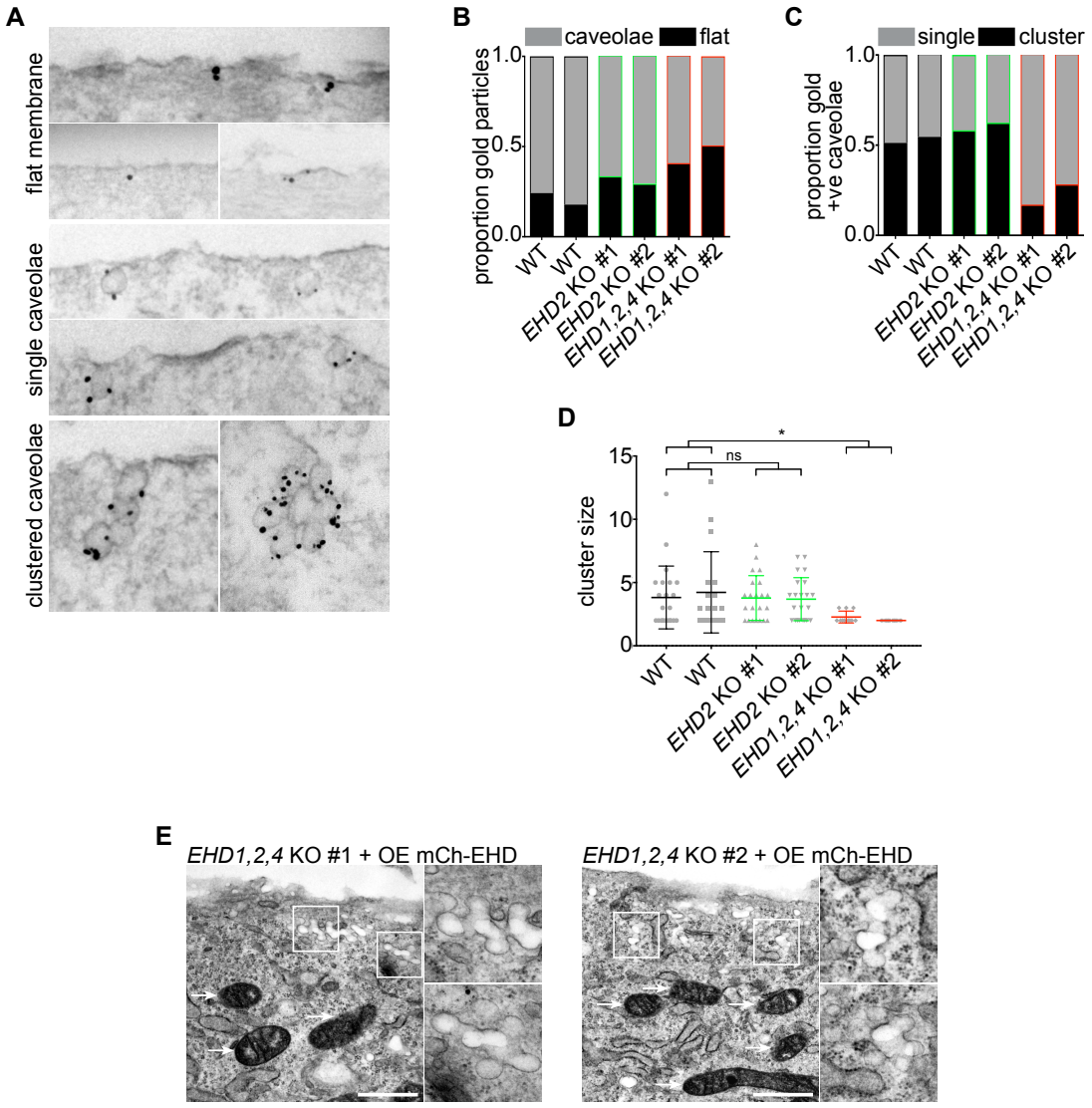

Figure 3.1.11 The formation of clustered arrays of caveolae is dependent on EHD proteins

A. Immunoelectron microscopy with anti-caveolin1 antibody to classify membrane morphology of caveolin1-positive regions. Examples of regions classified as flat membrane, single caveolae and clustered caveolae are shown. **B.** Quantification of the ratio between caveolin1-positive regions classified as flat or as morphological caveolae (single plus clustered caveolae) from immunoelectron microscopy. **C.** Quantification of the ratio between caveolin1-positive caveolae classified as single or as in clusters from immunoelectron microscopy. **D.** Quantification of the size of caveolar clusters (the number of caveolar bulbs present in a single structure) identified in immunoelectron microscopy. Student's t-test, *P≤0.05 and not significant. **E.** Electron micrographs of *EHD1,2,4* knockout cells expressing mitochondrially-targeted APEX, mCherry-EHD1, mCherry-EHD2 and mCherry-EHD4 by transient transfection. Cells were stained with diaminobenzidine, producing electron dense deposits in the mitochondria of transfected cells. Two cells are shown, arrows highlight mitochondria, the boxed regions are shown at higher magnification in the additional panels. Bar 500 nm.

3.1.12 Caveolin1 dynamics are increased in EHD1,2,4 knockout NIH 3T3 cells

To elucidate further the roles of EHD proteins in caveolar biology, FRAP experiments were conducted to assess the dynamics of caveolae in cells lacking EHD proteins. Previous FRAP experiments conducted in the laboratory on *EHD2* knockout cells with caveolin1-GFP expressed from the endogenous locus did not show a difference in the dynamics of caveolin1-GFP compared to wildtype cells [208]. However, other experiments using siRNA to knockdown EHD2 showed an increase in the mobility of caveolae [33, 34]. Wildtype and *EHD1,2,4* knockout cells expressing caveolin1-GFP from the endogenous locus were imaged live, photo-bleached and monitored for recovery. There is an increase in the recovery rate of caveolin1-GFP in *EHD1,2,4* knockout cells compared to wildtype (Figure 3.1.12 A). Whether or not this increase seen in the dynamics of caveolae is due to the endocytosis of caveolae is unclear. To clarify whether the increased dynamics of caveolae was due to endocytosis or not, surface proteins of wildtype and *EHD1,2,4* knockout cells were biotinylated with sulfo-NHS-S-biotin and internalised for 15 minutes. This was followed by MESNA treatment to remove non-internalised biotin moieties, and streptavidin labelling to reveal endocytic compartments. Only a small proportion of the labelled endocytosed biotin colocalised with caveolin1-GFP in both wildtype and *EHD1,2,4* knockout cells (Figure 3.1.12 B). Quantification confirmed this and also showed that there was no significant difference in the amount of endocytosis between wildtype and *EHD1,2,4* knockout cells (Figure 3.1.12 C), leading to the assumption that increased dynamic of caveolae may be due to lateral movements in the plasma membrane.

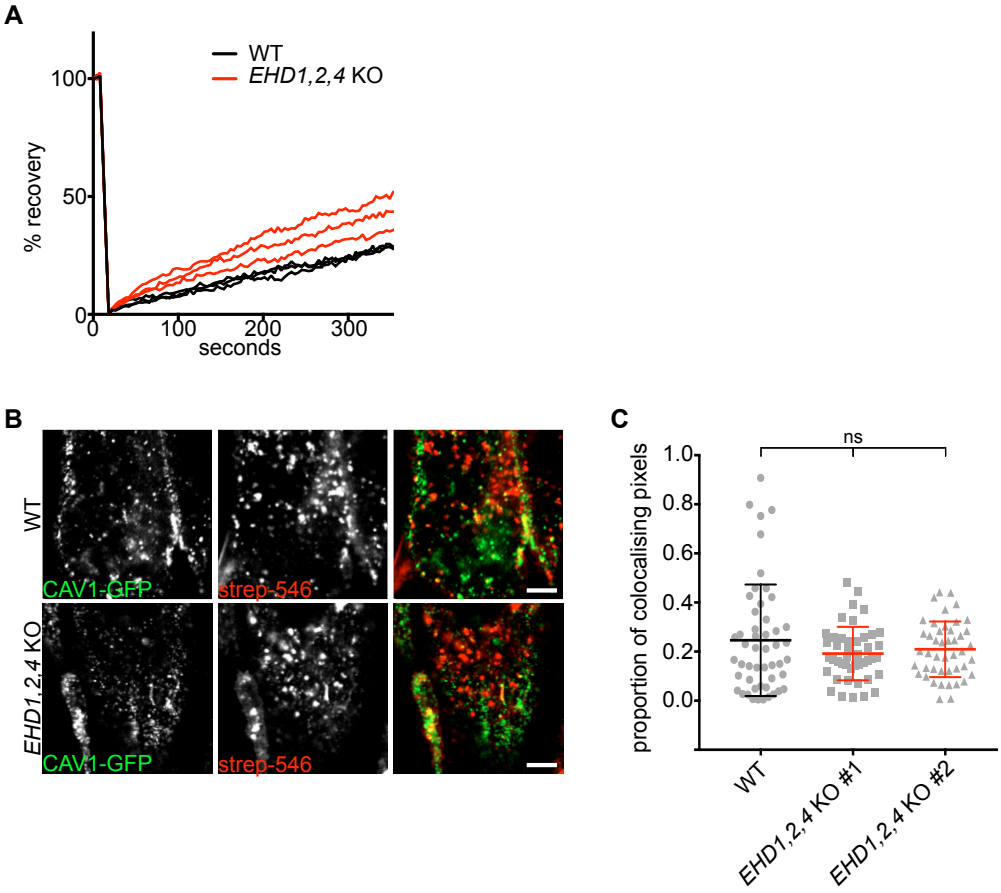

Figure 3.1.12 Caveolin1 dynamics are increased in *EHD1,2,4* knockout NIH 3T3 cells

A. Quantification of the mobility of caveolin1-GFP by FRAP. Each line is a mean from >7 individual photobleached regions from different experiments. **B.** Internalisation assay of wildtype and *EHD1,2,4* knockout NIH 3T3 cells with endogenously tagged caveolin1-GFP. Biotinylation of all surface proteins with sulfo-NHS-SS-biotin was followed by MESNA treatment to remove non-internalised biotin moieties and streptavidin-labelling to reveal endocytic compartments. Internalisation was for 15 minutes. Bar 5 µm. **C.** Quantification of internalisation assay to reveal intracellular caveolin1-GFP in wildtype and *EHD1,2,4* knockout NIH 3T3 cells. Student's t-test, not significant.
Experiments were conducted three times.

3.1.13 Caveolin1 turnover is increased in EHD1,2,4 knockout NIH 3T3 cells

The increase in caveolin1-GFP mobility in cells lacking EHD1, 2 and 4 may indicate unstable caveolae when EHD proteins are not present. Steady state levels of caveolin1 protein in wildtype and *EHD1,2,4* knockout cells were similar (Figure 3.1.13 A). However, quantitative PCR exhibited a significant increase in the abundance of *caveolin1* mRNA levels (Figure 3.1.13 B). Consistent with these findings, pulse-chase analysis using ^{35}S methionine showed that caveolin1 is degraded more quickly in *EHD1,2,4* knockout cells compared to wildtype (Figure 3.1.13 C and D).

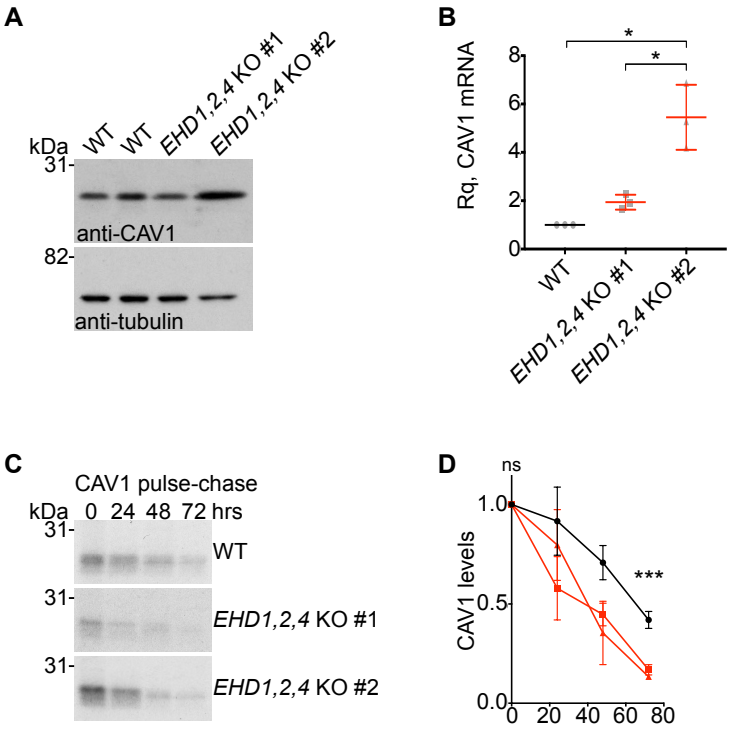

Figure 3.1.13 Caveolin1 turnover is increased in *EHD1,2,4* knockout NIH 3T3 cells

A. Western blots to show abundance of caveolin1 in two cultures of wildtype and two clones of *EHD1,2,4* triple knockout NIH 3T3 cells. **B.** Quantitative measurements of caveolin1 mRNA levels in wildtype and *EHD1,2,4* triple knockout NIH 3T3 cells using real-time PCR. Each point is a separate biological replicate itself based on four experimental replicates. Normalisation was to GAPDH. Student's t-test, *P≤0.05. **C.** Pulse-chase analysis of caveolin1 turnover in wildtype and *EHD1,2,4* knockout cell.. Cells were pulsed with ^{35}S methionine, lysed after the indicated times, before immunoprecipitation of caveolin1 and analysis by SDS-PAGE and autoradiography. **D.** Quantification of pulse-chase experiments as in C using densitometry of autoradiograms. One-way ANOVA, ***P≤0.001 and not significant.

Experiments A, C and D were conducted two times, and experiment B conducted three times.

3.1.14 EHD proteins are required for caveolae stability under repeated mechanical stress and cells lacking EHD proteins are more likely to rupture under repeated mechanical stress

An important function of caveolae is to protect cells from mechanical stress, potentially by flattening out and providing more membrane buffering [101, 102]. The kinetics by which caveolae flatten out and reform is still unclear [99]. EHD proteins have been reported to be involved in shaping membrane and perhaps may be an important component involved in the reformation of caveolae after flattening [178, 253].

Wildtype and *EHD1,2,4* knockout cells grown on deformable silicon chambers were subjected to cycles of stretching by 20% at 1.5 Hz for 1 hour and subsequently fixed and prepared for electron microscopy. Quantification of the number of morphologically-defined caveolae from these samples showed a considerable decrease of caveolae in cells lacking EHD proteins compared to wildtype (Figure 3.1.14 A). EHD proteins are indeed involved in the maintenance of caveolae when cells are under repeated mechanical stress, as seen in the experiments conducted in this study. Moreover, analysis of the cluster sizes confirmed the absence of caveolae clusters in *EHD1,2,4* knockout cells and showed that upon stretching, even the clusters of caveolae are decreased in wildtype cells, strengthening the argument that clustered arrays of caveolae are an important reservoir of membrane (Figure 3.1.14 B).

It is apparent that caveolae protect cells from mechanical stress-induced plasma membrane damage [101, 102]. A cytotoxicity assay was used to assess the ratio of intact (live) and damaged (dead) cells after repeated mechanical stress. A cell-permeant peptide substrate enters live, intact cells in which it is then cleaved by live-cell proteases to produce a fluorescent signal. This is added to cells along with a cell-impermeant peptide substrate that upon cleavage by dead-cell proteases released from cells with compromised plasma membrane, produces a different fluorescent signal. After stretching, a marked increase in the ratio of dead to live cells is seen in *EHD1,2,4* knockout cells compared to wildtype, and also compared to *caveolin1* knockout cells which was used as a control as previous experiments have shown that cells lacking caveolin1 are more susceptible to membrane damage upon stretch forces

(Figure 3.1.14 C). It should also be noted that there was already a significant difference in the ratio of intact to dead cells between wildtype and *EHD1,2,4* knockout cells prior to stretching (Figure 3.1.14 C). To support this observation, another assay for plasma membrane rupture was employed. Cells were incubated with high molecular weight fluorescent dextran, which will gain access to the cytosol of the cell should its plasma membrane integrity be compromised. To demonstrate that the increase for membrane rupture is due to the lack of EHD proteins, wildtype cells were labelled with a red cell tracker dye and seeded onto the chambers together with *EHD1,2,4* knockout cells. Thus, mitigating any potential variables as both cells containing and lacking EHD proteins would be subjected to the exact same experimental conditions. Cells were subjected to cycles of stretching by 20% at 1.5 Hz for 1 hour, this time whilst incubating with fluorescent dextran. Samples were imaged live and it was clear that cells lacking EHD proteins were more likely to contain fluorescent dextran than neighbouring wildtype cells (Figure 3.1.14 D (image acquired by Ben Nichols) and E). This corroborates the results observed by the cytotoxicity assay, that EHD proteins help preserve plasma membrane integrity when under stretch forces. To confirm further that the increase for membrane rupture is due to the lack of EHD proteins, *EHD1,2,4* knockout cells were transiently transfected with mCherry-tagged EHD1, EHD2 and EHD4. Cells that were transfected had clusters of caveolae restored, as seen in Figure 3.1.11 E. Again the cells were grown on deformable silicon chambers and subjected to cycles of stretching by 20% at 1.5 Hz for 1 hour, whilst incubating with fluorescent dextran. Samples were imaged live and as expected, untransfected cells lacking EHD proteins were more likely to contain fluorescent dextran than neighbouring transfected cells (Figure 3.1.14 F and G). It should be noted that caveolin1 protein levels did not change during the timeframe of the experiments (Figure 3.1.14 H).

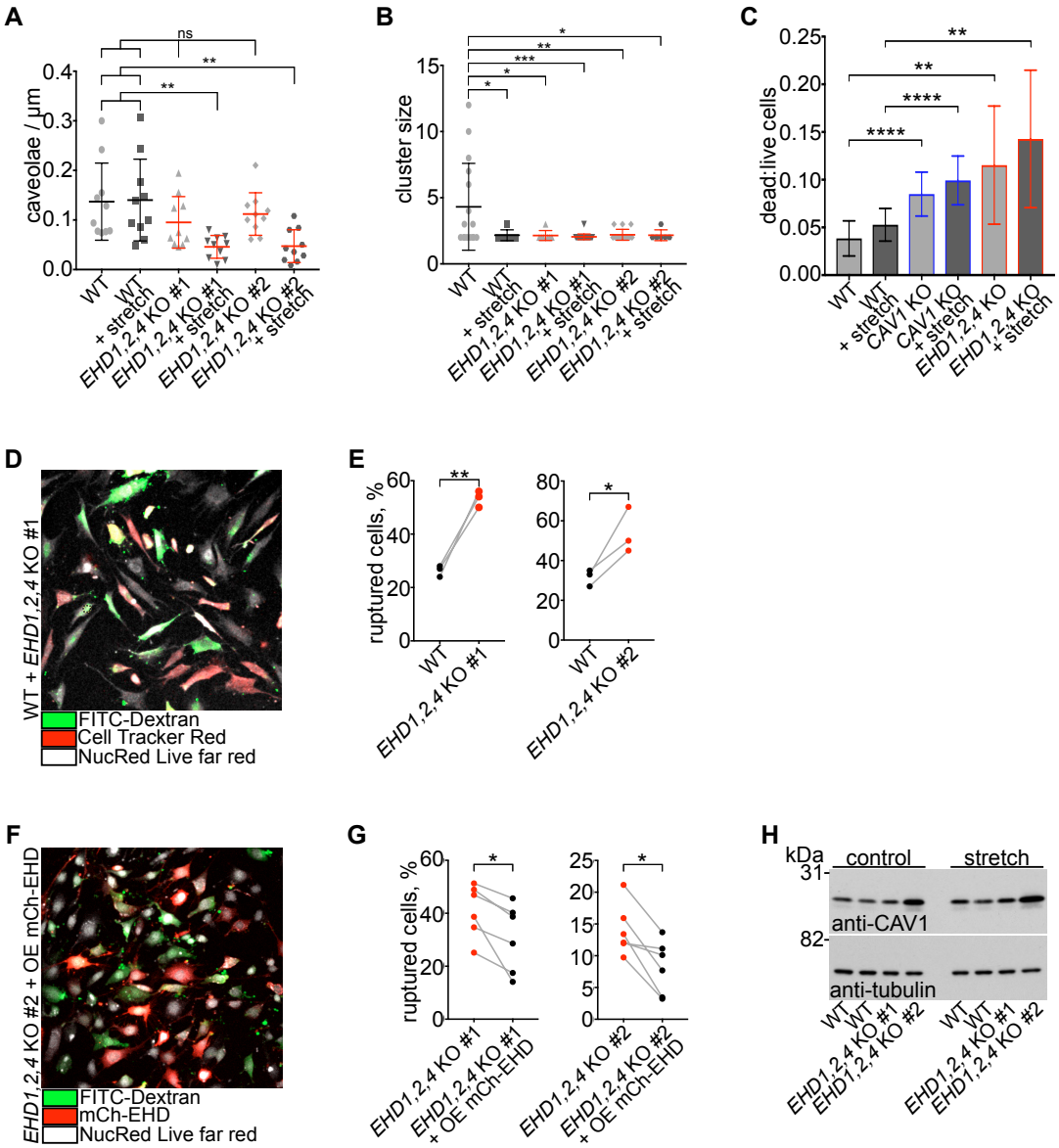
A
caveolae / µm
ns
**
**
**
WT
WT + stretch
EHD1,2,4 KO #1
EHD1,2,4 KO #1 + stretch
EHD1,2,4 KO #2
EHD1,2,4 KO #2 + stretch
B
cluster size
*
**
***
*
*
C
dead:live cells
**
**
****
****
WT
WT + stretch
CAV1 KO
CAV1 KO + stretch
EHD1,2,4 KO
EHD1,2,4 KO + stretch
D
WT + EHD1,2,4 KO #1
FITC-Dextran
Cell Tracker Red
NucRed Live far red
E
ruptured cells, %
**
*
WT
EHD1,2,4 KO #1
EHD1,2,4 KO #2
F
EHD1,2,4 KO #2 + OE mCh-EHD
FITC-Dextran
mCh-EHD
NucRed Live far red
G
ruptured cells, %
*
*
EHD1,2,4 KO #1
EHD1,2,4 KO #1 + OE mCh-EHD
EHD1,2,4 KO #2
EHD1,2,4 KO #2 + OE mCh-EHD
H
kDa
control
stretch
31-
82-
anti-CAV1
anti-tubulin
WT
WT
EHD1,2,4 KO #1
EHD1,2,4 KO #2
WT
WT
EHD1,2,4 KO #1
EHD1,2,4 KO #2

Figure 3.1.14 EHD proteins are required for caveolar stability under repeated mechanical stress and cells lacking EHD proteins are more likely to rupture under repeated mechanical stress

A. Quantification of morphologically-defined caveolae in *EHD1,2,4* triple knockout NIH 3T3 cells. One-way ANOVA with Dunnett's multiple comparison test, **P≤0.01 and not significant. **B.** Quantification of the sizes of clusters of caveolae from immunoelectron microscopy with cells fixed during repetitive stretching. One-way ANOVA with Dunnett's multiple comparison test, *P≤0.05, **P≤0.01 and ***P≤0.001. **C.** Cells grown on fibronectin-coated stretch chambers were stretched for 1 hour at 1.5 Hz by 20% in MultiTox-Fluor reagent and fluorescent intensity measured. Graph represents ratio between dead and live cells. Student's t-test, **P≤0.01 and ****P≤0.0001. **D.** Assay for plasma membrane rupture in wildtype and *EHD1,2,4* knockout NIH 3T3 cells, with wildtype cells stained with Cell Tracker Red. White signal is from NucRed Live 647 dye. Bar 5 μm. **E.** Quantification of the incidence of plasma membrane rupture in wildtype versus *EHD1,2,4* knockout cells as in D. Paired t-test, P≤0.05. **F.** Assay for plasma membrane rupture in *EHD1,2,4* knockout NIH 3T3 cells, some of which are transiently transfected with mCherry-EHD1, mCherry-EHD2 and mCherry-EHD4. White signal is from NucRed Live 647 dye. Bar 5 μm. **G.** Quantification of the incidence of plasma membrane rupture in non-transfected versus transfected *EHD1,2,4* knockout cells as in F. Paired t-test, P≤0.05. **H.** Caveolin1 protein expression levels in wildtype and *EHD1,2,4* knockout cells before and after 1 hour of stretching at 1.5 Hz by 20%.

Experiments A and B were conducted two times, and experiments C-H were conducted three times.

3.1.15 EHD1,2,3,4 quadruple knockout cells display the same phenotype as EHD1,2,4 triple knockout cells

Whilst EHD3 was not readily detected in the NIH 3T3 cell line used, *EHD1,2,3,4* quadruple knockout cells were produced nonetheless via CRISPR/Cas9 as described. Wildtype, *EHD1,2,4* knockout and *EHD1,2,3,4* knockout cells, with cavin1-mCherry expressed from the endogenous locus, were stained for caveolin1 with anti-caveolin1 antibody via indirect immunofluorescence. Images acquired do not show a distinguishable difference in the colocalisation between caveolin1 and cavin1, and the more scattered pattern of caveolin1 and cavin1 noted in *EHD1,2,4* knockout cells is also observed in the cells lacking all the EHD proteins (Figure 3.1.15 A). PCR genotyping as in Figure 3.1.5 B and C confirmed the mutation of the *EHD3* locus (Figure 3.1.15 B).

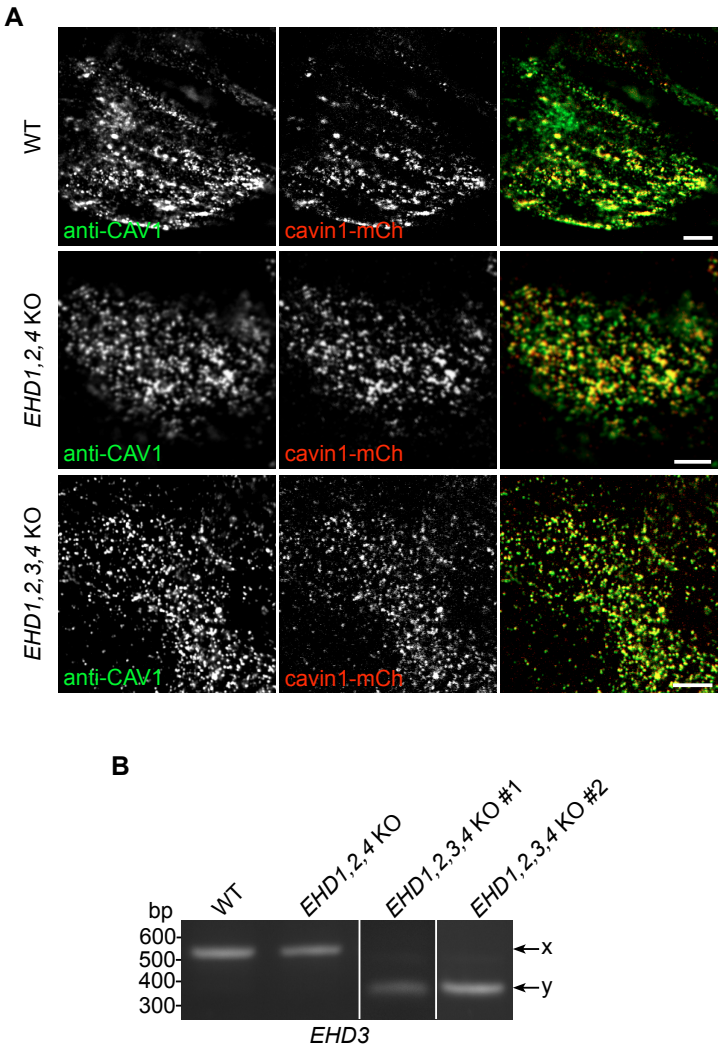

Figure 3.1.15 *EHD1,2,3,4* quadruple knockout cells display the same phenotype as *EHD1,2,4* triple knockout cells

A. Confocal images of wildtype NIH 3T3 cells, cells lacking EHD1, 2 and 4 and cells lacking EHD1, 2, 3, and 4 stained by indirect immunofluorescence with anti-caveolin1 antibody. All express cavin1-mCherry from the endogenous locus. Bar 5 µm. **B.** Agarose gel electrophoresis of PCR products as in Figure 3.1.5 B. No protein was detected by Western blot in all cases.

Experiment A was conducted three times, and experiment B was conducted two times.

3.1.16 Recruitment of PACSIN2 to caveolin1 is significantly increased in EHD1,2,4 triple knockout NIH 3T3 cells

A small fraction of PACSIN2 has previously been shown to colocalise to caveolae [127]. Wildtype and *EHD1,2,4* knockout cells both expressing cavin1-mCherry were labelled with an anti-PACSIN2 antibody. Confocal images revealed a notable increase in the colocalisation of PACSIN2 and caveolin1 in the *EHD1,2,4* triple knockout cells (Figure 3.1.16 A). Quantification, as previously described, of colocalisation between PACSIN2 and caveolin1 indeed showed an increase in *EHD1,2,4* knockout cells compared to wildtype (Figure 3.1.16 B). This change in distribution of PACSIN2 was not accompanied by a pronounced change in its expression levels (Figure 3.1.16 C). It is clear that lack of EHD proteins has an effect on PACSIN2, and it is possible that these components are affiliated and their functions redundant or overlapping.

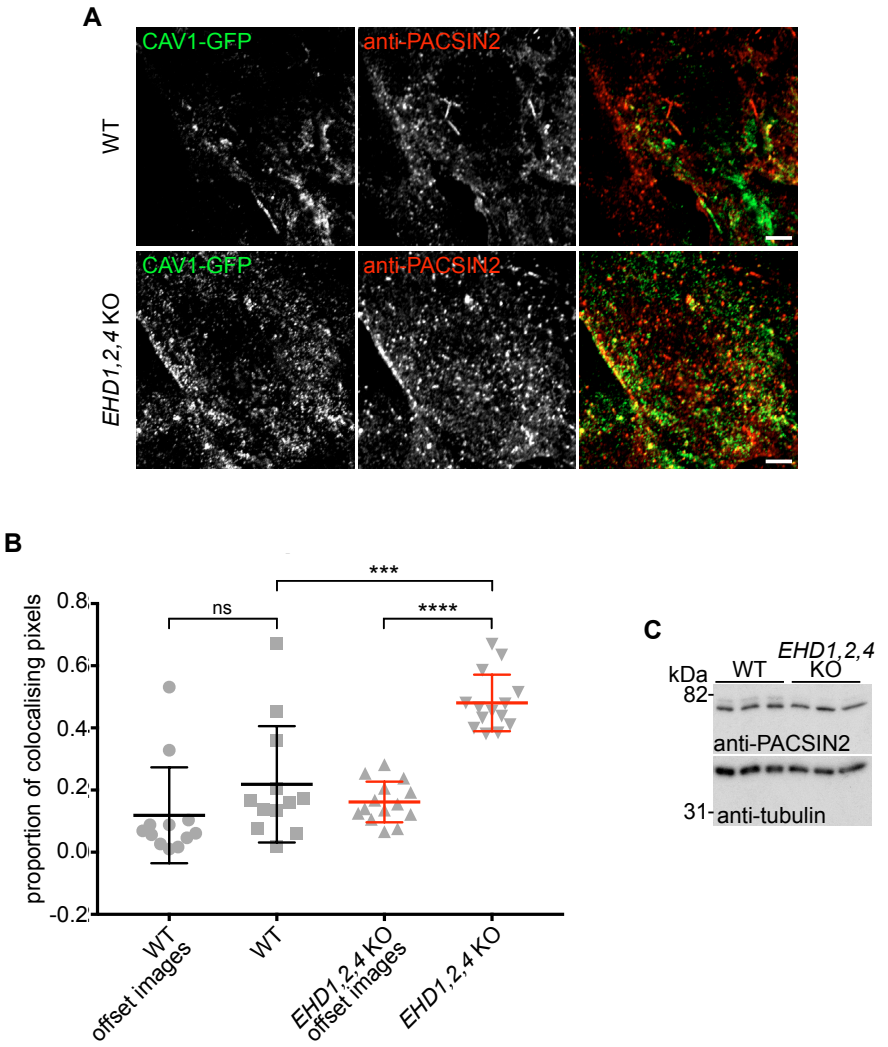

Figure 3.1.16 Recruitment of PACSIN2 to caveolae is significantly increased in *EHD1,2,4* triple knockout NIH 3T3 cells

A. Confocal images of wildtype and *EHD1,2,4* knockout NIH 3T3 cells stained by indirect immunofluorescence with anti-PACSIN2 antibody. Both express caveolin1-GFP from the endogenous locus. Bar 5 µm. **B.** Quantification of the co-localisation between PACSIN2 and caveolin1-GFP as in A. Images were analysed with the two fluorescence channels offset by approximately 0.8 µm to give an indication of the values expected due to chance overlap. Student's t-test, ***P≤0.001, ****P≤0.0001 and not significant. **C.** Western blots to show abundance of PACSIN2 proteins in three cultures of wildtype NIH 3T3 and three clones of *EHD1,2,4* knockout cells. Experiments were conducted three times.

3.2 Discussion

The data presented here describes three new key sets of findings pertinent to the function of EHD proteins at caveolae. Firstly, EHD1 and EHD4 are conclusively shown to be present in caveolae and the three EHD proteins can act independently of each other leading to possible functional redundancy. The lack of EHD2 results in the increase of EHD1 and most likely EHD4 present in caveolae, and only in the absence of all three EHD proteins are caveolar-related phenotypes readily detected. Secondly, the characteristic higher-order clusters of caveolae are contingent on the presence of all three EHD proteins (Figure 3.2). And finally, when cells lacking EHD1, EHD2 and EHD4 are subjected to repeated mechanical stress, the number of morphologically-defined caveolae is dramatically decreased and the plasma membrane is more likely to rupture.

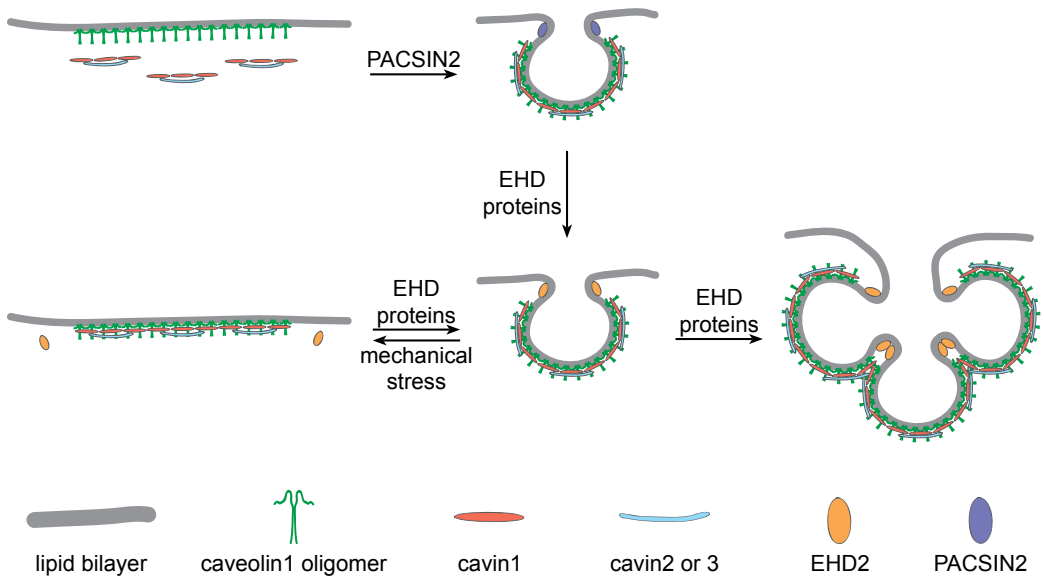

Figure 3.2 Speculative model for the involvement of EHD proteins in caveolar biology
Caveolin oligomers insert into the plasma membrane before cavin proteins associate with it. PACSIN2 may then help the invagination of caveolae. EHD proteins arrive and displace PACSIN2 to stabilise caveolae at the plasma membrane. EHD proteins are then responsible to generate clusters of caveolae, and to aid in the rapid reformation of caveolae upon mechanical stress.

Previous experiments have shown that EHD2 is located to the neck of caveolae, and is distinct from the proteins that comprise the caveolar coat complex, which forms the bulb of caveolae [33, 122]. There is very limited evidence available showing the association between other EHD proteins and caveolae [33]. This study employed the extensive use of genome-edited NIH 3T3 cell lines to elucidate the roles of EHD proteins in caveolar biology. Neither endogenous EHD3 protein or *EHD3* transcript were detected in the wildtype cell line and thus it was presumed to be not expressed (Figure 3.1.4 B and C). However, both EHD1 and EHD4 endogenous proteins and transcripts were detected, and overexpression of mCherry-tagged EHD1 and EHD4 revealed a limited amount of colocalisation with caveolin1 (Figure 3.1.4 A and C, and Figure 3.1.2 A and B). Genome editing of NIH 3T3 cells already expressing endogenous cavin1-mCherry to express either EHD1-GFP or EHD4-GFP from the endogenous locus allowed detection of the EHD proteins in caveolae (Figure 3.1.6) [21]. Immunoelectron microscopy showed EHD1 and EHD4 labelling close to the neck of caveolae, which suggested that like EHD2, EHD1 and EHD4 are also found at the neck region of caveolae (Figure 3.1.6). Despite being located in the same region as EHD2, EHD1 and EHD4 are also localised to elsewhere in the cell, as evident by confocal images (Figure 3.1.6 A). They are found in endocytic compartments and are seen to form tube-like structures in the cells, which have been observed previously [175, 254].

As seen by electron microscopy, the loss of EHD proteins does not have any noticeable effect on the shape of the caveolar bulb but it does alter the ultrastructural shape of the neck region, which is consistent with the EHD proteins location in the neck region of caveolae (Figure 3.1.10 C and D). In addition, characteristic higher-order clusters of caveolae are lost and upon mechanical stress the abundance of caveolae is altered (Figure 3.1.14 B). In cells lacking only EHD2 the neck of caveolae remains the same, which along with the confocal images of *EHD2* knockout cells labelled with anti-EHD1 antibodies, indicates that EHD1 and most probably also EHD4 aid in the maintenance of the caveolar neck (Figure 3.1.10 D and Figure 3.1.1 A). The higher-order clusters of caveolae appear to be linked via the necks of caveolae in electron microscopy, and with the EHD proteins located in the neck region, it is not surprising that these conglomerate clusters are lost (Figure 3.1.11 A, C and D).

Since caveolae abundance in the absence of EHD proteins is only affected during mechanical stress, it would seem that the caveolae are unable to rapidly re-form after stress (Figure 3.1.14 A). EHD proteins are recognised as mechano-enzymes that direct changes in membrane shape by utilising energy released by ATP hydrolysis [178]. With this in mind, EHD proteins may function to aid in the rapid re-formation of caveolae after stretch forces, as caveolae are still able to form in the absence of EHD proteins and the abundance is unchanged, thus EHD proteins are not part of the essential machinery in forming caveolae. It is worth noting that even in wildtype cells stretching causes the disassembly of large clusters of caveolae (Figure 3.1.14 B). It may be that clusters of caveolae are the first response to mechanical stress as they provide much more membrane when flattened out, and should the cells require more buffering, the rapid-forming individual caveolae provide this. Clusters may take time to configure and involve the recruitment of different proteins to aid in the formation. It is possible that EHD proteins at single caveolae directly aid in its rapid re-formation upon mechanical stress and that EHD proteins at higher-order clusters of caveolae aid in the formation in a stepwise manner, or by recruiting other proteins, which would increase the time taken to form the clusters. These differences observed are not due to differences in the abundance of caveolin1 protein as levels remain the same in wildtype and *EHD1,2,4* knockout cells with and without stretch forces (Figure 3.1.14 H).

Absence of EHD proteins increases the dynamics of caveolae, and this increase is not accompanied by an increase in the rate of endocytosis of caveolae (Figure 3.1.12). It suggests that EHD proteins are not required for caveolae endocytosis, but rather to stabilise caveolae at the plasma membrane, which is a proposed function of EHD2 at caveolae [33, 34]. Taking into account the above speculations, the stabilisation of caveolae at the plasma membrane may allow for its rapid re-formation should the cell require flattening of caveolae in response to mechanical stress. Another observation seen in the *EHD1,2,4* knockout cells is that the turnover of caveolin1 is affected. Steady state protein levels of caveolin1 remain unchanged but the transcript levels are increased in cells lacking EHD proteins (Figure 3.1.13). This is accompanied by an increase rate of degradation of caveolin1, thus steady state protein levels are comparable between the two. It is unclear whether EHD proteins are affecting caveolin1 degradation, thus increasing transcript levels as more protein needs to be

translated, or whether they are affecting transcript levels and therefore excess caveolin1 is degraded more quickly. One can imagine that the lack of higher-order clusters of caveolae in *EHD1,2,4* knockout cells causes a change in membrane tension, and to compensate for this the cell produces more caveolin1 transcript and protein. In this scenario, the excess caveolin1 is not utilised and needs to be degraded.

The loss of membrane convolutions introduced by caveolae is associated with a higher prospect of plasma membrane damage upon mechanical stress [101, 102]. This condition is also observed here where the lack of membrane convolutions is introduced by the lack of caveolae clusters in *EHD1,2,4* knockout cells (Figure 3.1.11 C and D). When these cells were subjected to repeated mechanical stress, the total number of caveolae was markedly decreased, and the plasma membrane of these cells were more susceptible to damage (Figure 3.1.14). These findings attest to the model of caveolae-derived membrane convolutions acting as a buffer for the cell during stretch forces, they flatten out providing more membrane and reducing the propensity for membrane damage. A question that may arise from an aspect of the cytotoxicity experiment is why the *caveolin1* knockout cells display less damage than the EHD proteins knockout cells (Figure 3.1.14 B). EHD proteins have other functions in the cell that are unrelated to caveolae, including the regulation of specific endocytic transport steps [174]. These transport steps may traffic important molecules required for membrane repair in response to mechanical stress. Thus, in cells lacking EHD proteins, membrane lesions are less likely to be repaired, whereas in the *caveolin1* knockout cells EHD proteins are still present and perhaps the membrane is repaired more efficiently. It should be noted that these experiments, and previously published experiments, do not distinguish whether or not the membrane protection is solely because of caveolae providing more membrane or if it is a downstream effect of caveolar components in response to mechanical stress. Caveolar components have been shown to have a signalling role and it may well be that caveolae sense the mechanical stress and send signals to the cell to protect itself [123].

It is known that EHD2 forms homo-oligomers and that EHD1 and EHD4 can hetero-oligomerise [175]. Data here shows that both EHD1 and EHD4 can bind to EHD2 and that the proteins can act independently of each other as lack of EHD1 or EHD4 does not affect the binding of the other to EHD2 (Figure 3.1.9). EHD1, and most likely

also EHD4, can compensate for lack of EHD2 at caveolae, and EHD2 is still recruited to caveolae in the absence of EHD1 and EHD4 (Figure 3.1.8). These observations support the functional redundancy element of EHD proteins in caveolar biology, and in EHD protein biology itself. However, exactly why there are multiple EHD proteins at caveolae is unclear. Perhaps each EHD protein has a slightly different effect on caveolae structure or recruit different binding partners. It is also unclear what mechanisms are regulating EHD1 and EHD4 to be recruited caveolae, as in wildtype cells only a small proportion of EHD1 or EHD4 is associated with caveolae. Perhaps EHD2 presence at caveolae indirectly or directly inhibits the efficient recruitment of EHD1 or EHD4, and without EHD2, other EHD proteins can be recruited more efficiently.

As well as EHD2 being associated with caveolae in the literature, PACSIN2 has also been related to caveolae [30, 127]. PACSIN proteins have been shown to bind EHD proteins through NPF motifs [182-184]. It may imply that PACSIN2 requires EHD proteins in order to bind to caveolae. However this is not the case as without EHD proteins, not only does PACSIN2 still colocalise to caveolae, but there is a significant increase in this colocalisation (Figure 3.1.16). Previous reports have shown limited colocalisation of PACSIN2 to caveolae and the reasoning for this was proposed that PACSIN2 is involved in the step in which flat caveolae are invaginated into the characteristic bulb-shaped caveolae [127]. It seems that EHD proteins may also be required for this step as there is more flat caveolae observed in *EHD1,2,4* knockout cells compared to wildtype. So in the absence of EHD proteins, it is likely that PACSIN2 protein levels would be increased to compensate. Alternatively, EHD proteins may regulate PACSIN2 efficiency, so without EHD proteins PACSIN2 is not as efficient at invaginating flat caveolae into flask-shaped caveolae, and the cell may attempt to rectify this by recruiting more PACSIN2 to caveolae. A study by Senju *et al*. has suggested that PACSIN2 phosphorylation decreases its membrane-binding activity and as a result decreases its stabilising effect on caveolae and triggers dynamin-mediated removal of caveolae [35]. It could be possible that EHD protein binding to PACSIN2 prevents its phosphorylation and therefore maintaining its membrane-binding activity. Taken with published data, this in turn could indirectly regulate dynamin2 by preventing it from removing caveolae. Another explanation could be that PACSIN2 may have different functions when it is unphosphorylated and

phosphorylated. In its unphosphorylated state, PACSIN2 along with EHD proteins function to invaginate caveolin1-rich membranes into caveolar bulbs. When the caveolar bulb is formed, EHD proteins remain at the neck of caveolae, and the changes in membrane curvature may lead to the phosphorylation of PACSIN2 and its subsequent release from the membrane, triggering dynamin2. All these interpretations are just speculations and are in no way exhaustive. Further experiments are required to fully understand the role of EHD proteins, and PACSIN2 and dynamin2, in relation to caveolae.

Chapter 4: Caveolae in adipocytes

It is evident that caveolae play a role in adipocytes from the striking phenotypes observed in mice and humans lacking caveolae [63, 209-211]. However, there are many uncertainties in the literature that require clarification. There is opposing evidence in the literature with regards to the association of the insulin receptor and caveolae, and the effects caveolae have on insulin signalling [45, 213-215, 217]. In addition, the insulin resistant phenotype observed may be due to increased fatty acid levels as that has been shown to induce insulin resistance and impaired insulin signalling [220, 221]. Free fatty acid levels are elevated in mice lacking caveolae and both CD36 and caveolin1 have been implicated to be involved in fatty acid uptake in adipocytes [59, 60, 226, 234, 235, 237, 255]. Despite this, it is unclear whether or not CD36 plays a key role in the uptake of fatty acids, as caveolin1 itself is reported to transport fatty acids independent of CD36 [59, 60]. Another possibility that avoids the confusion of the insulin receptor and CD36, is that caveolae may also have a mechanoprotective role in adipocytes, as shown in other cell types [101, 102]. In this model, the fragility of adipocytes lacking caveolae results in small adipocytes and a higher propensity for rupturing. This leads to the release of fatty acids causing lipotoxicity and hence the recruitment of macrophages and the generation of fibrosis. The disruption of adipocyte function and release of fatty acids are also responsible for the insulin-related phenotypes. It is clear that caveolae have a physiological role in adipocytes. However, it is not clear if this is due to the association of certain proteins such as the insulin receptor and CD36, with caveolae, or if it is due to the mechanoprotective roles of caveolae. This study aims to shed some clarification on the relationship between caveolae and the insulin receptor and CD36, and to see whether caveolae have a mechanoprotective role in adipocytes.

4.1 Results

4.1.1 Insulin receptor and CD36 are found in adipose tissue

Western blots of lysates from gonadal adipose tissue isolated from wildtype and *caveolin1* knockout mice confirmed that the insulin receptor and CD36 are expressed in this tissue (Figure 4.1.1). Expression levels of these proteins in adipose tissue are similar between wildtype and *caveolin1* knockout mice, suggesting that lack of caveolae does not affect the abundance of insulin receptor or CD36.

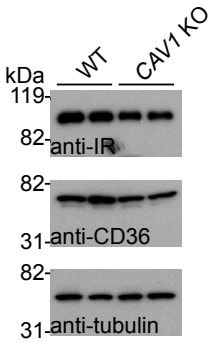

Figure 4.1.1 Insulin receptor and CD36 are found in adipose tissue
Adipose tissue from WT and *caveolin1* knockout mice were isolated and prepared for Western blot. Samples were blotted for insulin receptor beta subunit and CD36 with tubulin as the loading control.
Experiments were conducted three times.

4.1.2 Insulin receptor does not completely colocalise with caveolin1 in primary adipocytes

Pre-adipocytes were cultured and differentiated from gonadal adipose tissue of 6-8 week old mice and stained via indirect immunofluorescence with anti-insulin receptor antibody. Despite the insulin receptor being reported to colocalise extensively with caveolae, confocal microscopy here does not show significant colocalisation between insulin receptor and caveolin1 (Figure 4.1.2 A). Although there appears to be a similar pattern of staining between the insulin receptor and caveolin1, STED microscopy reveals that the limited colocalisation observed here in confocal images was due to the lower resolution of confocal microscopy, as areas that may display colocalisation in confocal images do not in the corresponding STED images (Figure 4.1.2 A, examples arrowed). Instead, the insulin receptor appears to be adjacent to caveolin1. Quantification of the STED images, as described in Materials and Methods, indicate that the observed colocalisation may have arisen by chance as the degree of pixel overlap (i.e. colocalisation) was similar between the original and offset images (Figure 4.1.2 B). As a control, the culture of adipocytes was also stained via indirect immunofluorescence with anti-caveolin1 antibody and two different secondary antibodies with different fluorophores to indicate colocalisation. With this approach, one would expect a significant difference in the amount of colocalising pixels between correctly aligned and offset images. Quantification of this showed a high proportion of colocalising pixels and a significant difference between the original and offset images, as expected (Figure 4.1.2 C).

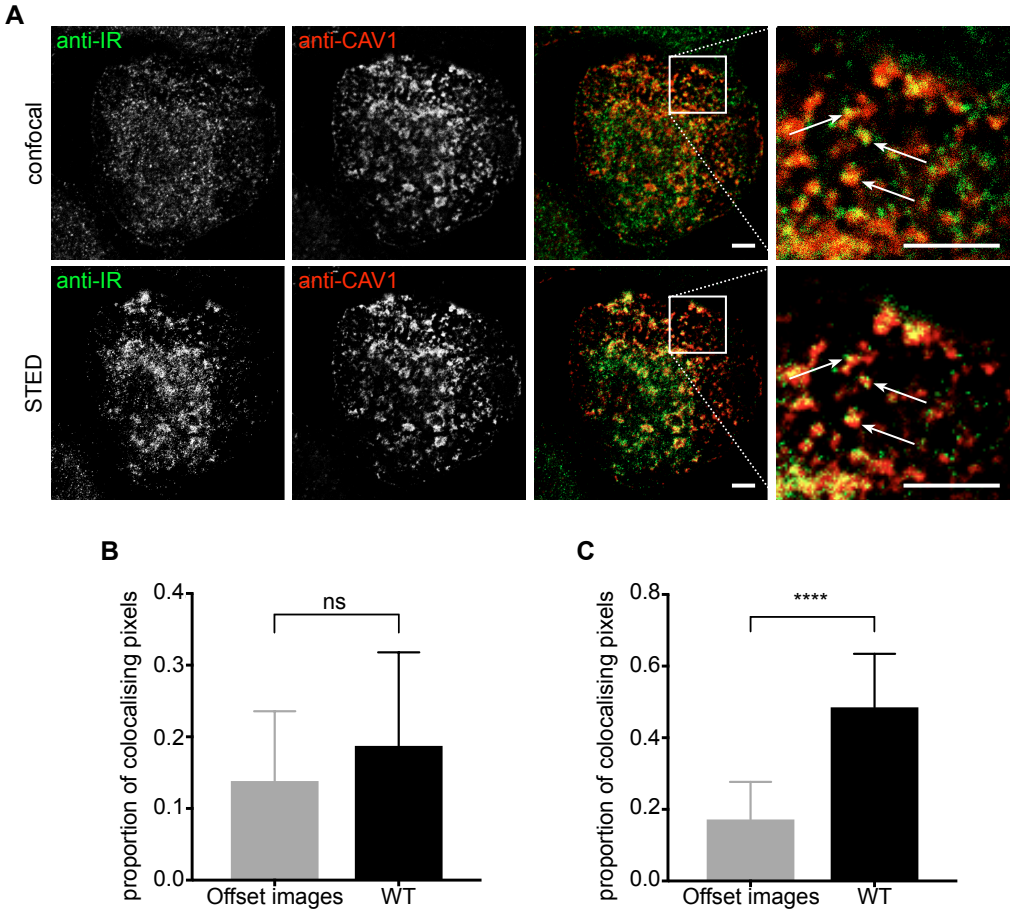

Figure 4.1.2 Insulin receptor does not completely colocalise with caveolin1 in primary adipocytes

A. Confocal and STED microscopy of primary adipocytes stained via indirect immunofluorescence with anti-insulin receptor and anti-caveolin1 antibodies. Bar 5 µm. **B.** Quantification of colocalisation between insulin receptor and caveolin1 in STED. Images were analysed with the two fluorescence channels offset by approx. 0.5 µm to give an indication of the values expected due to chance overlap. Student's t-test, not significant. **C.** Quantification of colocalisation between caveolin1 stained with two different colour fluorophore as a control. Images were analysed as in B. Student's t-test, ****P≤0.0001.

Experiments were conducted three times.

4.1.3 CD36 does not colocalise with caveolin1 in primary adipocytes

Pre-adipocytes were cultured and differentiated from gonadal adipose tissue of 6-8 week old mice and stained via indirect immunofluorescence with anti-CD36 antibody. Confocal microscopy shows that there is very limited colocalisation between CD36 and caveolin1 (Figure 4.1.3 A), and STED microscopy further indicates that the apparent colocalisation observed here is due to close proximity of the proteins. Quantification using a pixel-based mask, as in Figure 4.1.2 B and C, suggests that the colocalisation observed may have arisen by chance as there is no significant difference between wildtype and offset images (Figure 4.1.3 B).

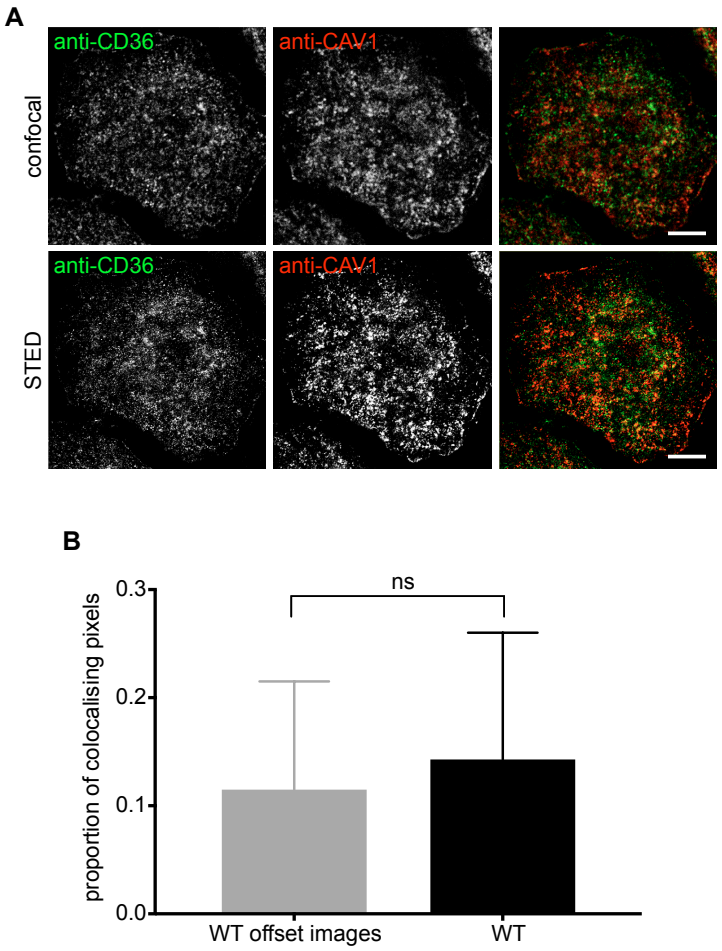

Figure 4.1.3 CD36 does not colocalise with caveolin1 in primary adipocytes
A. Confocal and STED microscopy of primary adipocytes stained via indirect immunofluorescence with anti-CD36 and anti-caveolin1 antibodies. Bar 5 µm. **B.** Quantification of colocalisation between CD36 and caveolin1 in STED. Images were analysed with the two fluorescence channels offset by approx. 0.5 µm to give an indication of the values expected due to chance overlap. Student's t-test, not significant.
Experiments were conducted three times.

4.1.4 Fatty acid uptake does not change significantly in caveolin1 knockout primary adipocytes

Since mice and human lacking caveolin1 display smaller adipocytes, perhaps this may be due to the inability of *caveolin1* knockout cells to uptake fatty acids efficiently [63, 64]. To test this, cultured and differentiated primary pre-adipocytes were loaded with ^{3}H-labelled oleic or palmitic acid at several time points, the cells were then lysed and measured for radioactivity. Uptake of both fatty acids increased as time progressed. However, there was no significant difference in the rate of uptake of oleic or palmitic acid between wildtype and *caveolin1* knockout adipocytes, (Figure 4.1.4 A and B respectively). This suggests that caveolin1 is not crucial in the uptake of fatty acids in adipocytes.

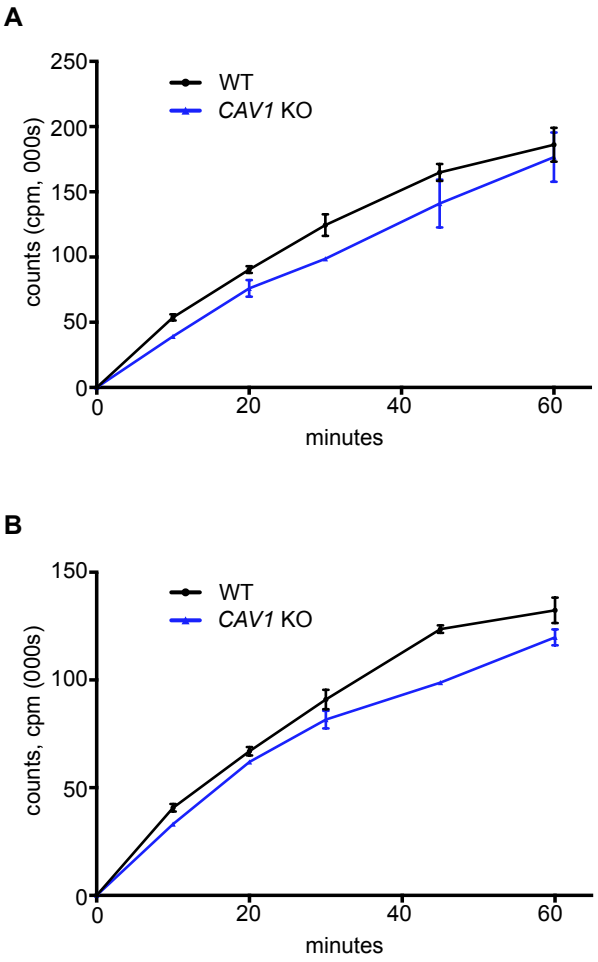

Figure 4.1.4 Fatty acid uptake does not change significantly in *caveolin1* knockout primary adipocytes

A. Wildtype and *caveolin1* knockout primary adipocytes were loaded with oleic acid for the times indicated. Cells were subsequently lysed and uptake measured. **B.** Wildtype and *caveolin1* knockout primary adipocytes were loaded with palmitic acid for the times indicated. Cells were subsequently lysed and uptake measured. Experiments were conducted two times.

4.1.5 Caveolae protect primary adipocytes from repeated mechanical stretch forces

According to the literature and previous published work from the laboratory, caveolae have a mechanoprotective role in cells including endothelial cells. Whether this is also true for adipocytes is not known. Here mouse primary pre-adipocytes were cultured and differentiated from wildtype and *caveolin1* knockout gonadal adipose tissue into flexible silicon chambers that fit into a stretching machine. The cells were stained with Nile Red to visualise lipid droplets, and with SYTOX green, a cell membrane impermeable dye that will stain the nucleus if cell membrane integrity is compromised. Cells were stretched and imaged live on a confocal microscope, with control samples left unstretched. Images acquired showed that upon stretching both wildtype and *caveolin1* knockout adipocytes contained more cells with SYTOX green uptake and were thus susceptible to the stretch forces (Figure 4.1.5 A). The images also showed that *caveolin1* knockout adipocytes were more susceptible to repeated stretch forces than wildtype adipocytes (Figure 4.1.5 A). These observations were confirmed by quantification of the percentage of damaged cells (Figure 4.1.5 B). As expected wildtype and *caveolin1* knockout unstretched control samples had similar low levels of cell damage. *Caveolin1* knockout adipocytes were significantly damaged upon stretching, and is also notably damaged compared to wildtype adipocytes that were also stretched.

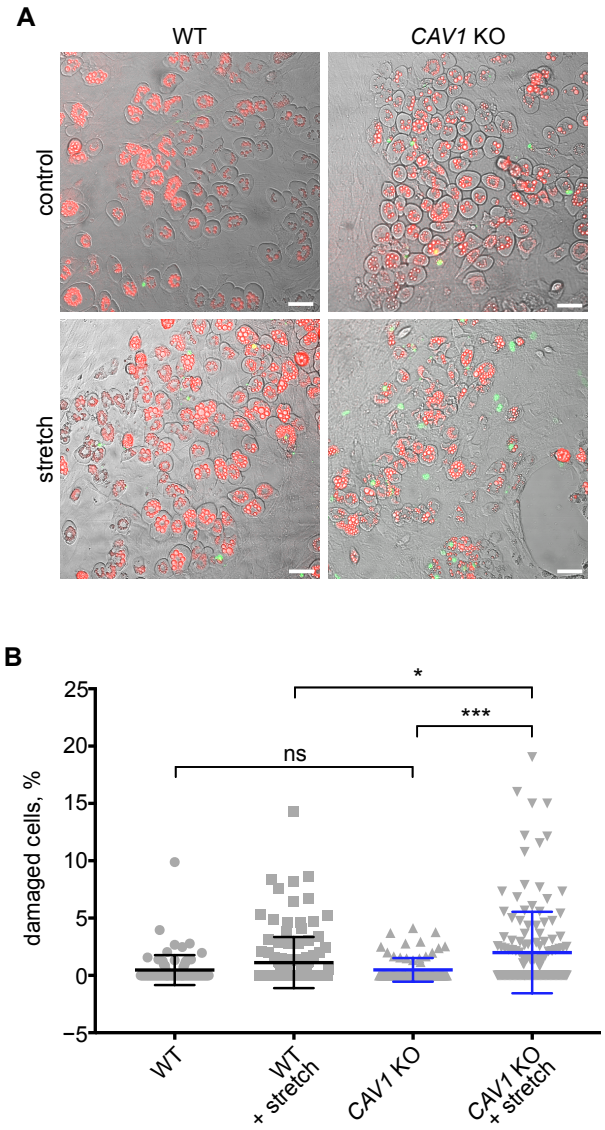

Figure 4.1.5 Caveolae protect primary adipocytes from repeated mechanical stretch forces

A. Confocal images of wildtype and *caveolin1* knockout primary adipocytes that were stained with Nile Red and subsequently stretched with SYTOX Green for 10 minutes at 1 Hz by 20% extensions. Bar 50 µm. **B.** Quantification of the incidence of plasma membrane rupture expressed as the proportion of the total number of adipocytes that have green nucleus staining. Each point represents one field of cells acquired from 6 individual experiments. Student's t-test, *P≤0.05, ***P≤0.001 and not significant. Experiments were conducted three times.

4.1.6 Caveolae have a potential mechanoprotective role in adipose tissue in vivo

In addition to assessing the mechanoprotective role of caveolae *in vitro*, this was also assessed *in vivo*. Mice aged approximately 20 weeks were injected with a propidium iodide and FITC-albumin solution and agitated on a machine, as described in Materials and Methods. Propidium iodide was used analogously to SYTOX green in that nuclei of cells will stain red if the cell membrane integrity is compromised. After stretching, subcutaneous adipose tissue was removed from the mice and imaged on a multiphoton confocal microscope, with control samples unagitated. Images acquired were quantified by the number of broken cells per 10 μm of tissue imaged. Images acquired from subcutaneous adipose tissue from male mice on a normal chow diet were quantified and revealed a significant difference between wildtype and *caveolin1* knockout when the mice were subjected to mechanical stress (Figure 4.1.6 A). There was no significant difference seen between wildtype and *caveolin1* knockout controls, nor in *caveolin1* knockout mice with and without stretching. Mice were fed a high fat to challenge the adipocytes and again, images were acquired from subcutaneous adipose tissue from both male and female mice with and without agitation. A notable difference was observed in the *caveolin1* knockout mice upon agitation (Figure 4.1.6 B). As expected, adipose tissue containing caveolae were not perturbed even upon mechanical stress (Figure 4.1.6 A and B). Even though the mechanical perturbation in these experiments is arbitrary and may vary from mouse to mouse, it is remarkable that statistically significant changes between wildtype and *caveolin1* knockout mice can be detected.

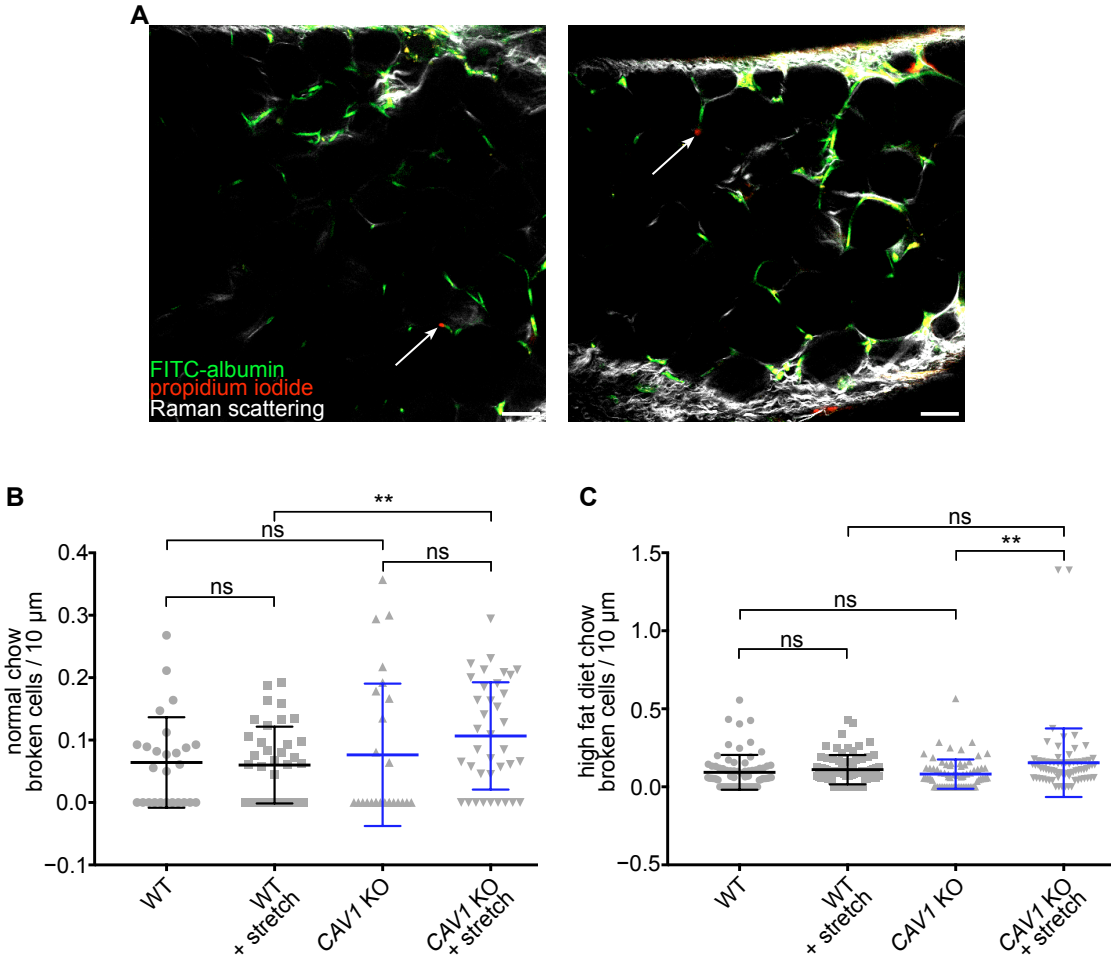

Figure 4.1.6 Caveolae have a potential mechanoprotective role in adipose tissue *in vivo*

A. Examples images of wildtype and *caveolin1* knockout adipose tissue from mice that were either agitated for 20 minutes or un-agitated. Mice were injected with FITC-albumin (green) to indicate blood vessels and propidium iodide (red) to stain the nuclei of damaged cells. White signal is as a result of Raman scattering of connective tissue. Bar 50 µm. **B.** Quantification of the incidence of plasma membrane rupture expressed as the number of broken cells per 10 µm of adipose tissue. Each point represents one field of cells acquired from 5 individual mice, with 5 images per mouse. Student's t-test, **P≤0.01 and not significant. **C.** Quantification of the incidence of plasma membrane rupture expressed as the number of broken cells per 10 µm of adipose tissue. Each point represents one field of cells acquired from 15 individual high-fat diet mice, with 5 images per mouse. Student's t-test, **P≤0.01 and not significant.

Experiments were conducted once.

4.2 Discussion

The results presented here shed a different light onto previously published data with regards to insulin receptor colocalisation to caveolae. In addition, the findings related to CD36 do not fully corroborate the current literature. Despite this, stretching experiments have shown a mechanoprotective role of caveolae in adipocytes, which is in agreement with this role of caveolae [101, 102].

Both human and mice lacking caveolae display a striking set of phenotypes [12, 16-18]. They are lipodystrophic, and mice lacking caveolae are insulin resistant and have impaired glucose tolerance. This has led to caveolae being associated with the insulin receptor and CD36, as a postulated role of caveolae is to act as a signalling platform for other proteins [44, 236, 237]. Both insulin receptor and CD36 are present in adipose tissue of wildtype and *caveolin1* knockout, however evidence indicating their relationship with caveolar proteins is dubious, especially since no difference is seen here in the levels of these proteins in wildtype and *caveolin1* knockout tissues (Figure 4.1.1).

Insulin receptor has been shown to colocalise with caveolae, despite this, super-resolution microscopy used here has not shown that this is the case (Figure 4.1.2) [44-46]. Previous experiments demonstrating this colocalisation were performed almost 20 years ago and used confocal microscopy only [45]. In addition to the development of super-resolution microscopy, confocal microscopy has developed and progressed much more since then and with better techniques it may be that observations noted during those studies may not be the case now. In the early experiments, colocalisation between caveolin1 and the insulin receptor was observed in isolated adipocyte plasma membrane sheets rather than the native cell [45, 217]. This technique may have lent to the increased colocalisation observed. Another error in technique that has led to caveolae being associated with the insulin receptor may be the use of overexpressed caveolin1 and the solubilisation of caveolae. A study performed by Nystrom *et al*. claims that caveolin1 can immunoprecipitate with the insulin receptor [77]. The immunoprecipitation was performed using overexpressed caveolin1 and the insulin receptor, ergo the expression levels of these proteins were not at their endogenous

levels. In addition, this study used 1% (v/v) Triton X-100 and 0.1% (w/v) SDS as the method of solubilisation, which may not be sufficient enough to fully solubilise caveolae as they are highly detergent-resistant membrane structures. If solubilisation of caveolae is not sufficient, any protein that displays similar resistance to solubilisation could co-immunoprecipitate with it. This seems to be the case for the insulin receptor, as Western blots and STED microscopy here reveals that the insulin receptor is indeed in adipocytes, thus if solubilisation was not sufficient it would not be implausible for the insulin receptor to co-immunoprecipitate with caveolin1. Although the insulin receptor has been reported to localise to the neck of caveolae in 3T3 L1 adipocytes by electron microscopy, it has not been replicated [214]. Commercial antibodies against the insulin receptor do not perform as expected, with most of them creating a significant level of background. It may also be non-specific binding or artefacts of electron microscopy. Intriguingly, although the insulin receptor does not colocalise with caveolin1, its proximity to caveolae suggests a degree of organisation, but the data implies that the insulin receptor is not directly recruited by caveolae.

Another postulated role of caveolae in adipocytes is that they protect the cells from fatty acid-mediated lipotoxicity. CD36 is a fatty acid translocase and CD36-mediated fatty acid uptake is said to require plasma membrane rafts. Despite studies indicating that CD36 is associated with caveolin1, there has been no evidence available to show the direct colocalisation of these two proteins. STED microscopy here reveals that CD36 and caveolin1 do not colocalise (Figure 4.1.3). Evidence such as the fractionations performed by Ring *et al*. show CD36 in the same fraction as caveolin1 [237]. This, again, may be due to the solubilisation methods employed in the experiment. Only 1% Triton X-100 was used as the detergent for solubilisation, which is not sufficient to fully solubilise detergent resistant membranes. Therefore, since CD36 is present in adipocytes and has been associated to lipid rafts, it is likely that it would run in the same fraction as caveolin1 because of its close proximity to caveolae [58, 236]. The study observed that in *caveolin1* knockout MEFs CD36 was absent from lipid raft-enriched membrane fractions, which contain detergent-resistant membranes. It implicates that caveolin1 is required for CD36 stabilisation at the plasma membrane, which may be true. However, the evidence does not indicate whether or not this effect is directly due to the lack of caveolin1. It may well be a

downstream effect of caveolae as they have been connected with signalling events [19].

A non-direct interaction between caveolin1 and CD36 correlates well with the fatty acid uptake data. Since CD36 is a fatty acid translocase, if it were directly affected by caveolin1 then one would expect that fatty acid uptake would be perturbed in cells lacking caveolin1. This was not the case, as there was no significant difference in uptake in wildtype and *caveolin1* knockout cells, nor between the two types of fatty acids used – the short-chain oleic acid and the long-chain saturated palmitic acid (Figure 4.1.4). Palmitic acid uptake was slightly less efficient than oleic acid and may be ascribed to the more saturated nature of palmitic acid. However, it should be noted that the lack of clear effects observed here is not necessarily dependent on CD36, and may be due to other fatty acid transport proteins functioning efficiently. It seems that fatty acid uptake remains normal in cells lacking caveolae so fatty acid-mediated lipotoxicity is most likely not due to the cell's inability to uptake fatty acid. It may be perhaps due to the smaller sized adipocytes when cells are missing caveolae as the cells cannot expand further without the help of extra membrane provided by caveolae.

The morphology of caveolae lends itself to being a reservoir for membrane and studies have indicated that this is in fact the case in endothelial and epithelial cells [98, 101, 102]. Adipocytes are inherently fragile cells due to their thin layer of cytoplasm and negligible cytoskeletal network, and the results shown here are in agreement with the mechanoprotective role of caveolae [256, 257]. Primary adipocytes lacking caveolae were more susceptible to repeated mechanical stretch forces than adipocytes containing caveolae (Figure 4.1.5). Whether this is due to a mechanical role of caveolae flattening out, or perturbation of caveolae signalling is yet to be established. The susceptibility of adipocytes lacking caveolae to stress forces and damage lends itself well to the characteristics seen in the adipose tissue of *caveolin1* knockout mice. The protective role of caveolae in adipocytes here is extended into *in vivo* studies, as when adipose tissue obtained from mice that were massaged across the abdomen, a significant, but more variable, difference was observed (Figure 4.1.6). This variation between *in vitro* and *in vivo* data may be due to differences between the mice and also may be due to the less direct agitation experienced by the mice. Primary adipocytes were grown directly on the substrate that

was stretched whereas the mice were agitated externally meaning that the skin may have protected the tissue from damage. It may also be due to the agitation not being vigorous enough. Despite the variables, caveolae are still seen to protect adipose tissue from mechanical forces, and perhaps with more robust stress a more pronounced result may be observed. The inflammation and macrophage infiltration seen in the adipose tissue of these mice, but not in wildtype mice, may be triggered by the more fragile and rupturing adipocytes.

The adipocyte-related phenotypes observed in mice and humans may be purely due to the lack of caveolae giving rise to more vulnerable cells, and not because caveolin1 is associated with the insulin receptor and CD36, and thus their downstream signalling pathways. Changes in adipocyte physiology may be sole the reason for the phenotypes seen. Lipodystrophy may occur because the cells lack the ability to expand and so cannot uptake the normal amount of fatty acids, rather than because fatty acid uptake is perturbed due to caveolin1 associations with CD36. Fatty acid-mediated lipotoxicity may result from the cell's inefficiency to store normal levels of fatty acids hence they remain outside of the cell and cause lipotoxicity that way, rather than being caused by inefficient uptake. It may also result from the cell's higher propensity to rupture and therefore release of fatty acids as it does so. These imbalances in adipocyte physiology may be contributing to the insulin resistant and glucose intolerant phenotype observed in mice, as studies have shown that perturbing adipocytes may lead to many complications in the normal functions [220, 221].

Chapter 5: Final discussion

Since their identification in 1953, work on caveolae has progressed. Major proteins involved have been identified. The structure and function of caveolae is slowly being unravelled. Caveolae have been implicated in processes from signalling to mechanoprotection to cancer. However, though our understanding of caveolae has advanced, confounding data in the literature has made it difficult to fully explain the roles of caveolae. Some uncertainties have arisen from unsuitable techniques employed to study caveolae, such as the overexpression of caveolin1 and insufficient solubilisation of caveolae. In addition, some important questions remain such as how exactly do caveolae assemble and disassemble, what exact proteins are involved and when are they involved? Also, do caveolae have a direct role in signalling or is it indirect? And is the mechanoprotective role of caveolae a direct effect of caveolae flattening out to buffer stretch forces, or is it because of signalling effects consequent to the flattening of caveolae? Advances in techniques such as super-resolution microscopy and genome editing, amongst others, will allow for the careful dissection of caveolar biology.

5.1 Formation and regulation of caveolae

Over the years, key proteins contributing to the morphology of caveolae have been identified and other protein players involved have also been discovered. Caveolin1 and cavin1 are the major proteins responsible for generating caveolae in non-muscle tissues. Caveolin1 is synthesised and homo-oligomerised in the endoplasmic reticulum, then transported to the Golgi where it assembles into larger complexes [133-135]. These assemblies are delivered to the plasma membrane where hetero-oligomeric cavin complexes associate with it, generating the caveolar bulb [25, 62]. Caveolae bulbs cannot form in the absence of either of the proteins and caveolin1 is degraded in the absence of cavin, vice versa. Flat patches of caveolae are seen in deep etched electron micrographs but whether or not these flat patches are caveolae in the process of budding, or whether they are caveolae that have flattened out after its formation is unclear [12, 123, 139].

Caveolae are composed of more than just the caveolar coat complex, EHD proteins, PACSIN2 and dynamin2 are involved. However, the exact mechanisms by which these proteins act is still in question. It is known that EHD2, located at the neck, cycles on and off caveolae. The slow ATP hydrolysis rate allows for the slow and tightly controlled dynamics of caveolae [33, 34, 178]. The absence of EHD proteins increases the dynamics of caveolae confirming the role of EHD proteins as stabilising caveolae at the membrane. In addition, clusters of caveolae are lost when EHD proteins are absent, highlighting a key role for EHD proteins in the formation of caveolar clusters. Additionally, EHD proteins appear to be involved in the quick re-formation of caveolae after disassembly. Individual caveolae are still present in cells lacking EHD proteins, but upon stretch forces, even the individual caveolae are lost, suggesting a role for EHD proteins in the quick assembly of caveolae after stress. As a consequence, the cells lacking EHD proteins are more likely to rupture. There is also an increase of flat caveolae in cells lacking EHD proteins, which reinforces the idea that EHD proteins are important for the formation of caveolae clusters.

It is evident that caveolae clusters, formed in the presence of EHD proteins, are important for protecting the cell. Yet in the absence of EHD proteins, caveolae still form, they are slightly more dynamic, but they do not endocytose more. This may be in part due to PACSIN2 as there is a significant increase in its recruitment to caveolae when EHD proteins are lacking. PACSIN2 bends membranes and is said to be involved in the step from flat to bulb [127]. EHD2 associates with caveolae to bend membrane at the neck and stabilises it until it disassembles and dissociates making caveolae more mobile. The increase of PACSIN2 recruitment to caveolae may be because EHD proteins are not there to stabilise caveolae, or perhaps EHD proteins are not there to release PACSIN2 to take its place, as limited colocalisation is seen between caveolae and PACSIN2 whereas colocalisation between EHD2 and caveolae is extensive [33, 127]. A probable model may be that upon formation of the bulb by caveolin1 and cavin1 oligomers, PACSIN2 recognises the curvature and binds. EHD2 is recruited, and in the absence of it, EHD1 and EHD4 compensate, and PACSIN2 is released, explaining its association to only a subpopulation of caveolae. However, when there is a lack of all EHD proteins, PACSIN2 is not released resulting in its increased localisation to caveolae. PACSIN2 is in its unphosphorylated state when it is released from caveolae by EHD proteins. When it is necessary for caveolae to bud

and endocytose, PACSIN2 is recruited, possibly by EHD proteins, and is phosphorylated, releasing autoinhibition of SH3 binding, allowing for dynamin2 to be recruited. This is speculative and further work into the dynamics of these associated proteins is required. Experiments using cells with endogenously tagged PACSIN2, and *PACSIN2* gene knockout cells will provide valuable insights into its role in caveolar biology.

5.2 Caveolae in signalling

There is no doubt that caveolae are involved in signalling pathways, but the question is whether or not caveolar proteins are the direct effectors, or if aberrant signalling is due to the loss of membrane organisation by caveolar bulbs [19, 123]. Proteins have been suggested to bind to caveolae through CBD/CSD interactions, but this has been undermined by the structural analysis of caveolin1 [85, 86]. In relation to adipocytes and the insulin receptor, the lack of obvious colocalisation between caveolae and the insulin receptor suggests that the effects of caveolae on insulin signalling may not be direct. This supports the data in the literature with regards to the dissociation of the insulin receptor and caveolae. Although the insulin receptor may not be directly associated with caveolae, it is possible that it resides in close proximity to the detergent resistant caveolae. And that in the absence of caveolae, the propensity for insulin receptor to accumulate decreases, thereby decreasing its activity. Caveolae may act as a platform for the signalling and function of proteins. This may be the case for CD36 whereby a lack of obvious colocalisation between caveolae and CD36 was observed, despite it being reported to associate with caveolae [59, 237]. Caveolin1 and CD36 have been reported to play a role in transmembrane fatty acid movement, both together and independently [54, 59, 226, 234, 235, 237]. The ability of caveolin1 alone to regulate fatty acid transport suggests that CD36 may not be so important but there are defects seen in mice lacking CD36. The results in this study indicated that fatty acid uptake was not influenced by caveolin1, and that it did not colocalise with CD36 [59]. So perhaps the increase in free fatty acid levels may be due to another reason. One such reason may be that adipocytes have less membrane to buffer tension and are more fragile. With that, when they experience stress or an increase in the uptake of fatty acids, they are more likely to break therefore releasing its contents.

This lipotoxicity may cause aberrant insulin signalling, implying that adipocyte-related phenotypes observed when lacking caveolae may not be due to the insulin receptor or CD36, but rather a mechanoprotective role of caveolae in adipocytes.

Despite the uncertainties in the field, the lack of caveolae includes more phenotypes other than the ones observed in relation to adipocytes and it cannot be denied that caveolae have a role in signalling. Whether the effects are directly due to caveolar proteins interacting with signalling proteins, or whether the effects are due to caveolae acting as signalling platforms requires clarification. Whilst the experiments in this study only investigate the association of caveolae with specific proteins, much work is needed to be done to confirm or contradict the other signalling proteins reported to be associated with caveolae. It is quite possible that although the signalling proteins do not bind directly to caveolar proteins, they may reside in the same detergent resistant fraction and as such are perturbed when caveolae are not present. Whether or not caveolae have a direct role in signalling is still unclear, but the effects of not having caveolae indicates its importance in signalling events.

5.3 Mechanoprotection

Caveolae have been shown to have a mechanoprotective role both in the literature and in the experiments in the studies here. The suggestion is that caveolae flatten out in response to mechanical stress thereby protecting the plasma membrane from rupture [98, 99]. However, what cannot be concluded from the experiments is that whether the mechanoprotective role of caveolae is solely due to the flattening of the convolutions or if the flattening of the bulbs initiates a signalling cascade which protects the cells from damage. Data have shown that upon stress cavin1 is released from caveolin1 and therefore caveolae are lost. The protective role of caveolae in this context may of course be due to the flattening of morphologically defined caveolar bulbs, but it could also be an effect of signalling due to the release of proteins from the detergent resistant region. In fact, it may also be due to cavin1, which was originally discovered as a regulator of transcription. It is clear that clusters of caveolae are important in protecting cells from membrane damage, but instead of the clusters providing even more membrane surface than individual caveolae, it could be

possible that clusters represent more aggregated signalling molecules that help protect the cell, and when caveolae clusters are absent cells are protected to a lesser extent. There is also the possibility that caveolae represent two lines of defence for the protection of the cell from mechanical stress. The first more immediate defence is the physical flattening of caveolae to provide more membrane surface area, and when that occurs the flattening triggers the second line of defence, the dissociation of proteins, some of which provide signals to the cell. These signals prepare the cell for membrane damage control such as triggering membrane repair pathways. The role of caveolae as mechanoprotectors is appealing and evidence for this is growing. Adipocyte-related phenotypes observed in mice and humans lacking caveolae can be explained by the simple concept of caveolae protecting cells from mechanical stress. In absence of caveolae, adipocytes are smaller in size due to a decrease in the capacity of the cells to provide more membrane surface area, as caveolae are not present to do so. Because of this, upon an increase of stress forces, the adipocytes rupture, releasing fatty acids and thus leading to lipotoxicity. This lipotoxicity affects insulin signalling causing insulin resistance and impaired glucose tolerance, phenotypes observed in mice and humans lacking caveolae.

5.4 Future directions

It is clear that there is more to the caveolar neck than EHD proteins. How exactly caveolae are formed is still unknown. Caveolins are synthesised at the rough endoplasmic reticulum where they homo-oligomerise and are transported to the Golgi. Here, they are assembled into larger complexes, which are then delivered to the plasma membrane. Cavin complexes that have assembled in the cytosol associate with caveolin at the plasma membrane. How this recruitment of cavin to membrane-bound caveolin occurs is unclear, and whether or not the association of cavin to membrane-bound caveolin initiates the formation of the bulb is also unclear. It is possible that the association of cavin to membrane-bound caveolin causes the plasma membrane to bend, and it is this curvature that recruits the membrane-shaping protein PACSIN2, to help invaginate caveolae. EHD proteins, mainly EHD2, could then get recruited, displace PACSIN2, and stabilise caveolae at the plasma membrane. Upon stretch forces, caveolae can flatten out and rapidly invaginate again with the aid of EHD

proteins. This possible mechanism regarding EHD proteins displacing PACSIN2 is highly speculative and further experiments are required to clarify the actual sequence of events.

To assess the functions of PACSIN2 in caveolar biology, it would be necessary to understand what happens to caveolae in the absence of PACSIN2. A more physiological method of achieving this would be to generate PACSIN2 knockout cells via genome-editing. Electron microscopy and immunofluorescence experiments would allow one to examine the morphology of caveolae and the distribution of caveolae, respectively. According to the speculative model presented in Figure 3.2, in the absence of PACSIN2, caveolae bulbs are not formed and thus cavin and caveolin proteins should remain at the plasma membrane as flat caveolae. In electron microscopy, this would present itself as a lack of caveolae bulbs accompanied by an increase in flat caveolae. And in immunofluorescence, cavin and caveolin should still colocalise with each other. However, if this is not the case it would be interesting to see if caveolae bulbs are still generated in the absence of PACSIN2 and EHD proteins. Experiments assessing the dynamics, abundance and turnover of caveolae in cells lacking PACSIN2, and PACSIN2 and EHD proteins would also aid in the dissection of how caveolae are generated and regulated.

The phenotypes observed in mice and humans lacking caveolae implicate caveolae as being involved in adipocyte metabolism. More exhaustive and robust experiments are required to fully understand the relationship between caveolae and adipocytes. In particular, whether caveolae affect the uptake of lipids and whether a more significant effect on adipocytes after mechanical force can be seen *in vivo* using a more vigorous approach. Experiments to investigate whether or not the adipocyte-related phenotypes are solely due to caveolae acting as a membrane buffer for tension, or if caveolae are involved in lipid uptake and regulation, would be valuable. These experiments can include lipid uptake experiments in cells with and without caveolae while also taking into account other methods of lipid uptake, such as transport through FATPs.

Since the discovery of caveolae, there has been much progress in the identification of the proteins involved and the complexes they form. The next big advance would be to elucidate the exact mechanisms by which these bulbs are formed. At which step are

the non-essential associated proteins recruited? Upon flattening out, what are the dynamics of re-formation? How exactly are clusters of caveolae formed? If EHD proteins are redundant with each other, are there perhaps other membrane-bending proteins, which have a similar function, involved? If so, then how and when? And what are the exact proteins associated to caveolar proteins and caveolar bulbs. By understanding the exact mechanisms of caveolae and the exact proteins involved, the precise functions of caveolae can be defined. Although there is still much controversy in the field regarding the association of different proteins and thus the functions of caveolae, these little tiny caves have intrigued researchers to this day.

Bibliography

1. Cooper, G.M., *Structure of the Plasma Membrane*, in *The Cell: A Molecular Approach*. 2000, Sinauer Associates.
2. Palade, G.E., *Fine structure of blood capillaries.* J Appl Phys, 1953. **24**: p. 1424.
3. Yamada, E., *The fine structure of the gall bladder epithelium of the mouse.* J Biophys Biochem Cytol, 1955. **1**(5): p. 445-58.
4. Rothberg, K.G., et al., *Caveolin, a protein component of caveolae membrane coats.* Cell, 1992. **68**(4): p. 673-82.
5. Scherer, P.E., et al., *Identification, sequence, and expression of caveolin-2 defines a caveolin gene family.* Proc Natl Acad Sci U S A, 1996. **93**(1): p. 131-5.
6. Way, M. and R.G. Parton, *M-caveolin, a muscle-specific caveolin-related protein.* FEBS Lett, 1996. **378**(1): p. 108-12.
7. Tang, Z., et al., *Molecular cloning of caveolin-3, a novel member of the caveolin gene family expressed predominantly in muscle.* J Biol Chem, 1996. **271**(4): p. 2255-61.
8. Vinten, J., et al., *Identification of a major protein on the cytosolic face of caveolae.* Biochim Biophys Acta, 2005. **1717**(1): p. 34-40.
9. McMahon, K.A., et al., *SRBC/cavin-3 is a caveolin adapter protein that regulates caveolae function.* Embo j, 2009. **28**(8): p. 1001-15.
10. Bastiani, M., et al., *MURC/Cavin-4 and cavin family members form tissue-specific caveolar complexes.* J Cell Biol, 2009. **185**(7): p. 1259-73.
11. Jansa, P., et al., *Cloning and functional characterization of PTRF, a novel protein which induces dissociation of paused ternary transcription complexes.* Embo j, 1998. **17**(10): p. 2855-64.
12. Liu, L., et al., *Deletion of Cavin/PTRF causes global loss of caveolae, dyslipidemia, and glucose intolerance.* Cell Metab, 2008. **8**(4): p. 310-7.
13. Gustincich, S. and C. Schneider, *Serum deprivation response gene is induced by serum starvation but not by contact inhibition.* Cell Growth Differ, 1993. **4**(9): p. 753-60.
14. Izumi, Y., et al., *A protein kinase Cdelta-binding protein SRBC whose expression is induced by serum starvation.* J Biol Chem, 1997. **272**(11): p. 7381-9.
15. Ogata, T., et al., *MURC, a muscle-restricted coiled-coil protein that modulates the Rho/ROCK pathway, induces cardiac dysfunction and conduction disturbance.* Mol Cell Biol, 2008. **28**(10): p. 3424-36.
16. Ardissone, A., et al., *Novel PTRF mutation in a child with mild myopathy and very mild congenital lipodystrophy.* BMC Med Genet, 2013. **14**: p. 89.
17. Dwianingsih, E.K., et al., *A Japanese child with asymptomatic elevation of serum creatine kinase shows PTRF-CAVIN mutation matching with congenital generalized lipodystrophy type 4.* Mol Genet Metab, 2010. **101**(2-3): p. 233-7.
18. Rajab, A., et al., *Fatal cardiac arrhythmia and long-QT syndrome in a new form of congenital generalized lipodystrophy with muscle rippling (CGL4) due to PTRF-CAVIN mutations.* PLoS Genet, 2010. **6**(3): p. e1000874.
19. Cheng, J.P. and B.J. Nichols, *Caveolae: One Function or Many?* Trends Cell Biol, 2016. **26**(3): p. 177-89.

20. Hayer, A., et al., *Caveolin-1 is ubiquitinated and targeted to intralumenal vesicles in endolysosomes for degradation.* J Cell Biol, 2010. **191**(3): p. 615-29.
21. Shvets, E., et al., *Dynamic caveolae exclude bulk membrane proteins and are required for sorting of excess glycosphingolipids.* Nat Commun, 2015. **6**: p. 6867.
22. Milici, A.J., et al., *Transcytosis of albumin in capillary endothelium.* J Cell Biol, 1987. **105**(6 Pt 1): p. 2603-12.
23. Pelkmans, L., et al., *Caveolin-stabilized membrane domains as multifunctional transport and sorting devices in endocytic membrane traffic.* Cell, 2004. **118**(6): p. 767-80.
24. Thomsen, P., et al., *Caveolae are highly immobile plasma membrane microdomains, which are not involved in constitutive endocytic trafficking.* Mol Biol Cell, 2002. **13**(1): p. 238-50.
25. Tagawa, A., et al., *Assembly and trafficking of caveolar domains in the cell: caveolae as stable, cargo-triggered, vesicular transporters.* J Cell Biol, 2005. **170**(5): p. 769-79.
26. Kirkham, M., et al., *Ultrastructural identification of uncoated caveolin-independent early endocytic vehicles.* J Cell Biol, 2005. **168**(3): p. 465-76.
27. Oh, P., et al., *Live dynamic imaging of caveolae pumping targeted antibody rapidly and specifically across endothelium in the lung.* Nat Biotechnol, 2007. **25**(3): p. 327-37.
28. Liu, L., et al., *Cavin-3 knockout mice show that cavin-3 is not essential for caveolae formation, for maintenance of body composition, or for glucose tolerance.* PLoS One, 2014. **9**(7): p. e102935.
29. Mohan, J., et al., *Cavin3 interacts with cavin1 and caveolin1 to increase surface dynamics of caveolae.* J Cell Sci, 2015. **128**(5): p. 979-91.
30. Senju, Y., et al., *Essential role of PACSIN2/syndapin-II in caveolae membrane sculpting.* J Cell Sci, 2011. **124**(Pt 12): p. 2032-40.
31. Henley, J.R., et al., *Dynamin-mediated internalization of caveolae.* J Cell Biol, 1998. **141**(1): p. 85-99.
32. Oh, P., D.P. McIntosh, and J.E. Schnitzer, *Dynamin at the neck of caveolae mediates their budding to form transport vesicles by GTP-driven fission from the plasma membrane of endothelium.* J Cell Biol, 1998. **141**(1): p. 101-14.
33. Stoeber, M., et al., *Oligomers of the ATPase EHD2 confine caveolae to the plasma membrane through association with actin.* Embo j, 2012. **31**(10): p. 2350-64.
34. Moren, B., et al., *EHD2 regulates caveolar dynamics via ATP-driven targeting and oligomerization.* Mol Biol Cell, 2012. **23**(7): p. 1316-29.
35. Senju, Y., et al., *Phosphorylation of PACSIN2 by protein kinase C triggers the removal of caveolae from the plasma membrane.* J Cell Sci, 2015. **128**(15): p. 2766-80.
36. Pelkmans, L., J. Kartenbeck, and A. Helenius, *Caveolar endocytosis of simian virus 40 reveals a new two-step vesicular-transport pathway to the ER.* Nat Cell Biol, 2001. **3**(5): p. 473-83.
37. Pelkmans, L., D. Puntener, and A. Helenius, *Local actin polymerization and dynamin recruitment in SV40-induced internalization of caveolae.* Science, 2002. **296**(5567): p. 535-9.

38. Damm, E.M., et al., *Clathrin- and caveolin-1-independent endocytosis: entry of simian virus 40 into cells devoid of caveolae.* J Cell Biol, 2005. **168**(3): p. 477-88.
39. Engel, S., et al., *Role of endosomes in simian virus 40 entry and infection.* J Virol, 2011. **85**(9): p. 4198-211.
40. Torgersen, M.L., et al., *Internalization of cholera toxin by different endocytic mechanisms.* J Cell Sci, 2001. **114**(Pt 20): p. 3737-47.
41. Hansen, G.H., et al., *Cholera toxin entry into pig enterocytes occurs via a lipid raft- and clathrin-dependent mechanism.* Biochemistry, 2005. **44**(3): p. 873-82.
42. Parton, R.G., *Ultrastructural localization of gangliosides; GM1 is concentrated in caveolae.* J Histochem Cytochem, 1994. **42**(2): p. 155-66.
43. Bitsikas, V., I.R. Correa, Jr., and B.J. Nichols, *Clathrin-independent pathways do not contribute significantly to endocytic flux.* Elife, 2014. **3**: p. e03970.
44. Stralfors, P., *Caveolins and caveolae, roles in insulin signalling and diabetes.* Adv Exp Med Biol, 2012. **729**: p. 111-26.
45. Gustavsson, J., et al., *Localization of the insulin receptor in caveolae of adipocyte plasma membrane.* Faseb j, 1999. **13**(14): p. 1961-71.
46. Fagerholm, S., et al., *Rapid insulin-dependent endocytosis of the insulin receptor by caveolae in primary adipocytes.* PLoS One, 2009. **4**(6): p. e5985.
47. Patel, H.H., F. Murray, and P.A. Insel, *G-protein-coupled receptor-signaling components in membrane raft and caveolae microdomains.* Handb Exp Pharmacol, 2008(186): p. 167-84.
48. Cheng, Z.J., et al., *Membrane microdomains, caveolae, and caveolar endocytosis of sphingolipids.* Mol Membr Biol, 2006. **23**(1): p. 101-10.
49. Sharma, D.K., et al., *Selective stimulation of caveolar endocytosis by glycosphingolipids and cholesterol.* Mol Biol Cell, 2004. **15**(7): p. 3114-22.
50. Schaefer, R.J., et al., *1,25 Dihydroxyvitamin D3 uptake is localized at caveolae and requires caveolar function.* J Biomed Nanotechnol, 2013. **9**(10): p. 1707-15.
51. Lin, H.Y., et al., *Caveolar endocytosis is required for human PSGL-1-mediated enterovirus 71 infection.* J Virol, 2013. **87**(16): p. 9064-76.
52. Thorn, H., et al., *Cell surface orifices of caveolae and localization of caveolin to the necks of caveolae in adipocytes.* Mol Biol Cell, 2003. **14**(10): p. 3967-76.
53. Murata, M., et al., *VIP21/caveolin is a cholesterol-binding protein.* Proc Natl Acad Sci U S A, 1995. **92**(22): p. 10339-43.
54. Trigatti, B.L., R.G. Anderson, and G.E. Gerber, *Identification of caveolin-1 as a fatty acid binding protein.* Biochem Biophys Res Commun, 1999. **255**(1): p. 34-9.
55. Martin, S. and R.G. Parton, *Caveolin, cholesterol, and lipid bodies.* Semin Cell Dev Biol, 2005. **16**(2): p. 163-74.
56. Pol, A., et al., *Dynamic and regulated association of caveolin with lipid bodies: modulation of lipid body motility and function by a dominant negative mutant.* Mol Biol Cell, 2004. **15**(1): p. 99-110.
57. Brasaemle, D.L., et al., *Proteomic analysis of proteins associated with lipid droplets of basal and lipolytically stimulated 3T3-L1 adipocytes.* J Biol Chem, 2004. **279**(45): p. 46835-42.
58. Pohl, J., et al., *Long-chain fatty acid uptake into adipocytes depends on lipid raft function.* Biochemistry, 2004. **43**(14): p. 4179-87.

59. Meshulam, T., et al., *Role of caveolin-1 and cholesterol in transmembrane fatty acid movement.* Biochemistry, 2006. **45**(9): p. 2882-93.
60. Simard, J.R., et al., *Caveolins sequester FA on the cytoplasmic leaflet of the plasma membrane, augment triglyceride formation, and protect cells from lipotoxicity.* J Lipid Res, 2010. **51**(5): p. 914-22.
61. Pol, A., et al., *Cholesterol and fatty acids regulate dynamic caveolin trafficking through the Golgi complex and between the cell surface and lipid bodies.* Mol Biol Cell, 2005. **16**(4): p. 2091-105.
62. Hayer, A., et al., *Biogenesis of caveolae: stepwise assembly of large caveolin and cavin complexes.* Traffic, 2010. **11**(3): p. 361-82.
63. Razani, B., et al., *Caveolin-1-deficient mice are lean, resistant to diet-induced obesity, and show hypertriglyceridemia with adipocyte abnormalities.* J Biol Chem, 2002. **277**(10): p. 8635-47.
64. Cohen, A.W., et al., *Caveolin-1-deficient mice show insulin resistance and defective insulin receptor protein expression in adipose tissue.* Am J Physiol Cell Physiol, 2003. **285**(1): p. C222-35.
65. Le Lay, S., et al., *Cholesterol-induced caveolin targeting to lipid droplets in adipocytes: a role for caveolar endocytosis.* Traffic, 2006. **7**(5): p. 549-61.
66. Frank, P.G., et al., *Caveolin-1 and regulation of cellular cholesterol homeostasis.* Am J Physiol Heart Circ Physiol, 2006. **291**(2): p. H677-86.
67. Pol, A., et al., *A caveolin dominant negative mutant associates with lipid bodies and induces intracellular cholesterol imbalance.* J Cell Biol, 2001. **152**(5): p. 1057-70.
68. Siddiqi, S., et al., *Intestinal caveolin-1 is important for dietary fatty acid absorption.* Biochim Biophys Acta, 2013. **1831**(8): p. 1311-21.
69. Ding, S.Y., et al., *Pleiotropic effects of cavin-1 deficiency on lipid metabolism.* J Biol Chem, 2014. **289**(12): p. 8473-83.
70. Pilch, P.F. and L. Liu, *Fat caves: caveolae, lipid trafficking and lipid metabolism in adipocytes.* Trends Endocrinol Metab, 2011. **22**(8): p. 318-24.
71. Couet, J., et al., *Identification of peptide and protein ligands for the caveolin-scaffolding domain. Implications for the interaction of caveolin with caveolae-associated proteins.* J Biol Chem, 1997. **272**(10): p. 6525-33.
72. Okamoto, T., et al., *Caveolins, a family of scaffolding proteins for organizing "preassembled signaling complexes" at the plasma membrane.* J Biol Chem, 1998. **273**(10): p. 5419-22.
73. Repetto, S., et al., *Insulin and IGF-I phosphorylate eNOS in HUVECs by a caveolin-1 dependent mechanism.* Biochem Biophys Res Commun, 2005. **337**(3): p. 849-52.
74. Shaul, P.W., et al., *Acylation targets emdothelial nitric-oxide synthase to plasmalemmal caveolae.* J Biol Chem, 1996. **271**(11): p. 6518-22.
75. Garcia-Cardena, G., et al., *Targeting of nitric oxide synthase to endothelial cell caveolae via palmitoylation: implications for nitric oxide signaling.* Proc Natl Acad Sci U S A, 1996. **93**(13): p. 6448-53.
76. Saltiel, A.R. and J.E. Pessin, *Insulin signaling in microdomains of the plasma membrane.* Traffic, 2003. **4**(11): p. 711-6.
77. Nystrom, F.H., et al., *Caveolin-1 interacts with the insulin receptor and can differentially modulate insulin signaling in transfected Cos-7 cells and rat adipose cells.* Mol Endocrinol, 1999. **13**(12): p. 2013-24.

78. Karlsson, M., et al., *Insulin induces translocation of glucose transporter GLUT4 to plasma membrane caveolae in adipocytes.* Faseb j, 2002. **16**(2): p. 249-51.
79. Gustavsson, J., S. Parpal, and P. Stralfors, *Insulin-stimulated glucose uptake involves the transition of glucose transporters to a caveolae-rich fraction within the plasma membrane: implications for type II diabetes.* Mol Med, 1996. **2**(3): p. 367-72.
80. Yamamoto, H., H. Komekado, and A. Kikuchi, *Caveolin is necessary for Wnt-3a-dependent internalization of LRP6 and accumulation of beta-catenin.* Dev Cell, 2006. **11**(2): p. 213-23.
81. Lin, D., et al., *Protein kinase Cgamma regulation of gap junction activity through caveolin-1-containing lipid rafts.* Invest Ophthalmol Vis Sci, 2003. **44**(12): p. 5259-68.
82. Couet, J., M. Sargiacomo, and M.P. Lisanti, *Interaction of a receptor tyrosine kinase, EGF-R, with caveolins. Caveolin binding negatively regulates tyrosine and serine/threonine kinase activities.* J Biol Chem, 1997. **272**(48): p. 30429-38.
83. Bernatchez, P.N., et al., *Dissecting the molecular control of endothelial NO synthase by caveolin-1 using cell-permeable peptides.* Proc Natl Acad Sci U S A, 2005. **102**(3): p. 761-6.
84. Taira, J., et al., *Caveolin-1 is a competitive inhibitor of heme oxygenase-1 (HO-1) with heme: identification of a minimum sequence in caveolin-1 for binding to HO-1.* Biochemistry, 2011. **50**(32): p. 6824-31.
85. Collins, B.M., et al., *Structure-based reassessment of the caveolin signaling model: do caveolae regulate signaling through caveolin-protein interactions?* Dev Cell, 2012. **23**(1): p. 11-20.
86. Byrne, D.P., C. Dart, and D.J. Rigden, *Evaluating caveolin interactions: do proteins interact with the caveolin scaffolding domain through a widespread aromatic residue-rich motif?* PLoS One, 2012. **7**(9): p. e44879.
87. Schlegel, A., et al., *A role for the caveolin scaffolding domain in mediating the membrane attachment of caveolin-1. The caveolin scaffolding domain is both necessary and sufficient for membrane binding in vitro.* J Biol Chem, 1999. **274**(32): p. 22660-7.
88. Epand, R.M., B.G. Sayer, and R.F. Epand, *Caveolin scaffolding region and cholesterol-rich domains in membranes.* J Mol Biol, 2005. **345**(2): p. 339-50.
89. Arbuzova, A., et al., *Membrane binding of peptides containing both basic and aromatic residues. Experimental studies with peptides corresponding to the scaffolding region of caveolin and the effector region of MARCKS.* Biochemistry, 2000. **39**(33): p. 10330-9.
90. Kirkham, M., et al., *Evolutionary analysis and molecular dissection of caveola biogenesis.* J Cell Sci, 2008. **121**(Pt 12): p. 2075-86.
91. Kwon, H., et al., *Caveolin-2 regulation of STAT3 transcriptional activation in response to insulin.* Biochim Biophys Acta, 2009. **1793**(7): p. 1325-33.
92. Kwon, H. and Y. Pak, *Prolonged tyrosine kinase activation of insulin receptor by pY27-caveolin-2.* Biochem Biophys Res Commun, 2010. **391**(1): p. 49-55.
93. Kwon, H., et al., *Fatty acylated caveolin-2 is a substrate of insulin receptor tyrosine kinase for insulin receptor substrate-1-directed signaling activation.* Biochim Biophys Acta, 2015. **1853**(5): p. 1022-34.

94. Gonzalez-Munoz, E., et al., *Caveolin-1 loss of function accelerates glucose transporter 4 and insulin receptor degradation in 3T3-L1 adipocytes.* Endocrinology, 2009. **150**(8): p. 3493-502.
95. Hernandez-Deviez, D.J., et al., *Caveolin regulates endocytosis of the muscle repair protein, dysferlin.* J Biol Chem, 2008. **283**(10): p. 6476-88.
96. Blouin, C.M., et al., *Plasma membrane subdomain compartmentalization contributes to distinct mechanisms of ceramide action on insulin signaling.* Diabetes, 2010. **59**(3): p. 600-10.
97. Hoffmann, C., et al., *Caveolin limits membrane microdomain mobility and integrin-mediated uptake of fibronectin-binding pathogens.* J Cell Sci, 2010. **123**(Pt 24): p. 4280-91.
98. Dulhunty, A.F. and C. Franzini-Armstrong, *The relative contributions of the folds and caveolae to the surface membrane of frog skeletal muscle fibres at different sarcomere lengths.* J Physiol, 1975. **250**(3): p. 513-39.
99. Sinha, B., et al., *Cells respond to mechanical stress by rapid disassembly of caveolae.* Cell, 2011. **144**(3): p. 402-13.
100. Gambin, Y., et al., *Single-molecule analysis reveals self assembly and nanoscale segregation of two distinct cavin subcomplexes on caveolae.* Elife, 2014. **3**: p. e01434.
101. Lo, H.P., et al., *The caveolin-cavin system plays a conserved and critical role in mechanoprotection of skeletal muscle.* J Cell Biol, 2015. **210**(5): p. 833-49.
102. Cheng, J.P., et al., *Caveolae protect endothelial cells from membrane rupture during increased cardiac output.* J Cell Biol, 2015. **211**(1): p. 53-61.
103. Zhao, Y.Y., et al., *Defects in caveolin-1 cause dilated cardiomyopathy and pulmonary hypertension in knockout mice.* Proc Natl Acad Sci U S A, 2002. **99**(17): p. 11375-80.
104. Woodman, S.E., et al., *Caveolin-3 knock-out mice develop a progressive cardiomyopathy and show hyperactivation of the p42/44 MAPK cascade.* J Biol Chem, 2002. **277**(41): p. 38988-97.
105. Hayashi, T., et al., *Identification and functional analysis of a caveolin-3 mutation associated with familial hypertrophic cardiomyopathy.* Biochem Biophys Res Commun, 2004. **313**(1): p. 178-84.
106. Vatta, M., et al., *Mutant caveolin-3 induces persistent late sodium current and is associated with long-QT syndrome.* Circulation, 2006. **114**(20): p. 2104-12.
107. Cronk, L.B., et al., *Novel mechanism for sudden infant death syndrome: persistent late sodium current secondary to mutations in caveolin-3.* Heart Rhythm, 2007. **4**(2): p. 161-6.
108. Bauer, P.M., et al., *Endothelial-specific expression of caveolin-1 impairs microvascular permeability and angiogenesis.* Proc Natl Acad Sci U S A, 2005. **102**(1): p. 204-9.
109. Galbiati, F., et al., *Caveolin-3 null mice show a loss of caveolae, changes in the microdomain distribution of the dystrophin-glycoprotein complex, and t-tubule abnormalities.* J Biol Chem, 2001. **276**(24): p. 21425-33.
110. McNally, E.M., et al., *Caveolin-3 in muscular dystrophy.* Hum Mol Genet, 1998. **7**(5): p. 871-7.
111. Woodman, S.E., et al., *Caveolinopathies: mutations in caveolin-3 cause four distinct autosomal dominant muscle diseases.* Neurology, 2004. **62**(4): p. 538-43.
112. Minetti, C., et al., *Mutations in the caveolin-3 gene cause autosomal dominant limb-girdle muscular dystrophy.* Nat Genet, 1998. **18**(4): p. 365-8.

113. Hayashi, Y.K., et al., *Human PTRF mutations cause secondary deficiency of caveolins resulting in muscular dystrophy with generalized lipodystrophy.* J Clin Invest, 2009. **119**(9): p. 2623-33.
114. Corrotte, M., et al., *Caveolae internalization repairs wounded cells and muscle fibers.* Elife, 2013. **2**: p. e00926.
115. Rizzo, V., et al., *Recruitment of endothelial caveolae into mechanotransduction pathways by flow conditioning in vitro.* Am J Physiol Heart Circ Physiol, 2003. **285**(4): p. H1720-9.
116. Boyd, N.L., et al., *Chronic shear induces caveolae formation and alters ERK and Akt responses in endothelial cells.* Am J Physiol Heart Circ Physiol, 2003. **285**(3): p. H1113-22.
117. Radel, C. and V. Rizzo, *Integrin mechanotransduction stimulates caveolin-1 phosphorylation and recruitment of Csk to mediate actin reorganization.* Am J Physiol Heart Circ Physiol, 2005. **288**(2): p. H936-45.
118. Yu, J., et al., *Direct evidence for the role of caveolin-1 and caveolae in mechanotransduction and remodeling of blood vessels.* J Clin Invest, 2006. **116**(5): p. 1284-91.
119. Sedding, D.G., et al., *Caveolin-1 facilitates mechanosensitive protein kinase B (Akt) signaling in vitro and in vivo.* Circ Res, 2005. **96**(6): p. 635-42.
120. Stan, R.V., *Structure of caveolae.* Biochim Biophys Acta, 2005. **1746**(3): p. 334-48.
121. Peters, K.R., W.W. Carley, and G.E. Palade, *Endothelial plasmalemmal vesicles have a characteristic striped bipolar surface structure.* J Cell Biol, 1985. **101**(6): p. 2233-8.
122. Ludwig, A., et al., *Molecular composition and ultrastructure of the caveolar coat complex.* PLoS Biol, 2013. **11**(8): p. e1001640.
123. Lamaze, C., et al., *The caveolae dress code: structure and signaling.* Curr Opin Cell Biol, 2017. **47**: p. 117-125.
124. Parton, R.G., et al., *Characterization of a distinct plasma membrane macrodomain in differentiated adipocytes.* J Biol Chem, 2002. **277**(48): p. 46769-78.
125. Echarri, A., et al., *Caveolar domain organization and trafficking is regulated by Abl kinases and mDia1.* J Cell Sci, 2012. **125**(Pt 13): p. 3097-113.
126. Stan, R.V., *Structure and function of endothelial caveolae.* Microsc Res Tech, 2002. **57**(5): p. 350-64.
127. Hansen, C.G., G. Howard, and B.J. Nichols, *Pacsin 2 is recruited to caveolae and functions in caveolar biogenesis.* J Cell Sci, 2011. **124**(Pt 16): p. 2777-85.
128. Pelkmans, L. and M. Zerial, *Kinase-regulated quantal assemblies and kiss-and-run recycling of caveolae.* Nature, 2005. **436**(7047): p. 128-33.
129. Drab, M., et al., *Loss of caveolae, vascular dysfunction, and pulmonary defects in caveolin-1 gene-disrupted mice.* Science, 2001. **293**(5539): p. 2449-52.
130. Dietzen, D.J., W.R. Hastings, and D.M. Lublin, *Caveolin is palmitoylated on multiple cysteine residues. Palmitoylation is not necessary for localization of caveolin to caveolae.* J Biol Chem, 1995. **270**(12): p. 6838-42.
131. Monier, S., et al., *Oligomerization of VIP21-caveolin in vitro is stabilized by long chain fatty acylation or cholesterol.* FEBS Lett, 1996. **388**(2-3): p. 143-9.
132. Parton, R.G. and M.A. del Pozo, *Caveolae as plasma membrane sensors, protectors and organizers.* Nat Rev Mol Cell Biol, 2013. **14**(2): p. 98-112.

133. Sargiacomo, M., et al., *Oligomeric structure of caveolin: implications for caveolae membrane organization.* Proc Natl Acad Sci U S A, 1995. **92**(20): p. 9407-11.
134. Monier, S., et al., *VIP21-caveolin, a membrane protein constituent of the caveolar coat, oligomerizes in vivo and in vitro.* Mol Biol Cell, 1995. **6**(7): p. 911-27.
135. Fernandez, I., et al., *Mechanism of caveolin filament assembly.* Proc Natl Acad Sci U S A, 2002. **99**(17): p. 11193-8.
136. Scheiffele, P., et al., *Caveolin-1 and -2 in the exocytic pathway of MDCK cells.* J Cell Biol, 1998. **140**(4): p. 795-806.
137. Hansen, C.G. and B.J. Nichols, *Exploring the caves: cavins, caveolins and caveolae.* Trends Cell Biol, 2010. **20**(4): p. 177-86.
138. Kovtun, O., et al., *Structural insights into the organization of the cavin membrane coat complex.* Dev Cell, 2014. **31**(4): p. 405-19.
139. Hill, M.M., et al., *PTRF-Cavin, a conserved cytoplasmic protein required for caveola formation and function.* Cell, 2008. **132**(1): p. 113-24.
140. Walser, P.J., et al., *Constitutive formation of caveolae in a bacterium.* Cell, 2012. **150**(4): p. 752-63.
141. Stoeber, M., et al., *Model for the architecture of caveolae based on a flexible, net-like assembly of Cavin1 and Caveolin discs.* Proc Natl Acad Sci U S A, 2016. **113**(50): p. E8069-e8078.
142. Ludwig, A., B.J. Nichols, and S. Sandin, *Architecture of the caveolar coat complex.* J Cell Sci, 2016.
143. Peter, B.J., et al., *BAR domains as sensors of membrane curvature: the amphiphysin BAR structure.* Science, 2004. **303**(5657): p. 495-9.
144. Shimada, A., et al., *Curved EFC/F-BAR-domain dimers are joined end to end into a filament for membrane invagination in endocytosis.* Cell, 2007. **129**(4): p. 761-72.
145. Plomann, M., et al., *PACSIN, a brain protein that is upregulated upon differentiation into neuronal cells.* Eur J Biochem, 1998. **256**(1): p. 201-11.
146. Qualmann, B. and R.B. Kelly, *Syndapin isoforms participate in receptor-mediated endocytosis and actin organization.* J Cell Biol, 2000. **148**(5): p. 1047-62.
147. Modregger, J., et al., *All three PACSIN isoforms bind to endocytic proteins and inhibit endocytosis.* J Cell Sci, 2000. **113 Pt 24**: p. 4511-21.
148. Ritter, B., et al., *PACSIN 2, a novel member of the PACSIN family of cytoplasmic adapter proteins.* FEBS Lett, 1999. **454**(3): p. 356-62.
149. Itoh, T. and P. De Camilli, *BAR, F-BAR (EFC) and ENTH/ANTH domains in the regulation of membrane-cytosol interfaces and membrane curvature.* Biochim Biophys Acta, 2006. **1761**(8): p. 897-912.
150. Suetsugu, S., K. Toyooka, and Y. Senju, *Subcellular membrane curvature mediated by the BAR domain superfamily proteins.* Semin Cell Dev Biol, 2010. **21**(4): p. 340-9.
151. Itoh, T., et al., *Dynamin and the actin cytoskeleton cooperatively regulate plasma membrane invagination by BAR and F-BAR proteins.* Dev Cell, 2005. **9**(6): p. 791-804.
152. Simpson, F., et al., *SH3-domain-containing proteins function at distinct steps in clathrin-coated vesicle formation.* Nat Cell Biol, 1999. **1**(2): p. 119-24.

153. Shimada, A., et al., *Mapping of the basic amino-acid residues responsible for tubulation and cellular protrusion by the EFC/F-BAR domain of pacsin2/Syndapin II.* FEBS Lett, 2010. **584**(6): p. 1111-8.
154. Wang, Q., et al., *Molecular mechanism of membrane constriction and tubulation mediated by the F-BAR protein Pacsin/Syndapin.* Proc Natl Acad Sci U S A, 2009. **106**(31): p. 12700-5.
155. Kessels, M.M., et al., *Complexes of syndapin II with dynamin II promote vesicle formation at the trans-Golgi network.* J Cell Sci, 2006. **119**(Pt 8): p. 1504-16.
156. Rao, Y., et al., *Molecular basis for SH3 domain regulation of F-BAR-mediated membrane deformation.* Proc Natl Acad Sci U S A, 2010. **107**(18): p. 8213-8.
157. Ferguson, S.M. and P. De Camilli, *Dynamin, a membrane-remodelling GTPase.* Nat Rev Mol Cell Biol, 2012. **13**(2): p. 75-88.
158. Sever, S., H. Damke, and S.L. Schmid, *Dynamin:GTP controls the formation of constricted coated pits, the rate limiting step in clathrin-mediated endocytosis.* J Cell Biol, 2000. **150**(5): p. 1137-48.
159. Cao, H., F. Garcia, and M.A. McNiven, *Differential distribution of dynamin isoforms in mammalian cells.* Mol Biol Cell, 1998. **9**(9): p. 2595-609.
160. van der Bliek, A.M., et al., *Mutations in human dynamin block an intermediate stage in coated vesicle formation.* J Cell Biol, 1993. **122**(3): p. 553-63.
161. Herskovits, J.S., et al., *Effects of mutant rat dynamin on endocytosis.* J Cell Biol, 1993. **122**(3): p. 565-78.
162. Damke, H., et al., *Induction of mutant dynamin specifically blocks endocytic coated vesicle formation.* J Cell Biol, 1994. **127**(4): p. 915-34.
163. Marks, B., et al., *GTPase activity of dynamin and resulting conformation change are essential for endocytosis.* Nature, 2001. **410**(6825): p. 231-5.
164. Shpetner, H.S. and R.B. Vallee, *Identification of dynamin, a novel mechanochemical enzyme that mediates interactions between microtubules.* Cell, 1989. **59**(3): p. 421-32.
165. Koenig, J.H. and K. Ikeda, *Disappearance and reformation of synaptic vesicle membrane upon transmitter release observed under reversible blockage of membrane retrieval.* J Neurosci, 1989. **9**(11): p. 3844-60.
166. van der Bliek, A.M. and E.M. Meyerowitz, *Dynamin-like protein encoded by the Drosophila shibire gene associated with vesicular traffic.* Nature, 1991. **351**(6325): p. 411-4.
167. Chen, M.S., et al., *Multiple forms of dynamin are encoded by shibire, a Drosophila gene involved in endocytosis.* Nature, 1991. **351**(6327): p. 583-6.
168. Ferguson, S.M., et al., *A selective activity-dependent requirement for dynamin 1 in synaptic vesicle endocytosis.* Science, 2007. **316**(5824): p. 570-4.
169. Nakata, T., et al., *Predominant and developmentally regulated expression of dynamin in neurons.* Neuron, 1991. **7**(3): p. 461-9.
170. Cook, T.A., R. Urrutia, and M.A. McNiven, *Identification of dynamin 2, an isoform ubiquitously expressed in rat tissues.* Proc Natl Acad Sci U S A, 1994. **91**(2): p. 644-8.
171. Raimondi, A., et al., *Overlapping role of dynamin isoforms in synaptic vesicle endocytosis.* Neuron, 2011. **70**(6): p. 1100-14.
172. Yao, Q., et al., *Caveolin-1 interacts directly with dynamin-2.* J Mol Biol, 2005. **348**(2): p. 491-501.

173. Bai, X., G. Meng, and X. Zheng, *Crystal structure of human PACSIN 2 F-BAR domain.* To be published.
174. Naslavsky, N. and S. Caplan, *EHD proteins: key conductors of endocytic transport.* Trends Cell Biol, 2011. **21**(2): p. 122-31.
175. George, M., et al., *Shared as well as distinct roles of EHD proteins revealed by biochemical and functional comparisons in mammalian cells and C. elegans.* BMC Cell Biol, 2007. **8**: p. 3.
176. Caplan, S., et al., *A tubular EHD1-containing compartment involved in the recycling of major histocompatibility complex class I molecules to the plasma membrane.* Embo j, 2002. **21**(11): p. 2557-67.
177. Sharma, M., N. Naslavsky, and S. Caplan, *A role for EHD4 in the regulation of early endosomal transport.* Traffic, 2008. **9**(6): p. 995-1018.
178. Daumke, O., et al., *Architectural and mechanistic insights into an EHD ATPase involved in membrane remodelling.* Nature, 2007. **449**(7164): p. 923-7.
179. Paoluzi, S., et al., *Recognition specificity of individual EH domains of mammals and yeast.* Embo j, 1998. **17**(22): p. 6541-50.
180. Salcini, A.E., et al., *Binding specificity and in vivo targets of the EH domain, a novel protein-protein interaction module.* Genes Dev, 1997. **11**(17): p. 2239-49.
181. Kieken, F., et al., *EH domain of EHD1.* J Biomol NMR, 2007. **39**(4): p. 323-9.
182. Kieken, F., et al., *Mechanism for the selective interaction of C-terminal Eps15 homology domain proteins with specific Asn-Pro-Phe-containing partners.* J Biol Chem, 2010. **285**(12): p. 8687-94.
183. Henry, G.D., et al., *Charge effects in the selection of NPF motifs by the EH domain of EHD1.* Biochemistry, 2010. **49**(16): p. 3381-92.
184. Braun, A., et al., *EHD proteins associate with syndapin I and II and such interactions play a crucial role in endosomal recycling.* Mol Biol Cell, 2005. **16**(8): p. 3642-58.
185. Grant, B., et al., *Evidence that RME-1, a conserved C. elegans EH-domain protein, functions in endocytic recycling.* Nat Cell Biol, 2001. **3**(6): p. 573-9.
186. Rapaport, D., et al., *Recycling to the plasma membrane is delayed in EHD1 knockout mice.* Traffic, 2006. **7**(1): p. 52-60.
187. Rainey, M.A., et al., *The endocytic recycling regulator EHD1 is essential for spermatogenesis and male fertility in mice.* BMC Dev Biol, 2010. **10**: p. 37.
188. Lin, S.X., et al., *Rme-1 regulates the distribution and function of the endocytic recycling compartment in mammalian cells.* Nat Cell Biol, 2001. **3**(6): p. 567-72.
189. Guilherme, A., et al., *Role of EHD1 and EHBP1 in perinuclear sorting and insulin-regulated GLUT4 recycling in 3T3-L1 adipocytes.* J Biol Chem, 2004. **279**(38): p. 40062-75.
190. Walseng, E., O. Bakke, and P.A. Roche, *Major histocompatibility complex class II-peptide complexes internalize using a clathrin- and dynamin-independent endocytosis pathway.* J Biol Chem, 2008. **283**(21): p. 14717-27.
191. Naslavsky, N., et al., *Rabenosyn-5 and EHD1 interact and sequentially regulate protein recycling to the plasma membrane.* Mol Biol Cell, 2004. **15**(5): p. 2410-22.
192. Pekar, O., et al., *EHD2 shuttles to the nucleus and represses transcription.* Biochem J, 2012. **444**(3): p. 383-94.

193. Galperin, E., et al., *EHD3: a protein that resides in recycling tubular and vesicular membrane structures and interacts with EHD1.* Traffic, 2002. **3**(8): p. 575-89.
194. Lee, D.W., et al., *ATP binding regulates oligomerization and endosome association of RME-1 family proteins.* J Biol Chem, 2005. **280**(17): p. 17213-20.
195. Hoernke, M., et al., *EHD2 restrains dynamics of caveolae by an ATP-dependent, membrane-bound, open conformation.* Proc Natl Acad Sci U S A, 2017. **114**(22): p. E4360-e4369.
196. Naslavsky, N., et al., *Interactions between EHD proteins and Rab11-FIP2: a role for EHD3 in early endosomal transport.* Mol Biol Cell, 2006. **17**(1): p. 163-77.
197. Naslavsky, N., et al., *EHD3 regulates early-endosome-to-Golgi transport and preserves Golgi morphology.* J Cell Sci, 2009. **122**(Pt 3): p. 389-400.
198. Gudmundsson, H., et al., *EH domain proteins regulate cardiac membrane protein targeting.* Circ Res, 2010. **107**(1): p. 84-95.
199. Bhattacharyya, S., et al., *Endocytic recycling protein EHD1 regulates primary cilia morphogenesis and SHH signaling during neural tube development.* Sci Rep, 2016. **6**: p. 20727.
200. Lu, Q., et al., *Early steps in primary cilium assembly require EHD1/EHD3-dependent ciliary vesicle formation.* Nat Cell Biol, 2015. **17**(3): p. 228-40.
201. Roland, J.T., et al., *Myosin Vb interacts with Rab8a on a tubular network containing EHD1 and EHD3.* Mol Biol Cell, 2007. **18**(8): p. 2828-37.
202. Yap, C.C., et al., *Alterations of EHD1/EHD4 protein levels interfere with L1/NgCAM endocytosis in neurons and disrupt axonal targeting.* J Neurosci, 2010. **30**(19): p. 6646-57.
203. Shao, Y., et al., *Pincher, a pinocytic chaperone for nerve growth factor/TrkA signaling endosomes.* J Cell Biol, 2002. **157**(4): p. 679-91.
204. Valdez, G., et al., *Pincher-mediated macroendocytosis underlies retrograde signaling by neurotrophin receptors.* J Neurosci, 2005. **25**(21): p. 5236-47.
205. Smith, C.A., et al., *The cell fate determinant numb interacts with EHD/Rme-1 family proteins and has a role in endocytic recycling.* Mol Biol Cell, 2004. **15**(8): p. 3698-708.
206. George, M., et al., *Ehd4 is required to attain normal prepubertal testis size but dispensable for fertility in male mice.* Genesis, 2010. **48**(5): p. 328-42.
207. Aboulaich, N., et al., *Vectorial proteomics reveal targeting, phosphorylation and specific fragmentation of polymerase I and transcript release factor (PTRF) at the surface of caveolae in human adipocytes.* Biochem J, 2004. **383**(Pt 2): p. 237-48.
208. Yeow, I., et al., *EHD Proteins Cooperate to Generate Caveolar Clusters and to Maintain Caveolae during Repeated Mechanical Stress.* Curr Biol, 2017.
209. Cao, H., et al., *Heterozygous CAV1 frameshift mutations (MIM 601047) in patients with atypical partial lipodystrophy and hypertriglyceridemia.* Lipids Health Dis, 2008. **7**: p. 3.
210. Shastry, S., et al., *Congenital generalized lipodystrophy, type 4 (CGL4) associated with myopathy due to novel PTRF mutations.* Am J Med Genet A, 2010. **152a**(9): p. 2245-53.
211. Schrauwen, I., et al., *A Frame-Shift Mutation in CAV1 Is Associated with a Severe Neonatal Progeroid and Lipodystrophy Syndrome.* PLoS One, 2015. **10**(7): p. e0131797.

212. Ost, A., et al., *Triacylglycerol is synthesized in a specific subclass of caveolae in primary adipocytes.* J Biol Chem, 2005. **280**(1): p. 5-8.
213. Souto, R.P., et al., *Immunopurification and characterization of rat adipocyte caveolae suggest their dissociation from insulin signaling.* J Biol Chem, 2003. **278**(20): p. 18321-9.
214. Foti, M., et al., *The neck of caveolae is a distinct plasma membrane subdomain that concentrates insulin receptors in 3T3-L1 adipocytes.* Proc Natl Acad Sci U S A, 2007. **104**(4): p. 1242-7.
215. Wharton, J., et al., *Dissociation of insulin receptor expression and signaling from caveolin-1 expression.* J Biol Chem, 2005. **280**(14): p. 13483-6.
216. Mastick, C.C., M.J. Brady, and A.R. Saltiel, *Insulin stimulates the tyrosine phosphorylation of caveolin.* J Cell Biol, 1995. **129**(6): p. 1523-31.
217. Kimura, A., et al., *The insulin receptor catalyzes the tyrosine phosphorylation of caveolin-1.* J Biol Chem, 2002. **277**(33): p. 30153-8.
218. Kabayama, K., et al., *Dissociation of the insulin receptor and caveolin-1 complex by ganglioside GM3 in the state of insulin resistance.* Proc Natl Acad Sci U S A, 2007. **104**(34): p. 13678-83.
219. Sekimoto, J., et al., *Dissociation of the insulin receptor from caveolae during TNFalpha-induced insulin resistance and its recovery by D-PDMP.* FEBS Lett, 2012. **586**(2): p. 191-5.
220. Yu, C., et al., *Mechanism by which fatty acids inhibit insulin activation of insulin receptor substrate-1 (IRS-1)-associated phosphatidylinositol 3-kinase activity in muscle.* J Biol Chem, 2002. **277**(52): p. 50230-6.
221. Itani, S.I., et al., *Lipid-induced insulin resistance in human muscle is associated with changes in diacylglycerol, protein kinase C, and IkappaB-alpha.* Diabetes, 2002. **51**(7): p. 2005-11.
222. Stralfors, P., *Autolysis of isolated adipocytes by endogenously produced fatty acids.* FEBS Lett, 1990. **263**(1): p. 153-4.
223. Su, X. and N.A. Abumrad, *Cellular fatty acid uptake: a pathway under construction.* Trends Endocrinol Metab, 2009. **20**(2): p. 72-7.
224. Pohl, J., et al., *Role of FATP in parenchymal cell fatty acid uptake.* Biochim Biophys Acta, 2004. **1686**(1-2): p. 1-6.
225. Abumrad, N.A., et al., *Cloning of a rat adipocyte membrane protein implicated in binding or transport of long-chain fatty acids that is induced during preadipocyte differentiation. Homology with human CD36.* J Biol Chem, 1993. **268**(24): p. 17665-8.
226. Coburn, C.T., et al., *Role of CD36 in membrane transport and utilization of long-chain fatty acids by different tissues.* J Mol Neurosci, 2001. **16**(2-3): p. 117-21; discussion 151-7.
227. Hamilton, J.A., *Fast flip-flop of cholesterol and fatty acids in membranes: implications for membrane transport proteins.* Curr Opin Lipidol, 2003. **14**(3): p. 263-71.
228. Doody, M.C., et al., *Mechanism and kinetics of transfer of a fluorescent fatty acid between single-walled phosphatidylcholine vesicles.* Biochemistry, 1980. **19**(1): p. 108-16.
229. Trigatti, B.L. and G.E. Gerber, *The effect of intracellular pH on long-chain fatty acid uptake in 3T3-L1 adipocytes: evidence that uptake involves the passive diffusion of protonated long-chain fatty acids across the plasma membrane.* Biochem J, 1996. **313 (Pt 2)**: p. 487-94.

230. Kampf, J.P. and A.M. Kleinfeld, *Fatty acid transport in adipocytes monitored by imaging intracellular free fatty acid levels.* J Biol Chem, 2004. **279**(34): p. 35775-80.
231. Herrmann, T., et al., *Mouse fatty acid transport protein 4 (FATP4): characterization of the gene and functional assessment as a very long chain acyl-CoA synthetase.* Gene, 2001. **270**(1-2): p. 31-40.
232. Schmelter, T., et al., *Biochemical demonstration of the involvement of fatty acyl-CoA synthetase in fatty acid translocation across the plasma membrane.* J Biol Chem, 2004. **279**(23): p. 24163-70.
233. Pohl, J., et al., *New concepts of cellular fatty acid uptake: role of fatty acid transport proteins and of caveolae.* Proc Nutr Soc, 2004. **63**(2): p. 259-62.
234. Coburn, C.T., et al., *Defective uptake and utilization of long chain fatty acids in muscle and adipose tissues of CD36 knockout mice.* J Biol Chem, 2000. **275**(42): p. 32523-9.
235. Hames, K.C., et al., *Free fatty acid uptake in humans with CD36 deficiency.* Diabetes, 2014. **63**(11): p. 3606-14.
236. Pohl, J., et al., *FAT/CD36-mediated long-chain fatty acid uptake in adipocytes requires plasma membrane rafts.* Mol Biol Cell, 2005. **16**(1): p. 24-31.
237. Ring, A., et al., *Caveolin-1 is required for fatty acid translocase (FAT/CD36) localization and function at the plasma membrane of mouse embryonic fibroblasts.* Biochim Biophys Acta, 2006. **1761**(4): p. 416-23.
238. Pownall, H.J. and J.A. Hamilton, *Energy translocation across cell membranes and membrane models.* Acta Physiol Scand, 2003. **178**(4): p. 357-65.
239. Briand, N., et al., *Distinct roles of endothelial and adipocyte caveolin-1 in macrophage infiltration and adipose tissue metabolic activity.* Diabetes, 2011. **60**(2): p. 448-53.
240. Martin, S., et al., *Caveolin-1 deficiency leads to increased susceptibility to cell death and fibrosis in white adipose tissue: characterization of a lipodystrophic model.* PLoS One, 2012. **7**(9): p. e46242.
241. Meshulam, T., et al., *Caveolins/caveolae protect adipocytes from fatty acid-mediated lipotoxicity.* J Lipid Res, 2011. **52**(8): p. 1526-32.
242. Ran, F.A., et al., *Genome engineering using the CRISPR-Cas9 system.* Nat Protoc, 2013. **8**(11): p. 2281-2308.
243. Wood, A.J., et al., *Targeted genome editing across species using ZFNs and TALENs.* Science, 2011. **333**(6040): p. 307.
244. Mali, P., et al., *RNA-guided human genome engineering via Cas9.* Science, 2013. **339**(6121): p. 823-6.
245. Cong, L., et al., *Multiplex genome engineering using CRISPR/Cas systems.* Science, 2013. **339**(6121): p. 819-23.
246. Urnov, F.D., et al., *Genome editing with engineered zinc finger nucleases.* Nat Rev Genet, 2010. **11**(9): p. 636-46.
247. Joung, J.K. and J.D. Sander, *TALENs: a widely applicable technology for targeted genome editing.* Nat Rev Mol Cell Biol, 2013. **14**(1): p. 49-55.
248. Jinek, M., et al., *A programmable dual-RNA-guided DNA endonuclease in adaptive bacterial immunity.* Science, 2012. **337**(6096): p. 816-21.
249. Garneau, J.E., et al., *The CRISPR/Cas bacterial immune system cleaves bacteriophage and plasmid DNA.* Nature, 2010. **468**(7320): p. 67-71.
250. Gasiunas, G., et al., *Cas9-crRNA ribonucleoprotein complex mediates specific DNA cleavage for adaptive immunity in bacteria.* Proc Natl Acad Sci U S A, 2012. **109**(39): p. E2579-86.

251. Razani, B., et al., *Caveolin-1 null mice are viable but show evidence of hyperproliferative and vascular abnormalities.* J Biol Chem, 2001. **276**(41): p. 38121-38.
252. Hansen, C.G., et al., *SDPR induces membrane curvature and functions in the formation of caveolae.* Nat Cell Biol, 2009. **11**(7): p. 807-14.
253. Melo, A.A., et al., *Structural insights into the activation mechanism of dynamin-like EHD ATPases.* Proc Natl Acad Sci U S A, 2017. **114**(22): p. 5629-5634.
254. Blume, J.J., et al., *EHD proteins are associated with tubular and vesicular compartments and interact with specific phospholipids.* Exp Cell Res, 2007. **313**(2): p. 219-31.
255. Pilch, P.F., et al., *Caveolae and lipid trafficking in adipocytes.* Clin Lipidol, 2011. **6**(1): p. 49-58.
256. Monteiro, R., et al., *Adipocyte size and liability to cell death.* Obes Surg, 2006. **16**(6): p. 804-6.
257. Eto, H., et al., *Characterization of structure and cellular components of aspirated and excised adipose tissue.* Plast Reconstr Surg, 2009. **124**(4): p. 1087-97.